SARS-CoV-2 causes periodontal fibrosis by deregulating mitochondrial β-oxidation

Yan Gao[1], Wai Ling Kok[1], Vikram Sharma[2], Charlotte Sara Illsley[1], Sally Hanks[1], Christopher Tredwin[1], Bing Hu[1*]

1. Stem Cells & Regenerative Medicine Laboratory, Peninsula Dental School, Faculty of Health, University of Plymouth, 16 Research Way, Plymouth, PL6 8BU, UK

2. School of Biomedical Sciences, Faculty of Health, University of Plymouth, 16 Research Way, Plymouth, PL6 8BU, UK

* Corresponding author

Professor Bing Hu

Email: bing.hu@plymouth.ac.uk

Running title: SARS-CoV-2 infection causes periodontal fibrosis

Key words: COVID-19; SARS-CoV-2; Tooth; Periodontal ligament; Fibrosis; Mitochondria

Word count: 3152

Reference count: 34

Figure/table counts: 5

Abstract

The global high prevalence of COVID-19 is a major challenge for health professionals and patients. SARS-CoV-2 virus mutate predominantly in the spike proteins, whilst the other key viral components remain stable. Previous studies have shown that the human oral cavity can potentially act as reservoir of the SARS-CoV-2 virus. COVID-19 can cause severe oral mucosa lesions and is likely to be connected with poor periodontal conditions. However, the consequence of SARS-CoV-2 viral infection on human oral health has not been systematically examined. In this research, we aimed to study the pathogenicity of SARS-CoV-2 viral components on human periodontal tissues and cells. We found that by exposing to SARS-CoV-2, especially to the viral envelope and membrane proteins, the human periodontal fibroblasts could develop fibrotic pathogenic phenotypes, including hyperproliferation that was concomitant induced together with increased apoptosis and senescence. The fibrotic degeneration was mediated by a down-regulation of mitochondrial β-oxidation in the fibroblasts. Fatty acid β-oxidation inhibitor, etomoxir treatment could mirror the same pathological consequence on the cells, similar to SARS-CoV-2 infection. Our results therefore provide novel mechanistic insights into how SARS-CoV-2 infection can affect human periodontal health at the cell and molecular level with potential new therapeutic targets for COVID-19 induced fibrosis.

Introduction

Since its outbreak, the coronavirus disease 2019 (COVID-19) pandemic has infected over 63 million people globally (https://covid19.who.int) and has been a major challenge to human health. The severe acute respiratory syndrome coronavirus 2 (SARS-CoV-2 virus) has multiple transmission routes such as through respiratory fluids, therefore is highly infectious (Ferretti et al. 2020). It has been reported that there were ever increasing "long COVID" (Lopez-Leon et al. 2021) and repeated infection cases (Wang et al. 2021), with the UK alone already having more than 2 million long COVID cases (Wise 2022). Although COVID-19 has been initially connected with acute inflammatory disease, which causes progressive pulmonary fibrosis (Spagnolo et al. 2020), increasing evidence have suggested that COVID-19 does affect other organs such as heart, skin, kidneys and brain (Wang et al. 2020). The human oral cavity and saliva have also been demonstrated to be an important reservoir of the SARS-CoV-2 virus (Huang et al. 2021), and saliva have been used for effective diagnosis of COVID-19 (Baghizadeh Fini 2020). Periodontal tissues are highly vulnerable to different infectious diseases and COVID-19 has been reported to be potentially connected with poor periodontal health (Qi et al. 2022). Furthermore, severe oral mucosa lesions including detachment of oral epithelium with inflammation and fibrosis have been reported in the COVID-19 patients (Henin et al. 2022; Pandiar et al. 2022). However, the molecular mechanisms under the potential pathological consequence of SARS-CoV-2 infection on human oral health have not been systematically investigated.

The evolution of SARS-CoV-2 has generated different variants that are responsible for infection speeds and symptoms (https://www.who.int/activities/tracking-SARS-CoV-2-variants). SARS-CoV-2 has four different structural protein components: envelope, membrane, nucleocapsid and spike (Figure 1A) (Huang et al. 2020). The mutations of SARS-CoV-2 predominantly occur in the spike proteins, particularly the receptor-binding

domain (RBD), whilst the other key viral components remain stable (Satarker and Nampoothiri 2020) (Harvey et al. 2021). A key step of SARS-CoV-2 infection is the binding of spike RBD to angiotensin-converting enzyme 2 (ACE2) receptor on the target cells (Ni et al. 2020) and co-receptor transmembrane serine protease 2 (TMPRSS2) to trigger viral internalization together with the molecular downstream cascades (Hoffmann et al. 2020). Currently, most of the COVID-19 related research and vaccine development have focused on the spike protein, leaving the other structural proteins' pathological functions remain to be elucidated.

As part of a series of research on the biological connection of COVID-19 with oral health, this study intended to apply human periodontal tissue and cells as examples to dissect the direct pathological effects of SARS-CoV-2 viral structural components.

Materials & methods

Cell culture

Human periodontal ligament fibroblasts (HPLF) were cultured in DMEM/F12 ((Gibco, 31331-028) containing 20% Fetal bovine serum (FBS) (Sigma, F7524), 1% penicillin-streptomycin (Hyclone, SV30079.01). Human gingival epithelial cells (HGEPp) were cultured in CnT-57 (CELLnTEC, CnT-57).

Viral infection

Plasmids for SARS-CoV-2 structural proteins were purchased from Addgene (Appendix Table 2). Lentiviral supernatant was collected according to the manual using 293FT cells. HPLFs were infected with lentiviruses carrying target sequences above with 10 μg/ml polybrene (Merck, TR-1003). After 2 h, dishes were topped up with fresh culture medium. Samples were collected at 6 h or 48 h. For overexpressing ACE2 (Addgene, Appendix Table 2) in HPLFs, the cells were infected with lentiviruses carrying target sequences above with 10 μg/ml polybrene (Merck). After 2 h, dishes were topped up with fresh normal culture medium. Samples were collected according to different time points. Infected cells were selected with 1 μg/ml puromycin (Thermo Scientific, 10781691) for 7-10 days.

Recombinant SARS-CoV-2 spike protein treatment

Recombinant SARS-CoV-2 spike protein with His-tag (Biotechne, 10549-CV) was diluted with culture medium to 500 ng/ml or 5 μg/ml and added into the cell culture medium. Samples were collected at 6 h or 48 h.

Mitochondria β-oxidation inhibition assay.

Etomoxir (Sigma, E1905) was diluted with culture medium to aimed concentration then added into cell culture medium. Samples were collected at 6 h or 48 h.

Human periodontal tissue 3D equivalents

5*10^4 of HPLFs were mixed with 150 µl gel mixture of rat tail collagen (Fisher, 11519816), DMEM (Fisher, 21969-035) and FBS (Ratio of volume 9:1:1) homogenously on ice. 2.3 µl 1M Sodium hydroxide solution (NaOH, Sigma 71687) was added into the mixture for neutralization, 150 µl gel was pipetted into a 0.4 µm culture insert (Greiner, 662641) incubated at 37°C for 1 h then fresh culture medium was added into the insert. Culture medium was replaced by CnT-57 before seeding 5*10^5 of HGEPp on top of the gel. HGEPp was cultured for 72 h before airlifting. Culture medium inside the insert was removed every day and the medium outside was changed every 2 days. Samples were frozen directly in OCT (Agar Scientific, AGR1180) at day 14 and sectioned at 20 µm for further analysis.

Hydrogel based 3D matrix production assay

1*10^6 of HPLFs were mixed with 100 µl bioink (CELLINK, CELLINK SKIN+) slowly and gently. Gels were pipetted into 6 well plate then 1.5 ml crosslinking agent (CELLINK) was added to cover the gel at RT for 5 min. Crosslinking agent was removed and 1.5 ml fresh culture media was added which was replaced every 2 days. Samples were frozen directly in OCT at day 7 and sectioned at 30 µm for further analysis.

Immunohistochemistry

For the details of immunostaining, BrdU incorporation assay, Terminal deoxynucleotidyl transferase dUTP nick end labelling (TUNEL) assay and Senescence assay details please see **Appendix materials & methods.**

Flow cytometry analysis

HPLFs and ACE2 overexpressed HPLFs were harvested and fixed in 2% PFA solution in 10 mM PBS for 10 min then washed with FACS buffer (1% BSA in PBS). 1*10^6 cells were resuspended in 500 µl flow cytometry permeabilization buffer (0.1% Tween-20 in PBS) for 15 min then washed with FACS buffer again. Cells were resuspended in 100 µl FACS buffer and APC His-Tag conjugated antibody was added, incubated for 2 h at room temperature then kept in dark at 4 °C degree overnight. Samples were analyzed using the BD FACSAria™ II (BD Biosciences). Data was acquired using red laser (633-640nm) for APC signal. Results were analyzed using the FlowJo software (Tree Star Inc., Version 10.8.1). Gates and regions were placed around populations of cells with common characteristics based on SSC and APC.

Western blotting

A NuPage® Electrophoresis System (Thermo Fisher Scientific), 4-12% Bis-Tris gradient gel (Thermo Fisher Scientific, NP0335BOX), and MOPS buffer (Thermo Fisher Scientific, NP0001), 25-40 µg protein were used for protein separation. Transfer of protein samples onto a 0.45 µm PVDF membrane (Thermo Fisher Scientific, LC2005) was carried out using a NuPage® XCell II Blot Module, and transfer buffer (Thermo Fisher Scientific, NP0006) with 10% methanol (Sigma, 322415). The iBind™ Western System (Thermo Fisher Scientific) was used for blocking, primary and secondary antibody incubations which details could be found above. A C-Digit scanner (LI-COR) was used for band detection with Image studio software (LI-COR, Version 3.1).

Proteomic analysis

Sample preparation, in-gel digestion, sample cleanup and mass spectrometric analysis was carried out as described previously (Dunn, J et al, 2018). For details please see **Appendix material & methods**.

Real-time PCR and data analysis

Real-time RT-PCR analysis was performed on a LightCycler 480 Real-Time system (Roche) for 45 cycles, using a SYBR Green I MasterMix (Roche, 04887352001) and primers. 36b4 gene was used as housekeeping gene. Analyses were performed using three technical replicates using the 2-ΔΔCt method.

Seahorse Mito Stress Test

3*10^3 of HPLFs per well were seeded into Seahorse XFe96 well plate (Agilent Technologies, 200941) for overnight. After 6 h and 48 h of viral infection, the medium was removed but a nominal 20 µl per well was left. Each well was washed twice with pre-warmed assay medium (Agilent Technologies, 103680). 80µl assay medium were added into each well, and cells were then incubated for 1 h at 37°C. Meanwhile, effector working solutions were prepared and loaded into ports of the XFe96 cartridge which was already rehydrated in XF buffer at 37°C overnight. The cartridge and the utility plate were inserted into XFe96 instrument to calibrate probes. Once the calibration was finished, the utility plate was replaced by cell plate and continued with the assay as indicated. When the progress was completed, cell plate was removed from the instrument. Medium was aspirated slowly from wells and all wells were gently washed with warmed assay buffer, Plates were stored at -20°C or continued with DNA assay for further normalization. Data were analyzed by Seahorse Analytics website and Wave software (Agilent Technologies, Version 2.6.3).

Statistics

Statistical analyses were performed using Prism software (GraphPad software, Version 9.4.1). Unpaired t-test was applied to all measurements. Data from Seahorse mito stress assay was analyzed by Seahorse Analytics website and Wave software (Agilent Technologies, Version 2.6.3). All quantification and real time RT-PCR results were presented using style of Mean and Standard Deviation (error bars). Observed differences were calculated for p-values: * $p<0.05$; ** $p<0.01$; ***: $p<0.001$; ****: $p<0.0001$.

Results

Human periodontal tissues and fibroblasts express SARS-CoV-2 receptors

To achieve robust evidence of the presence of SARS-CoV-2 receptors: ACE2 and TMPRSS2 in human periodontal tissue and cells, using immunofluorescence analysis, we confirmed that both ACE2 and TMPRSS2 were notably expressed in the gingiva epithelium, as well as in the periodontal ligament (PDL) cells (Figure 1B and C). By analyzing the cultured HPLF, we could also confirm the presence of the two receptors by immunofluorescence (Figure 1D) and western blotting analysis in those cells (Figure 1E). With an established collagen gel based 3D human gingiva tissue equivalent using gingival epithelial cells and HPLF (Appendix Figure 1A), we also observed consistent clear expression of ACE2 and TMPRSS2 both in the epithelial cells and PDL fibroblasts (Figure 1F).

SARS-CoV-2 has high affinity to PDL fibroblasts

We next explored the potentiality of SARS-CoV-2 in infecting PDL fibroblasts. By treating the cells with His Tag conjugated spike protein, followed by immunofluorescent analysis of the spike protein location using an anti-His Tag APC conjugated antibody (Appendix Figure 1B), we could observe clear association of the spike protein with the cells either under natural growing condition (Figure 1G), or in lentiviral mediated ACE2 overexpression condition (Figure 1H). The affinity of spike protein to the cells could be further validated by fluorescence activated cell sorting (FACS) analysis (Figure 1I and J). Therefore, we confirmed that SARS-CoV-2 indeed could infect PDL fibroblasts directly.

SARS-CoV-2 envelope and membrane proteins induce fibrotic pathogenic phenotypes in PDL fibroblasts

A key pathological hallmark of COVID-19 infection is fibrosis in the lung and potentially also in the other tissues (Spagnolo et al. 2020). To evaluate the consequence of COVID-19 infection on the PDL, we either adopted lentiviral mediated SARS-CoV-2 infection for envelope, membrane or nucleocapsid proteins (Gordon et al. 2020), or applied recombinant spike proteins at 500ng/ml or 5ug/ml, to cultured human PDL fibroblasts. We simulated acute and long infection by infecting or treating PDLs for 6 hours or 48 hours. Cell proliferation was evaluated using Bromodeoxyuridine (BrdU) incorporation followed by immunostaining for anti-BrdU antibodies. The results indicated that under our tested conditions, only membrane protein significantly increased cell proliferation at 6 hours, while at 48 hours, the envelope and membrane proteins could both elevate the BrdU incorporation index (Figure 2A and B; Appendix Figure 2A). Spike protein, on the contrary, could not modulate cell proliferation instead (Figure 2C and D; Appendix Figure 2B).

With Terminal deoxynucleotidyl transferase dUTP nick end labelling (TUNEL), we then evaluated apoptosis status in the cells. The results indicated that at 48 hours, again only the envelope and membrane proteins, but not the nucleocapsid nor spike proteins could increase apoptosis (Figure 2E-H; Appendix 3A and B). In the meanwhile, for cellular senescence status in the tested conditions, the results showed that at 6 and 48 hours, only the envelope and membrane protein groups resulted in a significant increase in senescent cells (Figure 2I-L; Appendix 4A and B).

We then investigated extracellular matrix production by focusing on Collagen I and MMP1, the two key components and enzymes responsible for PDL tissue integrity. Interestingly, western blotting analysis revealed that all the SARS-CoV-2 structure proteins could induce Collagen I production (Figure 3A-F), and reduce MMP1 production, spike protein elevated MMP1 expression under one of the two tested doses (Figure 3A-F). Real time RT-PCR analysis suggested the Collagen I expression induction and MMP1

downregulation were modulated at transcription levels (Figure 3G and H). By applying a hydrogel based 3D culture system, we evaluated Collagen I and MMP1 production and deposition at three dimensions. The results showed that Collagen I deposition were again highly elevated, especially in the envelope and membrane protein groups (Figure 3I and J). And membrane and nucleocapsid proteins could bring down the MMP1 expression (Figure 3K and L).

Together, with the evidence of elevated fibroblast proliferation, apoptosis and senescence concomitantly, alongside increased matrix deposition and reduced metalloprotease production, our results pointed out that the SARS-CoV-2's envelope and membrane were the most potent components to induce a fibrotic degeneration phenotype in PDL cells.

SARS-CoV-2 envelope and membrane proteins down-regulate mitochondrial β-oxidation

To understand the molecular regulation mechanisms behind the observed pathological consequence of SARS-CoV-2 infection, we performed proteomic analysis on the treated PDL fibroblasts, by focusing on the effects of the envelope, membrane and nucleocapsid proteins. We then identified a group of proteins that were both suppressed at 6 and 48 hours post infection (Figure 4A; Appendix Table 1). Among the significantly down-regulated proteins, the trifunctional enzyme subunit alpha, isoform 2 of very long-chain specific acyl-CoA dehydrogenase, cytochrome c oxidase subunit 2 and isoform cytoplasmic of fumarate hydratase are all essential enzymes in mitochondria functions and mitochondrial β-oxidation (Figure 4A). Particularly the trifunctional enzyme subunit alpha (HADHA), isoform 2 of very long-chain specific acyl-CoA dehydrogenase were connected with mitochondrial fatty acid

β-oxidation. In addition, western blotting analysis could further confirm that HADHA was indeed down-regulated by SARS-CoV-2 structural protein infection (Figure 4B-E).

We therefore conducted Seahorse Mito stress test (Appendix Figure 5) for evaluating if and how the mitochondria fatty acid pathway's function could be affected by SARS-CoV-2 infection. The results showed that indeed, both SARS-CoV-2 envelope and membrane protein, could inhibit fatty acid β-oxidation at both 6 hours and 48 hours' time points (Figure 4F and G).

Chemical inhibition of mitochondrial β-oxidation can mirror the fibrotic pathological consequence of SARS-CoV-2 infection

To validate the effect of fatty acid β-oxidation pathway inhibition, we next treated the cells with etomoxir, a specific inhibitor of the pathway through inhibiting carnitine palmitoyltransferase I (CPT1), a key regulatory enzyme for fatty acid to be imported into mitochondria (Figure 5A). The results indicated that etomoxir treatment could indeed mirror the same pathological consequence on the fibroblasts, similar to SARS-CoV-2 infection. We again observed significantly increased cell proliferation (Figure 5B; Appendix figure 6), apoptosis (Figure 5C; Appendix figure 6), and senescence (Figure 5D and E), together with elevated Collagen I production (Figure 5F and G). Similarly, in the hydrogel based three dimension PDL fibroblasts culture, Collagen I deposition was highly increased in the etomoxir treated samples (Figure 5H and I).

Discussion

COVID-19 infection can cause a series of symptoms. Among them, fibrosis particularly in lung tissues has evoked significant attention due to the severe consequence on patient life and health quality. Although the current dominant SARS-CoV-2 variants (such as the Omicron) induce milder symptoms in human bodies, the exact pathological consequence of COVID-19 to different human tissues and organs, particularly for oral cavity tissues are still missing, possibly due to the difficulty of distinguishing conventional periodontal diseases from COVID-19 connections. Current concepts of COVID-19 etiology suggest lung fibrosis caused by SARS-CoV-2 infection can be mainly due to damages on lung epithelial cells that trigger acute inflammation followed by fibroblast hyperproliferation (Merad and Martin 2020). However, as SARS-CoV-2 infection is rapid and it is difficult to distinguish if the deeper cells (such as fibroblasts) can also be infected directly, such as in oral cavity the epithelial barrier could be rapidly disrupted upon infection (Henin et al. 2022) . We therefore cannot neglect the potential direct infection consequence of SARS-CoV-2 on fibroblasts. In particular, PDL is one of the most vulnerable human tissues that extrinsic virus and bacteria can often enter PDL directly in pathological conditions (Kononen et al. 2019). Consistent with this concept, previous reports have shown that ACE2 expression were elevated in the periodontal fibroblasts under gingivitis and periodontitis conditions(Santos et al. 2015), and could be induced by lipopolysaccharide, inflammatory cytokines etc. (Sena et al. 2021). As such, it is reasonable to postulate that SARS-CoV-2 can also directly infect PDL fibroblasts in the already damaged PDL, and can induce further pathological changes or enhance existing periodontal lesions. Attentions therefore should be made by dental clinicians to the patients who got COVID-19 and appeared to be diagnosed with periodontal disease at the same time, particularly for those long COVID and repeated infected cases.

Our results also suggested SARS-CoV-2 infection indeed can directly induce fibrotic disease phenotypes in fibroblasts through distinct pathways. Mitochondrial fatty acid β-oxidation is the major pathway responsible for fatty acids degradation, hence is essential for human body energy homeostasis. Impeding the pathway can cause different disorders (Merritt et al. 2018). Very recent studies have observed mitochondrial dysregulation in COVID-19 patient blood cells (Ajaz et al. 2021; Guntur et al. 2022). Interestingly, the dysfunction of the fatty acid oxidation has been previously connected with fibrosis particularly in the lung and kidney (Geng et al. 2021; Jang et al. 2020){Merritt, 2018 #12}. For the first time, our findings further confirmed that in the fibroblasts, SARS-CoV-2 could induce fibrotic degeneration directly, through down-regulating fatty acid β-oxidation, particularly by the virus' envelope and membrane proteins.

Among the SARS-CoV-2's structural proteins: envelope, membrane, nucleocapsid and spike, the first three proteins are stable structure proteins for all the reported variants, while so far all of the identified mutations happen inside the spike proteins (Harvey et al. 2021). Although spike protein is still the target especially for COVID-19 vaccine development, increasing evidence suggest the other SARS-CoV-2 structural proteins might have unexpected important roles in inducing COVID-19 symptoms. Previous structural analysis of the envelope protein suggested it might be important for virus pathogenicity (Mandala et al. 2020). The envelope protein can also physically increase intra-Golgi pH and forms cation channel(Cabrera-Garcia et al. 2021), and biochemically modulate spike protein in the meantime (Boson et al. 2021). The most abundant protein: the membrane protein in the SARS-CoV-2 virus, is rationally important for virus assembly (Zhang et al. 2022). Our results further confirmed that the envelope and membrane proteins are actually responsible for the fibrosis phenotypes in the cells by down regulating the key fatty acid β-oxidation regulator

such as the trifunctional enzyme subunit alpha. The molecular mechanism behind this regulation axis would require further biochemical analysis.

In this study, our results provide novel mechanistic insights into how SARS-CoV-2 infection can affect human health, particularly for inducing fibrosis, at the cell and molecular level. The findings could be possibly extended to the other body systems to explain and explore the fibrosis pathology and treatment.

Acknowledgement

We would like to thank the helps provided by Dr Jane Carré for assisting Seahorse analysis, Dr Paul Waines for FACS operation, and Prof. Simon Whawell for critical reading. This study was supported by a research grant from the European Orthodontic Society to Bing Hu. Yan Gao received a fellowship from the Peninsula Dental Social Enterprise.

Author contributions

Yan Gao: Contributed to conception and design, acquisition, analysis, and interpretation, critically revised the manuscript.

Wai Ling Kok: Contributed to acquisition and analysis and critically revised the manuscript.

Vikram Sharma: Contributed to acquisition and analysis and critically revised the manuscript.

Charlotte Sara Illsley: Contributed to conception and design, and critically revised the manuscript.

Sally Hanks: Contributed to conception and design, and critically revised the manuscript.

Christopher Tredwin: Contributed to conception and design, and critically revised the manuscript.

Bing Hu: Contributed to conception and design, interpretation, and drafted and critically revised the manuscript.

All authors gave their final approval and agree to be accountable for all aspects of the work. The authors declare that there is no conflict of interest regarding the publication of this article.

Material and data availability statement

The materials used and datasets generated during and/or analyzed during the current study are available from Professor Bing Hu on reasonable request.

References

Ajaz S, McPhail MJ, Singh KK, Mujib S, Trovato FM, Napoli S, Agarwal K. 2021. Mitochondrial metabolic manipulation by sars-cov-2 in peripheral blood mononuclear cells of patients with covid-19. Am J Physiol Cell Physiol. 320(1):C57-C65.

Baghizadeh Fini M. 2020. Oral saliva and covid-19. Oral Oncol. 108:104821.

Boson B, Legros V, Zhou B, Siret E, Mathieu C, Cosset FL, Lavillette D, Denolly S. 2021. The sars-cov-2 envelope and membrane proteins modulate maturation and retention of the spike protein, allowing assembly of virus-like particles. J Biol Chem. 296:100111.

Cabrera-Garcia D, Bekdash R, Abbott GW, Yazawa M, Harrison NL. 2021. The envelope protein of sars-cov-2 increases intra-golgi ph and forms a cation channel that is regulated by ph. J Physiol. 599(11):2851-2868.

Ferretti L, Wymant C, Kendall M, Zhao L, Nurtay A, Abeler-Dorner L, Parker M, Bonsall D, Fraser C. 2020. Quantifying sars-cov-2 transmission suggests epidemic control with digital contact tracing. Science. 368(6491).

Geng J, Liu Y, Dai H, Wang C. 2021. Fatty acid metabolism and idiopathic pulmonary fibrosis. Front Physiol. 12:794629.

Gordon DE, Jang GM, Bouhaddou M, Xu J, Obernier K, O'Meara MJ, Guo JZ, Swaney DL, Tummino TA, Huttenhain R et al. 2020. A sars-cov-2-human protein-protein interaction map reveals drug targets and potential drug-repurposing. bioRxiv.

Guntur VP, Nemkov T, de Boer E, Mohning MP, Baraghoshi D, Cendali FI, San-Millan I, Petrache I, D'Alessandro A. 2022. Signatures of mitochondrial dysfunction and impaired fatty acid metabolism in plasma of patients with post-acute sequelae of covid-19 (pasc). Metabolites. 12(11).

Harvey WT, Carabelli AM, Jackson B, Gupta RK, Thomson EC, Harrison EM, Ludden C, Reeve R, Rambaut A, Consortium C-GU et al. 2021. Sars-cov-2 variants, spike mutations and immune escape. Nat Rev Microbiol. 19(7):409-424.

Henin D, Pellegrini G, Carmagnola D, Lanza Attisano GC, Lopez G, Ferrero S, Amendola A, De Angelis D, Tanzi E, Dellavia C. 2022. Morphological and immunopathological aspects of lingual tissues in covid-19. Cells. 11(7).

Hoffmann M, Kleine-Weber H, Schroeder S, Kruger N, Herrler T, Erichsen S, Schiergens TS, Herrler G, Wu NH, Nitsche A et al. 2020. Sars-cov-2 cell entry depends on ace2 and tmprss2 and is blocked by a clinically proven protease inhibitor. Cell. 181(2):271-280 e278.

Huang N, Perez P, Kato T, Mikami Y, Okuda K, Gilmore RC, Conde CD, Gasmi B, Stein S, Beach M et al. 2021. Sars-cov-2 infection of the oral cavity and saliva. Nat Med. 27(5):892-903.

Huang Y, Yang C, Xu XF, Xu W, Liu SW. 2020. Structural and functional properties of sars-cov-2 spike protein: Potential antivirus drug development for covid-19. Acta Pharmacol Sin. 41(9):1141-1149.

Jang HS, Noh MR, Kim J, Padanilam BJ. 2020. Defective mitochondrial fatty acid oxidation and lipotoxicity in kidney diseases. Front Med (Lausanne). 7:65.

Kononen E, Gursoy M, Gursoy UK. 2019. Periodontitis: A multifaceted disease of tooth-supporting tissues. J Clin Med. 8(8).

Lopez-Leon S, Wegman-Ostrosky T, Perelman C, Sepulveda R, Rebolledo PA, Cuapio A, Villapol S. 2021. More than 50 long-term effects of covid-19: A systematic review and meta-analysis. Sci Rep. 11(1):16144.

Mandala VS, McKay MJ, Shcherbakov AA, Dregni AJ, Kolocouris A, Hong M. 2020. Structure and drug binding of the sars-cov-2 envelope protein transmembrane domain in lipid bilayers. Nat Struct Mol Biol. 27(12):1202-1208.

Merad M, Martin JC. 2020. Pathological inflammation in patients with covid-19: A key role for monocytes and macrophages. Nat Rev Immunol. 20(6):355-362.

Merritt JL, 2nd, Norris M, Kanungo S. 2018. Fatty acid oxidation disorders. Ann Transl Med. 6(24):473.

Ni W, Yang X, Yang D, Bao J, Li R, Xiao Y, Hou C, Wang H, Liu J, Yang D et al. 2020. Role of angiotensin-converting enzyme 2 (ace2) in covid-19. Crit Care. 24(1):422.

Pandiar D, Ramani P, Krishnan RP, Y D. 2022. Histopathological analysis of soft tissue changes in gingival biopsied specimen from patients with underlying corona virus disease associated mucormycosis (cam). Med Oral Patol Oral Cir Bucal. 27(3):e216-e222.

Qi X, Northridge ME, Hu M, Wu B. 2022. Oral health conditions and covid-19: A systematic review and meta-analysis of the current evidence. Aging Health Res. 2(1):100064.

Santos CF, Morandini AC, Dionisio TJ, Faria FA, Lima MC, Figueiredo CM, Colombini-Ishikiriama BL, Sipert CR, Maciel RP, Akashi AP et al. 2015. Functional local renin-angiotensin system in human and rat periodontal tissue. PLoS One. 10(8):e0134601.

Satarker S, Nampoothiri M. 2020. Structural proteins in severe acute respiratory syndrome coronavirus-2. Arch Med Res. 51(6):482-491.

Sena K, Furue K, Setoguchi F, Noguchi K. 2021. Altered expression of sars-cov-2 entry and processing genes by porphyromonas gingivalis-derived lipopolysaccharide, inflammatory cytokines and prostaglandin e(2) in human gingival fibroblasts. Arch Oral Biol. 129:105201.

Spagnolo P, Balestro E, Aliberti S, Cocconcelli E, Biondini D, Casa GD, Sverzellati N, Maher TM. 2020. Pulmonary fibrosis secondary to covid-19: A call to arms? Lancet Respir Med. 8(8):750-752.

Wang J, Kaperak C, Sato T, Sakuraba A. 2021. Covid-19 reinfection: A rapid systematic review of case reports and case series. J Investig Med. 69(6):1253-1255.

Wang T, Du Z, Zhu F, Cao Z, An Y, Gao Y, Jiang B. 2020. Comorbidities and multi-organ injuries in the treatment of covid-19. Lancet. 395(10228):e52.

Wise J. 2022. Covid-19: Two million people in the uk are estimated to be experiencing long covid, says ons. BMJ. 377:o1391.

Zhang Z, Nomura N, Muramoto Y, Ekimoto T, Uemura T, Liu K, Yui M, Kono N, Aoki J, Ikeguchi M et al. 2022. Structure of sars-cov-2 membrane protein essential for virus assembly. Nat Commun. 13(1):4399.

Figure legends

Figure 1. Human periodontal cells express ACE2 and TMPRSS2, and prone to SARS-CoV-2 infection.

A. Illustration of SARS-CoV-2's key structure proteins;

B and C. Immunofluorescence analysis of ACE2 or TMPRSS2 co-expression with Vimentin in human periodontal tissues. using specific antibodies and Alexa 568 (red) or Alexa 488 (green) conjugated secondary antibodies. Dotted lines mark epithelia-mesenchymal junctions. Arrows indicate typical clusters of fibroblasts with co-expression of the indicated markers.

D. Immunofluorescence analysis of ACE2 or TMPRSS2 in human periodontal ligament fibroblasts (HPLF).

E. Western blotting analysis of ACE2 and TMPRSS2 expression in human periodontal ligament fibroblasts (HPLF) under normal growing condition, and lentiviral mediated ACE2 overexpression. Lamin B1 was used as loading control. All the blots were performed sequentially on the same membrane.

F. Immunofluorescence analysis of ACE2 or TMPRSS2 in human gingiva equivalent (also see Appendix Figure 1A).

G and H. Normal HPLF or the cells with ACE2 overexpression was treated with His tagged spike (S) protein first then traced using Anti-His Tag APC conjugated antibodies. For controls, the spike protein was omitted (also see Appendix Figure 1B).

I and J: FACS analysis of the samples showed in E and F. Note the anti-His Tag APC antibody did show background but the shifting of the florescence peak could still be visualized (H). n: particle (cell) count.

Bars: 100um

Figure 2. SARS-CoV-2 envelope and membrane protein could induce PDL fibroblast proliferation, apoptosis and senescence.

A-D. BrdU incorporation analysis on the PDL fibroblasts treated with indicated conditions and time. Each data dot represent one random field in triplicated samples. Dunnett's test was used for statistical analysis. Representative images can be found from Appendix Figure 2.

E-H. TUNEL analysis on the PDL fibroblasts treated with indicated conditions and time. Each data dot represent one random field in triplicated samples. Dunnett's correction was used for statistical analysis. Representative images can be found from Appendix Figure 3.

I-L. Quantification of senescence-associated β-galactosidase positive cells (for identifying senescence) images on the indicated conditions. Each data dot represent one random field in triplicated samples. Representative images can be found from Appendix Figure 4.

ns: no significance; ** $p<0.01$; ***: $p<0.001$.

Figure 3. SARS-CoV-2 infection could induce collagen matrix deposition and MMP1 reduction.

A-F. Western blotting analysis of Collagen I and MMP1 production in the cells under indicated conditions. A shows blotting results. B and C represents statistical analysis (each dot represents a single individual measurement). Dunnett's test was used for statistical analysis.

ns: no significance;

G and H. Real time RT-PCR analysis of Collagen 1 and MMP1 transcription in the indicated conditions.

I-L. Representative three dimensional analysis of Collagen I and MMP1 expression in the indicated conditions at 7 days after seeding the cells and infection in the hydrogel. The gel were stained using anti-Collagen I and MMP1 specific antibodies and developed with Alexa

568 (red) or 488 (Green) conjugated secondary antibodies. Each data dot represent one random field in triplicated samples.

ns: no significance; * $p<0.05$; ** $p<0.01$; ***: $p<0.001$; ****: $p<0.0001$.

Bars: 100um

Figure 4. Envelope and membrane proteins are responsible to SARS-CoV-2 infection to PDL fibroblasts caused deregulate of mitochondria fatty acid β-oxidation pathway.

A. Summary of proteomic analysis results of PDL fibroblasts treated with indicated conditions and time points. Only proteins showed <0.50 or >1.5 fold changes were included. For full data analysis please see Appendix Table 1.

B-E. Western blotting analysis of HADHA expression in HPLF treated under indicated viral infection conditions either for 6 hours (B and C), or 48 hours (D and E). C and E represent statistical analysis (each dot represents a single individual measurement). ***: $p<0.001$; ****: $p<0.0001$. Lamin B1 was used as loading control. All the blots were performed sequentially on the same membrane.

F and G. 6 and 48 hours Seahorse palmitate oxidation stress tests under indicated conditions either with vehicle alone or Etomoxir. Note for both time points, envelope group were down-regulated with/without etomoxir treatments, while membrane group also showed down regulation but only in the etomoxir treated samples.

Figure 5. Mitochondrial fatty acid β-oxidation inhibition mirrored fibrotic degeneration phenotypes in PDL fibroblasts.

A. Schematic drawing of fatty acid β-oxidation pathway (left) and the Etomoxir functioning mechanism (right).

B and C. BrdU and TUNEL analysis of etomoxir treated cells. For representative images please see Appendix Figure 6. Each data dot represent one random field in triplicated samples.

D and E. Representative senescence-associated β-galactosidase assay on indicated conditions. Note increased senescence in the etomoxir treated samples. Each data dot represent one random field in triplicated samples.

F and G. Western blotting analysis of Collagen I expression in HPLF under etomoxir treatment or vehicle (DMSO) alone. Lamin B1 was used as loading control. All the blots were performed sequentially on the same membrane. G represents statistical analysis (each dot represents a single individual measurement).

H and I. Representative 3D analysis of Collagen I expression in the indicated conditions at 48 hours after seeding the cells and etomoxir treatment in the hydrogel. The gel was stained using anti-Collagen I specific antibodies and developed with Alexa 568 (red) conjugated secondary antibodies. Each data dot represent one random field in triplicated samples.

* $p<0.05$; ** $p<0.01$; ***: $p<0.001$; ****: $p<0.0001$.

Bars: 100um

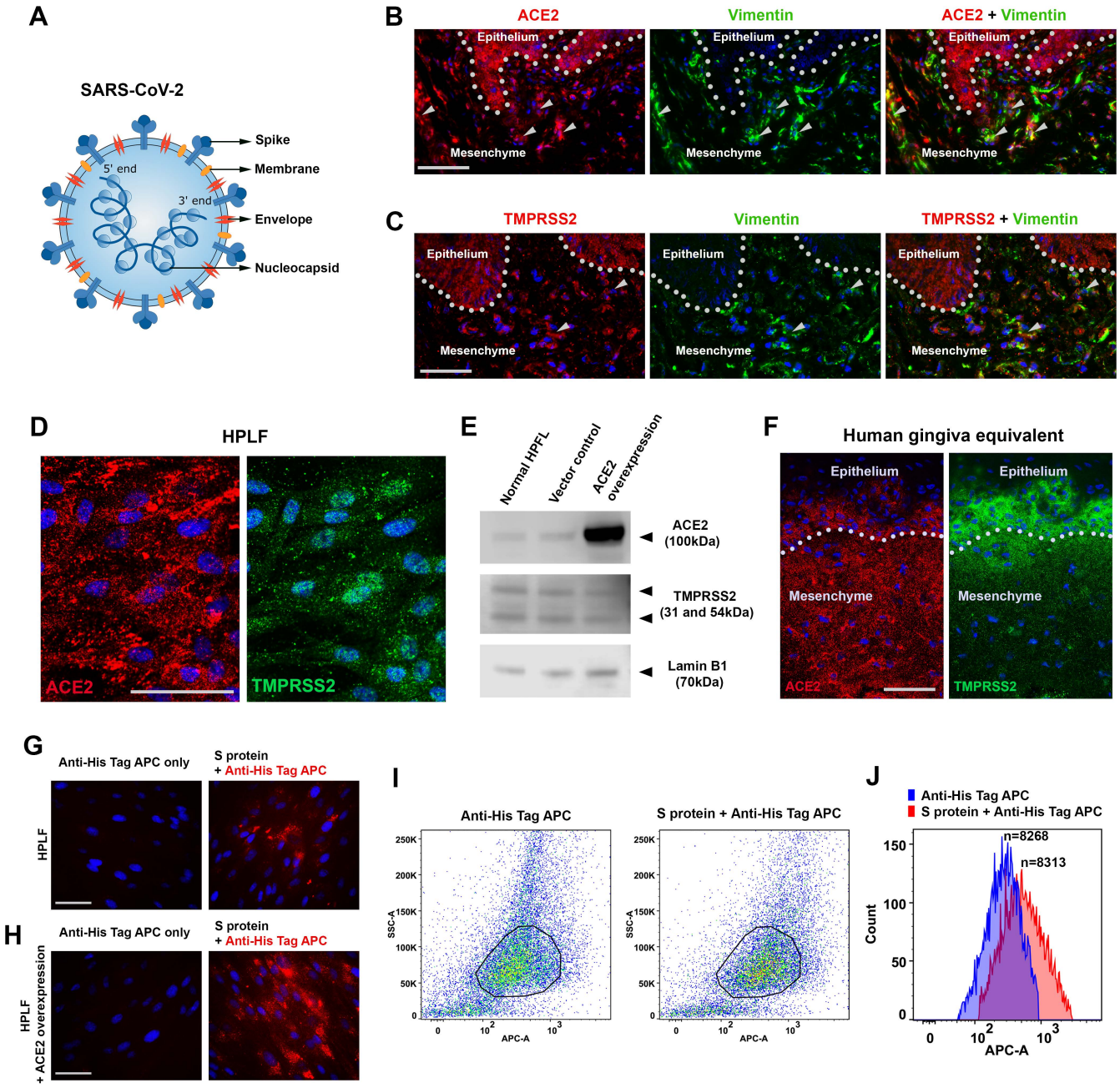
A
SARS-CoV-2
5' end
3' end
Spike
Membrane
Envelope
Nucleocapsid
B
ACE2
Vimentin
ACE2 + Vimentin
Epithelium
Mesenchyme
C
TMPRSS2
Vimentin
TMPRSS2 + Vimentin
Epithelium
Mesenchyme
D
HPLF
ACE2
TMPRSS2
E
Normal HPFL
Vector control
ACE2 overexpression
ACE2 (100kDa)
TMPRSS2 (31 and 54kDa)
Lamin B1 (70kDa)
F
Human gingiva equivalent
Epithelium
Mesenchyme
ACE2
TMPRSS2
G
Anti-His Tag APC only
S protein + Anti-His Tag APC
HPLF
H
Anti-His Tag APC only
S protein + Anti-His Tag APC
HPLF + ACE2 overexpression
I
Anti-His Tag APC
S protein + Anti-His Tag APC
SSC-A
APC-A
J
Anti-His Tag APC
S protein + Anti-His Tag APC
n=8268
n=8313
Count
APC-A

Figure 1

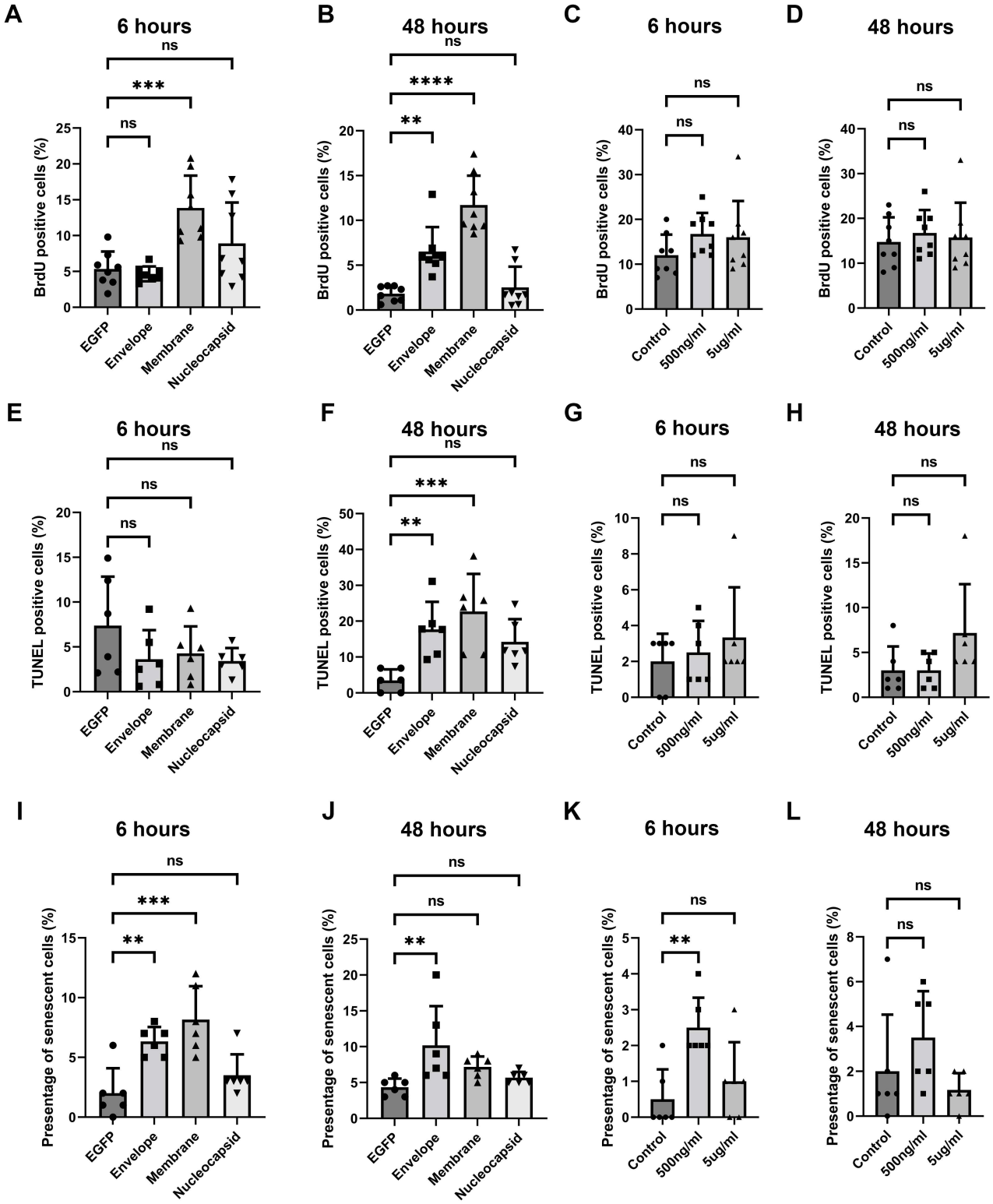
A
6 hours
ns
***
ns
BrdU positive cells (%)
EGFP
Envelope
Membrane
Nucleocapsid
B
48 hours
ns
****
**
BrdU positive cells (%)
EGFP
Envelope
Membrane
Nucleocapsid
C
6 hours
ns
ns
BrdU positive cells (%)
Control
500ng/ml
5ug/ml
D
48 hours
ns
ns
BrdU positive cells (%)
Control
500ng/ml
5ug/ml
E
6 hours
ns
ns
ns
TUNEL positive cells (%)
EGFP
Envelope
Membrane
Nucleocapsid
F
48 hours
ns
***
**
TUNEL positive cells (%)
EGFP
Envelope
Membrane
Nucleocapsid
G
6 hours
ns
ns
TUNEL positive cells (%)
Control
500ng/ml
5ug/ml
H
48 hours
ns
ns
TUNEL positive cells (%)
Control
500ng/ml
5ug/ml
I
6 hours
ns
***
**
Presentage of senescent cells (%)
EGFP
Envelope
Membrane
Nucleocapsid
J
48 hours
ns
ns
**
Presentage of senescent cells (%)
EGFP
Envelope
Membrane
Nucleocapsid
K
6 hours
ns
**
Presentage of senescent cells (%)
Control
500ng/ml
5ug/ml
L
48 hours
ns
ns
Presentage of senescent cells (%)
Control
500ng/ml
5ug/ml

Figure 2

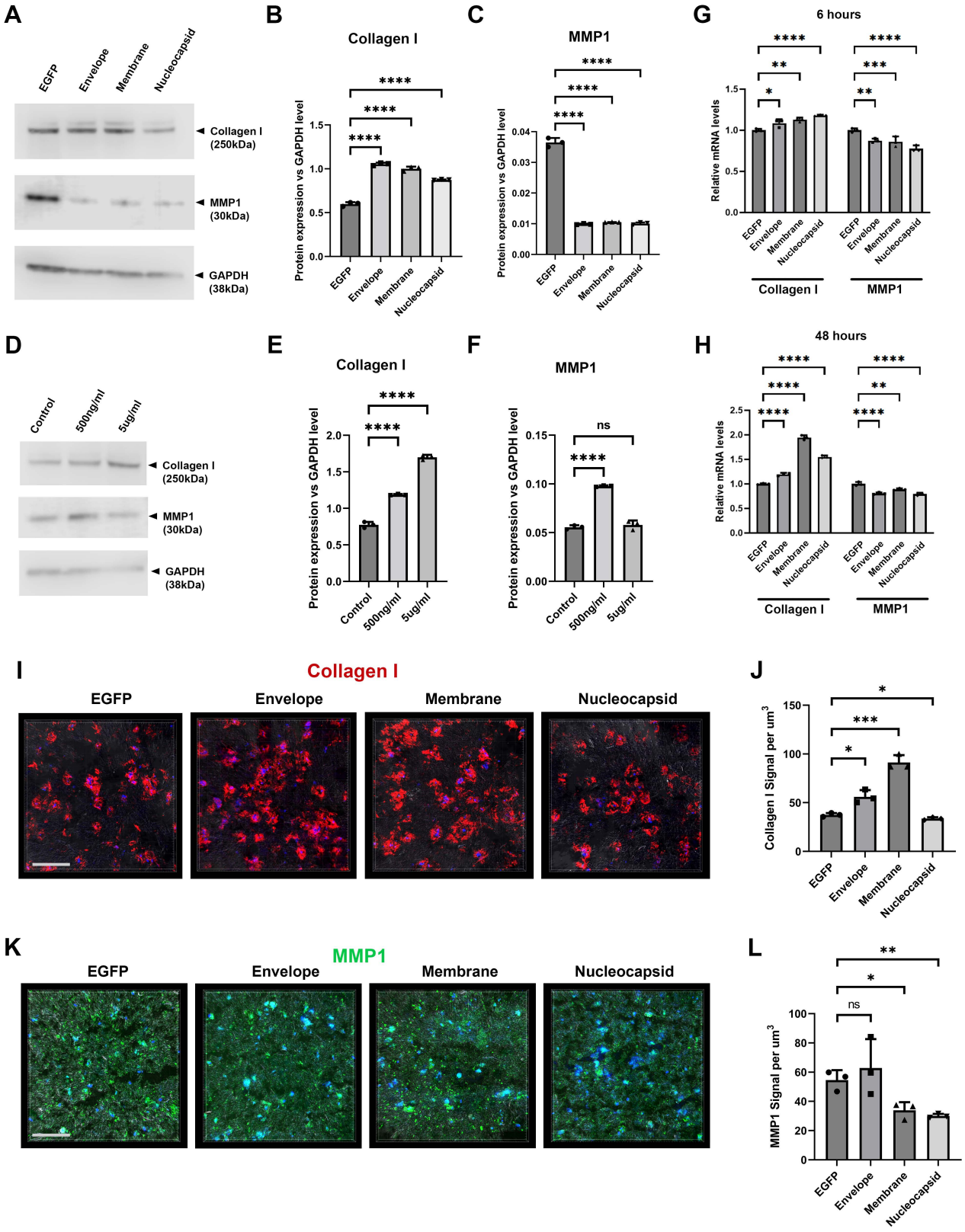
A
EGFP
Envelope
Membrane
Nucleocapsid
Collagen I (250kDa)
MMP1 (30kDa)
GAPDH (38kDa)
B
Collagen I
Protein expression vs GAPDH level
C
MMP1
Protein expression vs GAPDH level
G
6 hours
Relative mRNA levels
Collagen I
MMP1
D
Control
500ng/ml
5ug/ml
Collagen I (250kDa)
MMP1 (30kDa)
GAPDH (38kDa)
E
Collagen I
Protein expression vs GAPDH level
F
MMP1
Protein expression vs GAPDH level
ns
H
48 hours
Relative mRNA levels
I
Collagen I
EGFP
Envelope
Membrane
Nucleocapsid
J
Collagen I Signal per um3
K
MMP1
EGFP
Envelope
Membrane
Nucleocapsid
L
MMP1 Signal per um3
ns

Figure 3

A

Protein expression levels (based on proteomic analysis results)

	Envelope vs. EGFP		Membrane vs. EGFP		Nucleocapsid vs. EGFP	
	6h	48h	6h	48h	6h	48h
Proteasome subunit beta type-2	0.37	0.30				
Trifunctional enzyme subunit alpha (HADHA)	0.38	0.25	0.45	0.14		
60S ribosomal protein L29	2.47	2.21				
Isoform 2 of Very long-chain specific acyl-CoA dehydrogenase			0.19	0.09		
60S ribosomal protein L27a			0.22	0.16		
Isoform 2 of Ran-specific GTPase-activating protein			0.34	0.43		
Tubulin beta-2A chain					0.36	0.36
Cytochrome c oxidase subunit 2					0.37	0.21
Isoform Cytoplasmic of Fumarate hydratase					0.45	0.27

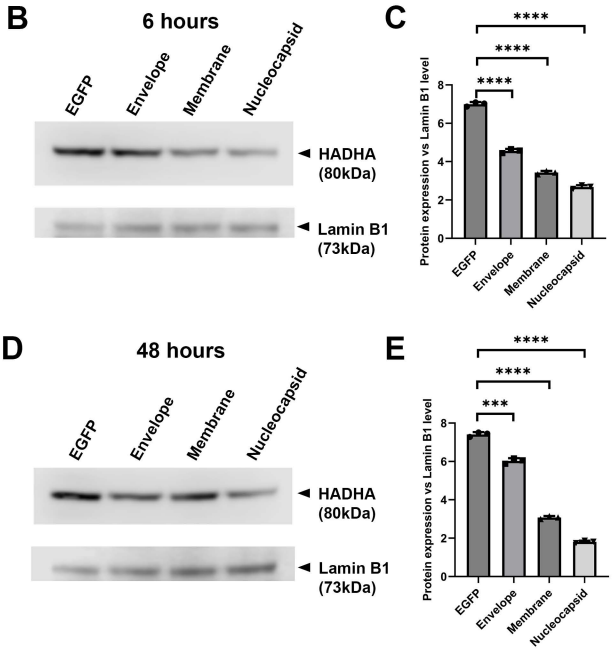

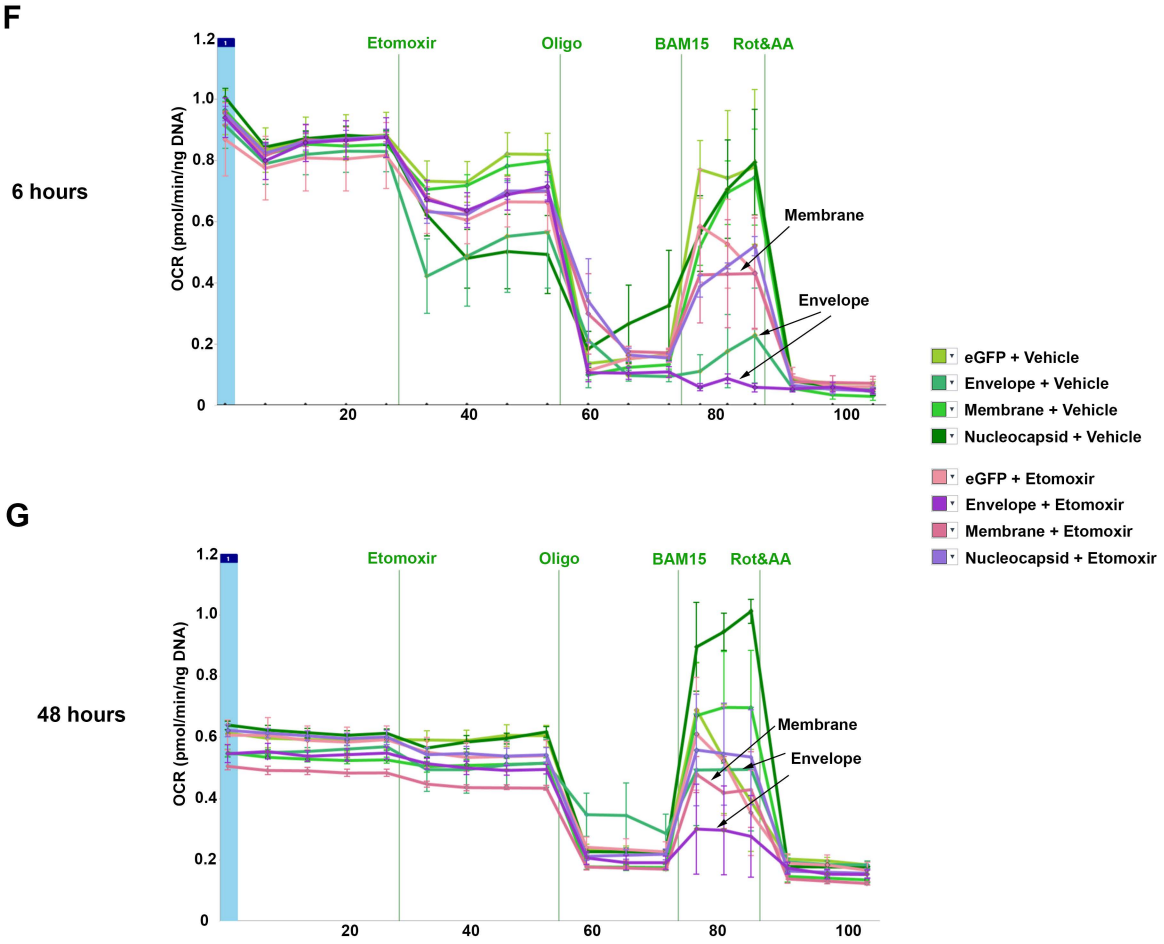

Figure 4

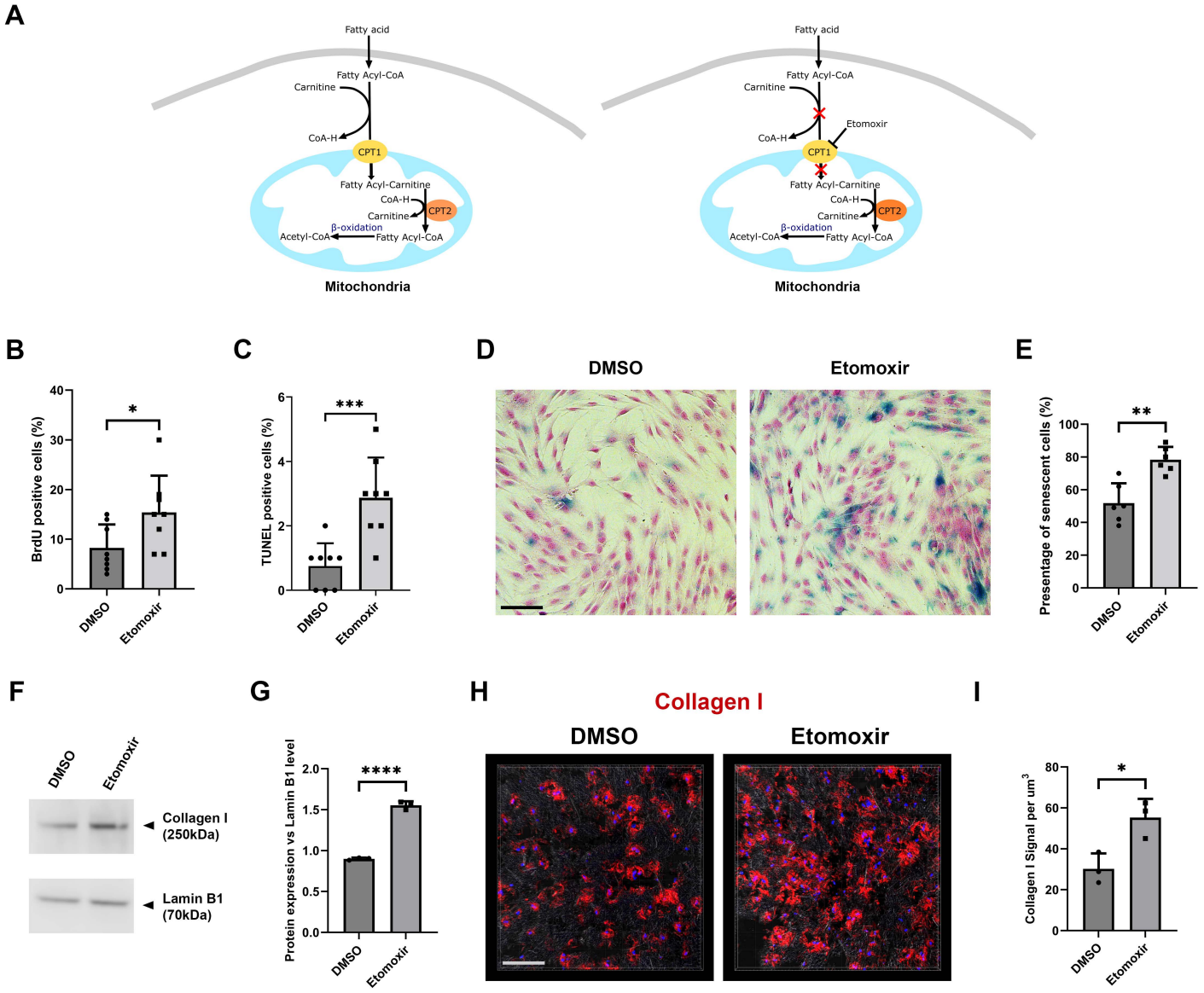
A
Fatty acid
Fatty Acyl-CoA
Carnitine
CoA-H
CPT1
Fatty Acyl-Carnitine
CoA-H
Carnitine
CPT2
β-oxidation
Acetyl-CoA
Fatty Acyl-CoA
Mitochondria
Etomoxir
B
BrdU positive cells (%)
DMSO
Etomoxir
C
TUNEL positive cells (%)
D
DMSO
Etomoxir
E
Presentage of senescent cells (%)
F
Collagen I (250kDa)
Lamin B1 (70kDa)
G
Protein expression vs Lamin B1 level
H
Collagen I
I
Collagen I Signal per um3

Figure 5

SARS-CoV-2 causes periodontal fibrosis by deregulating mitochondrial β-oxidation

Yan Gao[1], Wai Ling Kok[1], Vikram Sharma[2], Charlotte Sara Illsley[1], Sally Hanks[1], Christopher Tredwin[1], Bing Hu[1*]

1. Stem Cells & Regenerative Medicine Laboratory, Peninsula Dental School, Faculty of Health, University of Plymouth, 16 Research Way, Plymouth, PL6 8BU, UK

2. School of Biomedical Sciences, Faculty of Health, University of Plymouth, 16 Research Way, Plymouth, PL6 8BU, UK

* Corresponding author

Professor Bing Hu

Email: bing.hu@plymouth.ac.uk

Appendix Materials & Methods

Appendix Figure 1 to 6

Appendix Table 1 and 2

Appendix Materials & Methods

Immunostaining

Human oral cavity cancer tissue array that contains normal human gingiva tissues, HnTMA108 was purchased from Creative Bioarray. Slides were heated to 60°C for 20 min before being twice washed in xylenes (Sigma Aldrich 534056) for 10 mins. rehydrated with 100% industrial methylated spirit (IMS) (VWR, 23684.360) for 5 min, before being washed for 2 min in 95% IMS and then 70% IMS. Antigen retrieval was performed by 95°C water bath, slide was submerged in pre-warmed 0.01 M citrate buffer solution (citric acid (Sigma Aldrich, C2404) & 0.05% Tween-20 (Sigma Aldrich, P9416)), pH 8.0 for 20 min. Slide was washed briefly in tap water before washed 3 times in phosphate buffered saline (PBS, Sigma, P4417) containing 0.1% Triton-X100, (Sigma, X100) (PBST) for 5 min per wash. Non-Specific binding was blocked by incubation for 60 min with PBST containing 5% Donkey Serum (Sigma, D9663). Primary antibodies were incubated overnight at 4°C. Slide was washed 3 times in PBST before incubation with secondary antibodies for 2 h at room temperature. Nuclei were counterstained with 2 µg/ml DAPI (Sigma Aldrich, D9542) for 10 min then slide was mounted with Dako fluorescent mounting medium (Dako North America Inc., S3023). IF images were captured using a Leica DMI6000 confocal microscope with a Leica TCS SP8 attachment at a scanning thickness of 1 µm per section. The microscope is running LAS X (Leica, Version 3.7.3.23245) software from Leica. Images for comparison were taken using the same settings and post imaging processing was conducted using Adobe Photoshop (Adobe, Version 24.0.1).

For frozen section, the slides were air-dried for 1 h then fixed with 4% paraformaldehyde (PFA; Sigma in PBS) for 30 min, then washed twice with PBST 5 min each. Primary antibodies were incubated overnight at 4°C. Slides were washed three times in PBST before incubation with secondary antibodies for 2 h at room temperature. Nuclei were counterstained with 2 µg/ml DAPI for 10 min.

Images were captured using a Leica DMI6000 confocal microscope with a Leica TCS SP8 attachment. The microscope is running LAS X (Leica, Version 3.7.3.23245) software. Images for

comparison were taken using the same settings and post imaging processing was conducted using Adobe Photoshop (Adobe, Version 24.0.1). Images of 3D equivalents were visualized by Imaris software (Bitplane, Version 9.0.2).

BrdU incorporation assay

5*10^3 of HPLFs were seeded into a black 96 well plate (GBO, 655090). After the spike protein treatment or lentiviral infection, BrdU cell prolife labelling reagent (Amersham-GE, RPN201, 1:1000) was diluted in complete cell culture medium then added into dishes for 2-3 h. Cells were washed 3 more times with PBS for 2 min each, then fixed in 4% PFA for 30 min followed by washing twice in PBS. Cells were treated with 100 µl 2N hydrochloric acid (HCl) (Sigma, H1758-100ml) for 30 min before they were stained with anti-BrdU antibody (Abcam, ab6326, 1:500). The antibody staining procedures were exactly as above except that the blocking buffer was prepared with 2.5% bovine serum albumin (BSA) (Sigma. A2153) in PBST. Images were processed in Image J software (National Institutes of Health, Bethesda, MD, USA, Version 1.53k). BrdU-positive cells and total cell number were quantified using 'Analyze Particles' function.

Terminal deoxynucleotidyl transferase dUTP nick end labelling (TUNEL) assay

5*10^3 of HPLFs were seeded into black 96 well plate. After the spike protein treatment or lentiviral infection, cells were washed briefly for 5 sec in PBS twice, then fixed in 4% PFA for 30 min and washed twice in PBS 5 min each. Cells were permeabilized by PBST for 2 min on ice then incubated in 50 µl TUNEL mixture (In Situ Cell Death Detection Kit, Fluorescein, version 17, Roche) for 2 h at 37°C in humid atmosphere. After the washing and mounting, images were taken by Leica IM8 conducted using Adobe Photoshop.

Senescence assay

5*10^4 of HPLFs were seeded in 24 well plate. After the spike protein treatment or lentiviral infection, cells were washed briefly with PBS, the fixative solution from the senescence kit (Senescence b-galactosidase kit, Cell Signalling, 9860S) was added to each well for 15 min at room temperature. Cells were rinsed 2 times with PBS then β-Galactosidase Staining Solution, pH 6.0, was added into each well, and at the meantime pH 4.0 was added into spare wells as positive control. The plate was incubated at 37°C at least overnight in a dry incubator without CO_2. Cells were washed twice with PBS then stained with nuclear fast red solution (Sigma, N8002) for 20 min then washed with distilled H_2O. All wells were mounted with 70% glycerol (Sigma, G2025) and images were taken with Leica IM8 conducted using Adobe Photoshop.

Proteomic analysis

HPLFs were seeded in 6cm dishes and performed viral infection and protein treatment for 6 h and 48 h. To collect protein after each time points, culture media was removed from the culture dishes and cells were washed in pre-cooled HBSS twice. HBSS was removed and replaced with ice-cold RIPA buffer (ThermoFisher, 89901) supplemented with Halt™ Protease and Phosphatase Inhibitor Cocktail (ThermoFisher , 78440) at 1:100. The cells were detached from the dish using a cell scraper and then collected into an Eppendorf tube on ice then incubated for 30 min with frequent agitation for efficient cell lysis and solubilisation of proteins. Tubes were spun down at 15,000 rpm for 15 min at 4°C so the supernatant containing the protein could be collected and stored at -80°C until ready to load onto a gel. 15 µg protein samples were run on a Nupage 4-12% Bis-Tris protein gel at 200V for 45 min. Gel was rinsed with water before fixing in 40% ethanol and 10% acetic acid for 15 min with gentle agitation. After washing the gel twice in water, the gel was stained overnight in QC colloidal Coomassie Blue G-250 (Biorad, 161-0803). The gel was destained for 1 h with changes of water every 15 min until protein bands were visible. Every sample lane was cut into 4 fractions and each fraction further cut into 1-2 mm cubes for equilibration. In-gel digestion, sample cleanup and mass

spectrometric analysis was carried out as described previously (Dunn, J et al, 2018). All samples were stored at -20°C or analyze directly using mass spectrometry.

Appendix Figures

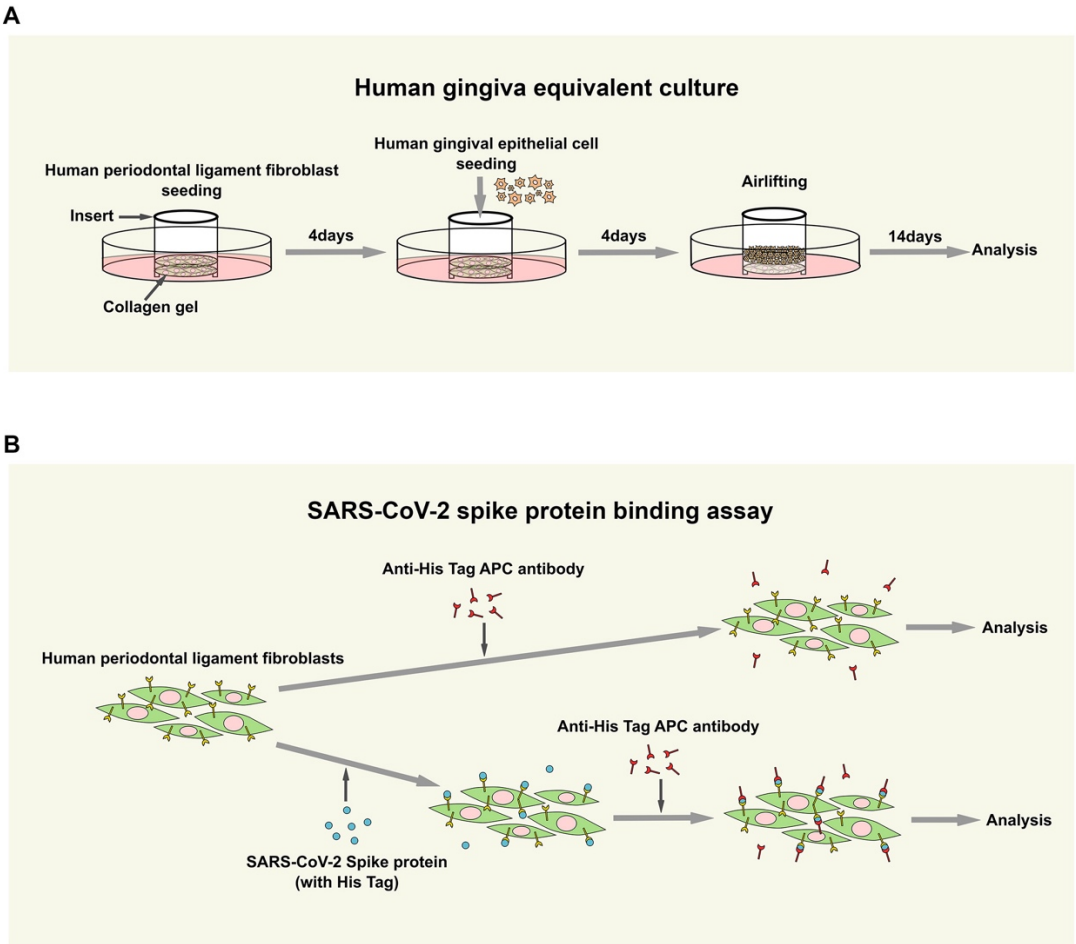

Appendix Figure 1. Illustration of human gingiva equivalent culture and spike protein binding assay.

A. For human gingiva equivalent culture, HPLF were seeded into collagen gel supported by a cell culture insert cylinder. 4 days later human gingival epithelial cells were seeded on top of the culture. After a further 4 days, the culture were lifted to air-liquid interface to allow stratification for 14 days before further analysis.

B. To test the binding of spike protein to HPLF cells, the cells were treated with His Tag conjugated spike protein first then traced using anti-His Tag APC conjugated antibodies. For control, the spike proteins were omitted.

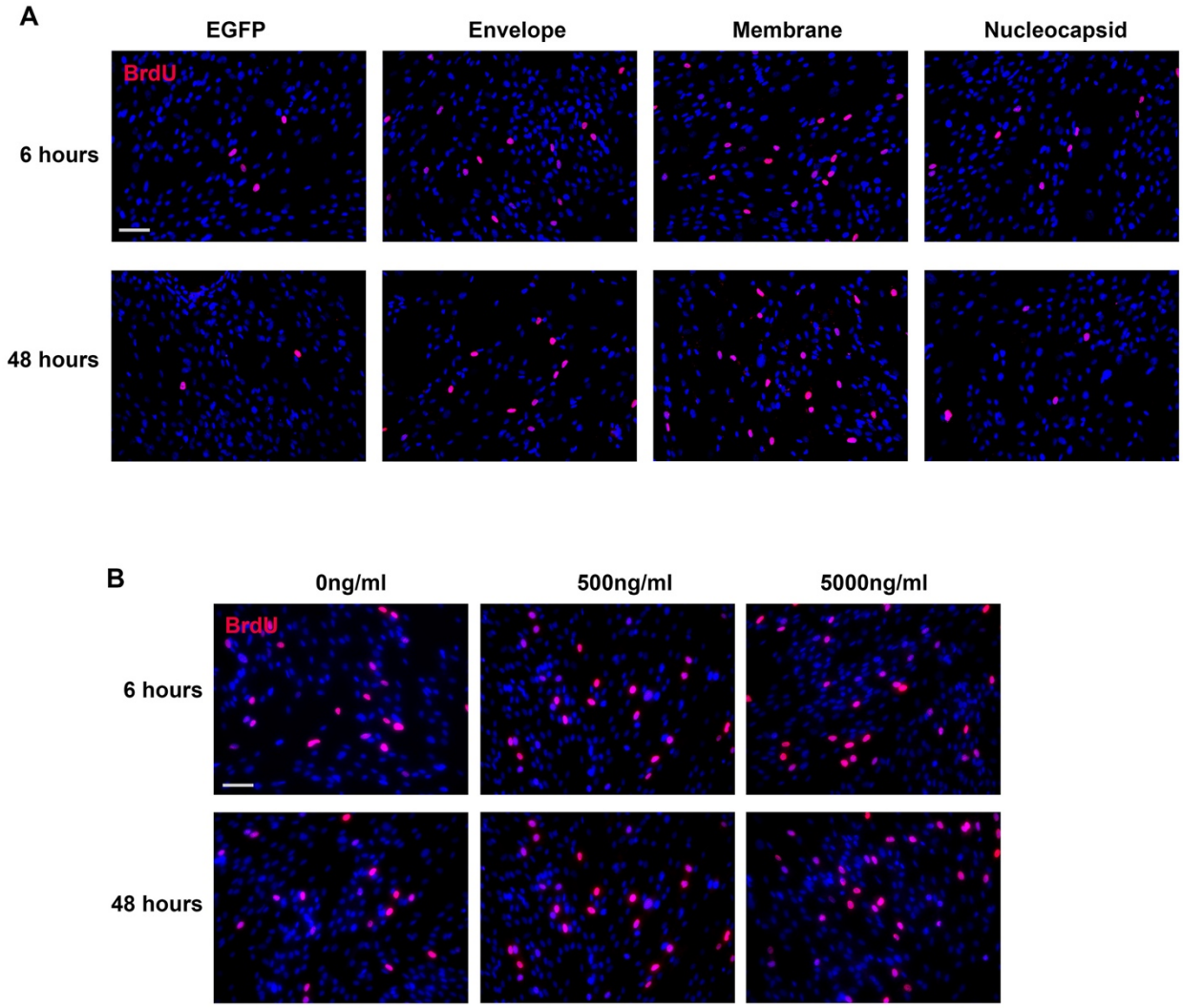

Appendix Figure 2. SARS-CoV-2 envelope and membrane protein could induce PDL fibroblast proliferation.

Representative field images of BrdU incorporation analysis in the indicated conditions. Quantitative analysis can be found from Figure 2 A-D.

Bars: 100um

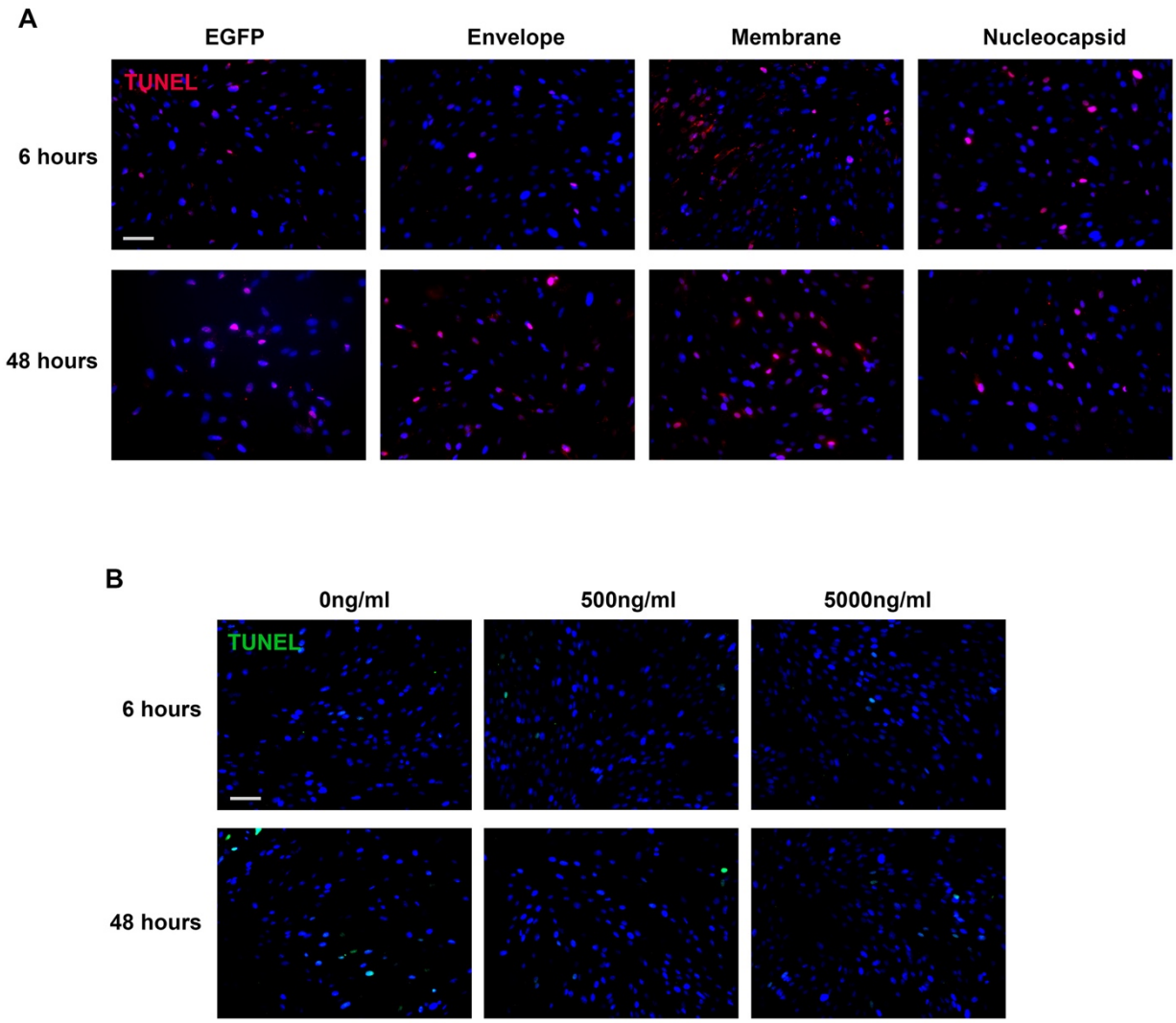

Appendix Figure 3. SARS-CoV-2 envelope and membrane protein could induce PDL fibroblast apoptosis.

Representative field images of TUNEL analysis in the indicated conditions. Quantitative analysis can be found from Figure 2 E-H.

Bars: 100um

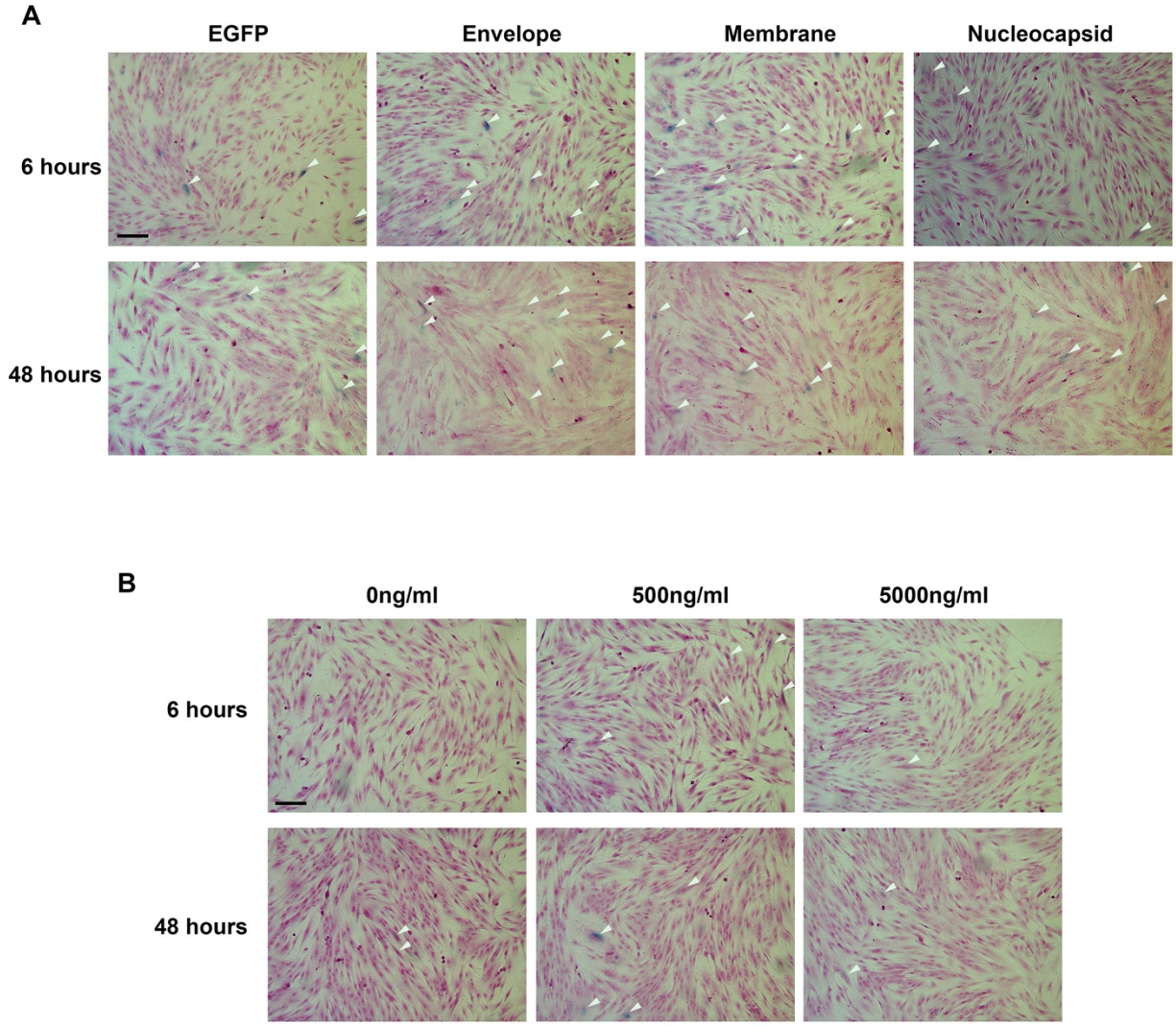

Appendix Figure 4. SARS-CoV-2 envelope and membrane protein could induce PDL fibroblast senescence.

Representative field images of senescence analysis in the indicated conditions. The cells were countered stained with nuclear fast red. Note increased blue staining (marking senescent cells) in the envelope and membrane groups. Quantitative analysis can be found from Figure 2 I-L. White arrows indicate representative positive cells.

Bars: 100um

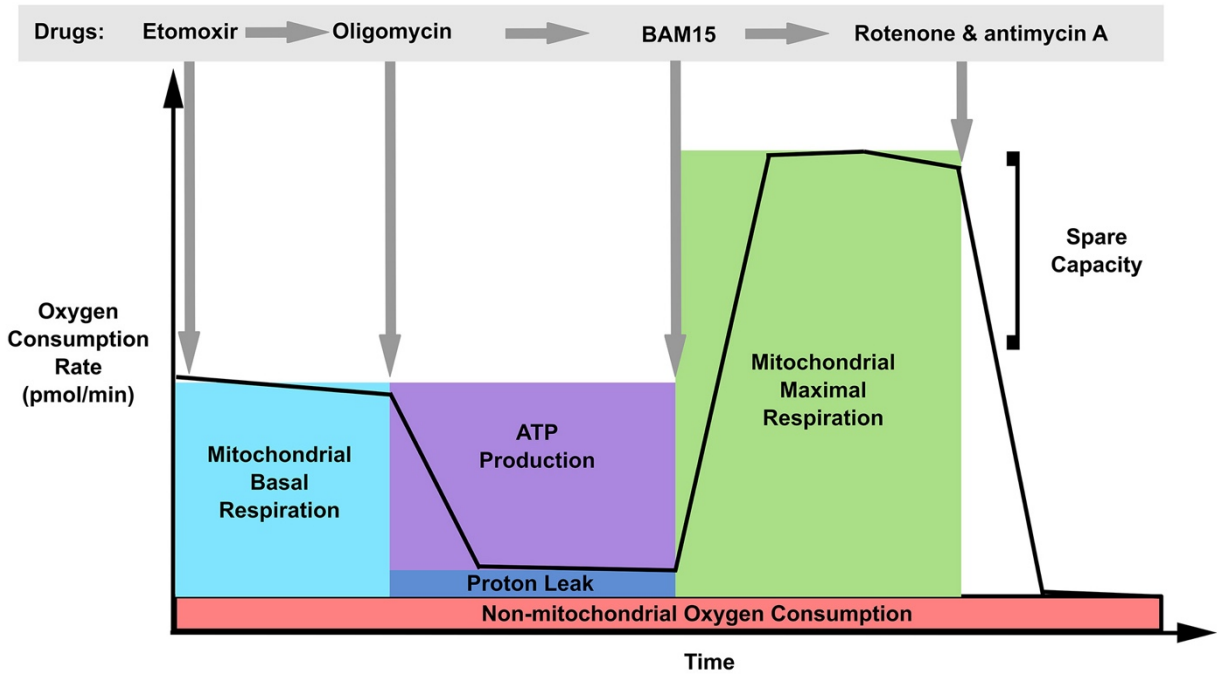

Appendix Figure 5. Illustration of Seahorse mito stress test, for which drugs were added sequentially into the cell culture and what have been measured by the machine.

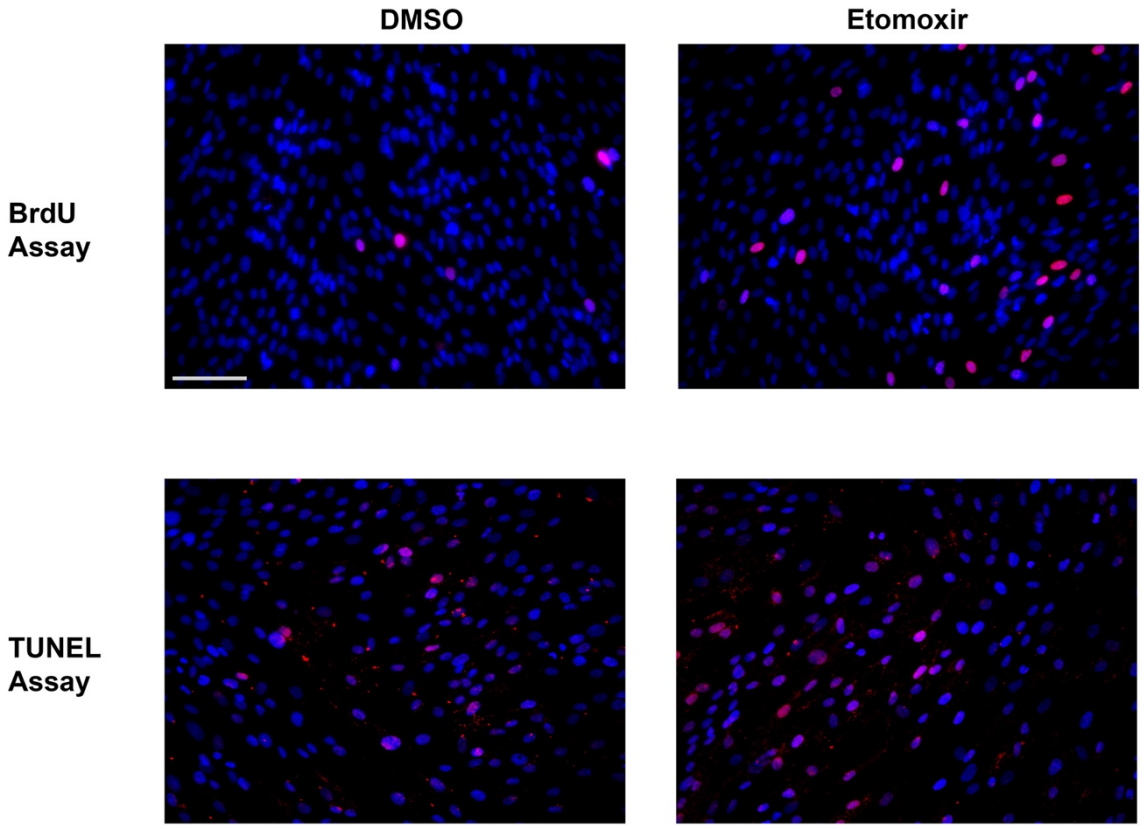

Appendix Figure 6. Mitochondrial fatty acid β-oxidation inhibition mirrored fibrotic degeneration phenotypes in PDL fibroblasts.

Representative field images of BrdU incorporation and TUNEL analysis in the indicated conditions. Quantitative analysis can be found from Figure 5 B and C.

Appendix Table 1

The original proteomic analysis data of the effects of SARS-CoV-2 structural proteins, as showed in Figure 4A.

Accession	Protein	LFQ intensity EGFP 6hrs	LFQ intensity Envelope 6hrs	LFQ intensity Membrane 6hrs	LFQ intensity Nucleocapsid 6hrs
H3BTL1	H3BTL1_HUMAN Microtubule-associated protein 1 light chain 3 beta, isoform CRA_f OS	20.10239029	19.10513687	20.0364418	20.03939056
Q99613-2	EIF3C_HUMAN Isoform 2 of Eukaryotic translation initiation factor 3 subunit C OS	18.629179	19.96310425	20.06723404	20.2131176
F8VZJ2	F8VZJ2_HUMAN Nascent polypeptide-associated complex subunit alpha OS	22.0500946	21.60272598	18.8843956	21.94813538
O00148	DX39A_HUMAN ATP-dependent RNA helicase DDX39A OS	20.24852562	19.92243576	20.19075012	20.36442184
O00159-2	MYO1C_HUMAN Isoform 2 of Unconventional myosin-Ic OS	20.42316437	20.65970612	21.64368057	18.09388161
O00231	PSD11_HUMAN 26S proteasome non-ATPase regulatory subunit 11 OS	21.50232315	20.77643585	18.8217926	21.38958359
O00232-2	PSD12_HUMAN Isoform 2 of 26S proteasome non-ATPase regulatory subunit 12 OS	19.38958931	18.97323799	18.15907097	19.32212639
O00299	CLIC1_HUMAN Chloride intracellular channel protein 1 OS	23.82948685	23.17922211	23.2844677	23.52719116
O00303	EIF3F_HUMAN Eukaryotic translation initiation factor 3 subunit F OS	20.16717339	19.47286606	18.07906342	19.43161583
O00410	IPO5_HUMAN Importin-5 OS	21.63754654	21.14910889	21.34261513	21.50586319
A0A2R8Y5G6	A0A2R8Y5G6_HUMAN RNA helicase OS	20.2237606	20.15783119	20.38268661	20.18555832
O14818	PSA7_HUMAN Proteasome subunit alpha type-7 OS	21.17542076	21.4470787	21.25014496	22.0280323
P19105	ML12A_HUMAN Myosin regulatory light chain 12A OS	22.9598732	22.81103897	22.7803669	23.33674431
O15143	ARC1B_HUMAN Actin-related protein 2/3 complex subunit 1B OS	21.7553997	21.41776848	20.67959976	21.02337074
O15144	ARPC2_HUMAN Actin-related protein 2/3 complex subunit 2 OS	21.11825943	20.74419022	20.81472015	20.75881767
A0A286YF22	A0A286YF22_HUMAN D-3-phosphoglycerate dehydrogenase OS	22.21483803	20.47070313	20.90087509	21.23543739
O43242	PSMD3_HUMAN 26S proteasome non-ATPase regulatory subunit 3 OS	18.42886925	19.4923172	18.51243401	20.35412407
O43707	ACTN4_HUMAN Alpha-actinin-4 OS	24.45920181	24.34854317	24.44373131	24.58663368
O43795-2	MYO1B_HUMAN Isoform 2 of Unconventional myosin-Ib OS	19.75842857	19.13761139	19.4098053	17.52830315
O43852	CALU_HUMAN Calumenin OS	23.00316048	23.20448685	23.1497612	22.97472
O60506-4	HNRPQ_HUMAN Isoform 4 of Heterogeneous nuclear ribonucleoprotein Q OS	18.74744225	22.43349266	21.80931282	22.75505257
O60664-4	PLIN3_HUMAN Isoform 4 of Perilipin-3 OS	23.39806557	22.11977959	21.64412117	22.92772293
O60701	UGDH_HUMAN UDP-glucose 6-dehydrogenase OS	23.65567398	23.56685829	23.33824158	23.71785164
O60763	USO1_HUMAN General vesicular transport factor p115 OS	19.5602951	20.07678986	20.93315506	19.38621902
O75083	WDR1_HUMAN WD repeat-containing protein 1 OS	22.13138199	21.2696228	23.37650108	23.52037239
E5RIW3	E5RIW3_HUMAN Tubulin-specific chaperone A OS	20.52305603	19.03895187	20.3042984	20.24493027
O75369-2	FLNB_HUMAN Isoform 2 of Filamin-B OS	23.54580688	23.33183289	23.51544952	23.3334713
B4DJV2	B4DJV2_HUMAN Citrate synthase OS	20.92810249	20.59532356	20.07365608	21.55524826
O75396	SC22B_HUMAN Vesicle-trafficking protein SEC22b OS	21.74324417	21.7069149	21.60792542	20.76983452
O76003	GLRX3_HUMAN Glutaredoxin-3 OS	20.27491951	19.94077301	18.5617981	20.08108902
O94979-3	SC31A_HUMAN Isoform 3 of Protein transport protein Sec31A OS	20.96845818	21.05278206	20.82539749	20.87927246
O95373	IPO7_HUMAN Importin-7 OS	20.65709114	20.65333557	21.17102814	20.54726791
O95782-2	AP2A1_HUMAN Isoform B of AP-2 complex subunit alpha-1 OS	19.28873253	18.351408	18.48805237	19.44828987
O95816	BAG2_HUMAN BAG family molecular chaperone regulator 2 OS	19.18461418	19.14443588	19.68760109	19.34550858

P00338	LDHA_HUMAN L-lactate dehydrogenase A chain OS	25.44344711	25.19159508	25.05527687	25.45575714
P00367	DHE3_HUMAN Glutamate dehydrogenase 1, mitochondrial OS	20.72550583	20.42521667	20.81932831	20.7519722
P00387-2	NB5R3_HUMAN Isoform 2 of NADH-cytochrome b5 reductase 3 OS	21.65530205	21.77398491	21.40265274	22.45176506
P00403	COX2_HUMAN Cytochrome c oxidase subunit 2 OS	20.24376869	18.19075394	20.23958015	18.82337379
P00505-2	AATM_HUMAN Isoform 2 of Aspartate aminotransferase, mitochondrial OS	20.64368057	20.42624092	19.4458847	19.96225739
P00558	PGK1_HUMAN Phosphoglycerate kinase 1 OS	24.08772278	23.93939209	23.55262375	23.79451561
P00568	KAD1_HUMAN Adenylate kinase isoenzyme 1 OS	19.53301811	20.11629295	19.46778107	18.75499535
P02452	CO1A1_HUMAN Collagen alpha-1(I) chain OS	23.09102058	23.28248978	23.32072258	22.52114105
P02545	LMNA_HUMAN Prelamin-A/C OS	25.78877831	25.64861488	25.65376091	25.40311432
P02751-5	FINC_HUMAN Isoform 5 of Fibronectin OS	19.21175766	20.52219391	21.38642883	19.76073647
P02786	TFR1_HUMAN Transferrin receptor protein 1 OS	19.10517883	20.29356194	20.46383476	18.64682007
P04075	ALDOA_HUMAN Fructose-bisphosphate aldolase A OS	25.22262001	25.09051132	25.17108154	25.27159691
P04080	CYTB_HUMAN Cystatin-B OS	20.52611732	19.50829697	20.25234222	20.95091438
P04083	ANXA1_HUMAN Annexin A1 OS	25.49655724	25.25198174	25.19745636	25.76468658
P04181	OAT_HUMAN Ornithine aminotransferase, mitochondrial OS	19.78298378	18.27453041	19.64839745	19.92171097
P04350	TBB4A_HUMAN Tubulin beta-4A chain OS	19.22675705	18.80141258	20.51595306	19.99050903
P04406	G3P_HUMAN Glyceraldehyde-3-phosphate dehydrogenase OS	25.86968994	25.795681	25.68059349	26.01186371
K7EM73	K7EM73_HUMAN Calcium-activated neutral proteinase small subunit (Fragment) OS	20.34028053	21.09706306	20.18728256	21.22464561
A0A6Q8PFK8	A0A6Q8PFK8_HUMAN Heat shock protein beta-1 OS	22.90451813	23.41905403	22.59400177	24.08909798
P04843	RPN1_HUMAN Dolichyl-diphosphooligosaccharide--protein glycosyltransferase subunit 1 OS	22.59996033	22.73931503	22.67497635	22.67910576
P04844-2	RPN2_HUMAN Isoform 2 of Dolichyl-diphosphooligosaccharide--protein glycosyltransferase subunit 2 OS	21.00449753	21.7910614	21.34098625	21.54443932
P05023-3	AT1A1_HUMAN Isoform 3 of Sodium/potassium-transporting ATPase subunit alpha-1 OS	21.17102814	18.53874207	20.76530838	19.07042313
P05141	ADT2_HUMAN ADP/ATP translocase 2 OS	22.5421505	22.79127884	22.61236572	22.96227455
P05387	RLA2_HUMAN 60S acidic ribosomal protein P2 OS	20.0263443	19.84896278	19.8745079	20.33527184
P05388	RLA0_HUMAN 60S acidic ribosomal protein P0 OS	22.12786102	23.20111084	23.83614922	22.81395721
P05455	LA_HUMAN Lupus La protein OS	20.18555832	20.52085304	18.54012489	20.43267632
H7C4K3	H7C4K3_HUMAN Integrin beta-1 OS	22.45108604	22.80725098	23.01367569	22.93646622
P06576	ATPB_HUMAN ATP synthase subunit beta, mitochondrial OS	22.97744751	23.98988533	23.63433647	23.94476318
R4GN98	R4GN98_HUMAN Protein S100 (Fragment) OS	20.53221893	22.26570702	22.08384895	20.79827881
P06733	ENOA_HUMAN Alpha-enolase OS	26.81433296	26.25585747	25.92379379	26.77341652
P06744	G6PI_HUMAN Glucose-6-phosphate isomerase OS	21.22564507	21.50329399	22.13433075	21.45317268
P06748-3	NPM_HUMAN Isoform 3 of Nucleophosmin OS	23.91488075	23.17753601	23.01529312	23.60625458
P06753-2	TPM3_HUMAN Isoform 2 of Tropomyosin alpha-3 chain OS	24.84282875	25.24285316	24.69620132	24.69109726
P07195	LDHB_HUMAN L-lactate dehydrogenase B chain OS	23.87483406	24.55174446	24.20015335	24.21489716
P07237	PDIA1_HUMAN Protein disulfide-isomerase OS	23.87389565	24.38929367	24.5389576	24.61605072
P07355	ANXA2_HUMAN Annexin A2 OS	26.3249855	26.16036797	26.40963364	26.59448624
Q5JP53	Q5JP53_HUMAN Tubulin beta chain OS	25.56784439	25.24590302	24.97814751	24.51701164
P07737	PROF1_HUMAN Profilin-1 OS	25.31572151	24.98984146	24.69280052	25.51267815
P07741-2	APT_HUMAN Isoform 2 of Adenine phosphoribosyltransferase OS	19.49337769	19.55965996	19.41886902	19.26836014
P07814	SYEP_HUMAN Bifunctional glutamate/proline--tRNA ligase OS	20.97729111	20.52209854	20.81158829	20.95496559
A0A7I2V668	A0A7I2V668_HUMAN Cathepsin B OS	18.59151268	19.28309441	18.92534637	20.0256691

P07900	HS90A_HUMAN Heat shock protein HSP 90-alpha OS	24.97701073	24.96798325	24.85262489	24.31568718
P07954-2	FUMH_HUMAN Isoform Cytoplasmic of Fumarate hydratase, mitochondrial OS	21.47427177	19.83877563	18.75895691	20.33145142
A0A087WTA8	A0A087WTA8_HUMAN Collagen alpha-2(I) chain OS	19.50655174	20.52200317	20.08925819	18.34784698
P08133-2	ANXA6_HUMAN Isoform 2 of Annexin A6 OS	21.31440163	20.74706268	22.89498711	20.61063194
P08195-2	4F2_HUMAN Isoform 2 of 4F2 cell-surface antigen heavy chain OS	20.74369621	20.62631416	20.87252426	21.52616501
P08238	HS90B_HUMAN Heat shock protein HSP 90-beta OS	26.66275215	26.74239731	26.63740921	26.3826313
P08670	VIME_HUMAN Vimentin OS	28.09763145	28.45575714	28.18338203	28.07418633
P08708	RS17_HUMAN 40S ribosomal protein S17 OS	20.42121506	20.89081955	19.0922699	20.2166748
P08758	ANXA5_HUMAN Annexin A5 OS	26.03416443	25.64617157	25.64603424	26.01497269
C9J9K3	C9J9K3_HUMAN 40S ribosomal protein SA (Fragment) OS	23.82997131	23.51689148	23.25066566	23.94556618
P09211	GSTP1_HUMAN Glutathione S-transferase P OS	23.67152405	23.38508606	23.45989037	23.40210533
P09382	LEG1_HUMAN Galectin-1 OS	25.39008141	24.85357666	24.82914734	25.43990135
P09493-3	TPM1_HUMAN Isoform 3 of Tropomyosin alpha-1 chain OS	23.12140846	23.01855659	22.72708702	23.17525291
P09651-3	ROA1_HUMAN Isoform 2 of Heterogeneous nuclear ribonucleoprotein A1 OS	23.24212646	23.56790352	23.55882454	23.16250992
P09936	UCHL1_HUMAN Ubiquitin carboxyl-terminal hydrolase isozyme L1 OS	21.78048706	21.51016998	21.51527977	21.37081909
J3QS39	J3QS39_HUMAN Polyubiquitin-B (Fragment) OS	25.05804634	24.82701683	24.93737221	25.38742256
P0DMV8-2	HS71A_HUMAN Isoform 2 of Heat shock 70 kDa protein 1A OS	22.42190742	22.63862991	22.50331879	22.5267849
P0DP25	CALM3_HUMAN Calmodulin-3 OS	21.64552879	21.67882729	21.98693848	21.82629013
P10599	THIO_HUMAN Thioredoxin OS	23.13769531	22.60306549	22.52657127	22.82549286
A0A7I2V599	A0A7I2V599_HUMAN 60 kDa heat shock protein, mitochondrial OS	23.39479828	23.44733238	24.19151878	24.08172226
P11021	BIP_HUMAN Endoplasmic reticulum chaperone BiP OS	25.55800819	25.57282639	25.71832085	25.92592239
P11142	HSP7C_HUMAN Heat shock cognate 71 kDa protein OS	26.54789734	26.72455406	26.61568642	26.60724258
P11279	LAMP1_HUMAN Lysosome-associated membrane glycoprotein 1 OS	17.32139587	19.31709862	19.2150135	20.2681942
P11413	G6PD_HUMAN Glucose-6-phosphate 1-dehydrogenase OS	23.88892555	23.74745178	23.55168533	23.64735222
V9GYY3	V9GYY3_HUMAN C-1-tetrahydrofolate synthase, cytoplasmic OS	19.85201454	20.60909843	17.56593513	20.80475235
P11940-2	PABP1_HUMAN Isoform 2 of Polyadenylate-binding protein 1 OS	21.51590538	22.08718872	22.50006294	22.46543121
P12004	PCNA_HUMAN Proliferating cell nuclear antigen OS	20.3467865	18.33042145	19.56888008	20.10712433
A0A087X0S5	A0A087X0S5_HUMAN Collagen alpha-1(VI) chain OS	18.71038246	20.07195473	20.02998734	19.10149193
P12110-3	CO6A2_HUMAN Isoform 2C2A of Collagen alpha-2(VI) chain OS	18.38016319	18.76461792	19.70730209	18.65681839
P12111-2	CO6A3_HUMAN Isoform 2 of Collagen alpha-3(VI) chain OS	20.01154327	18.73948097	18.68630219	19.30571556
P12236	ADT3_HUMAN ADP/ATP translocase 3 OS	21.83865166	21.45498085	21.2160244	21.11667442
E7ETK5	E7ETK5_HUMAN Inosine-5-monophosphate dehydrogenase 2 OS	20.26739502	19.94535255	20.17840195	20.36463547
P12814	ACTN1_HUMAN Alpha-actinin-1 OS	24.16867256	23.90655708	24.06923676	24.06767845
P12956	XRCC6_HUMAN X-ray repair cross-complementing protein 6 OS	22.48537064	22.75951004	21.96677017	22.26014709
P13010	XRCC5_HUMAN X-ray repair cross-complementing protein 5 OS	20.98161697	21.04693413	18.7273922	21.02418137
P13489	RINI_HUMAN Ribonuclease inhibitor OS	19.07761192	19.36923981	20.75564384	21.56532478
P13639	EF2_HUMAN Elongation factor 2 OS	25.42521667	25.36131859	25.49347496	25.31458092
P13667	PDIA4_HUMAN Protein disulfide-isomerase A4 OS	22.20329285	21.50198364	22.4616394	22.20401001
P13693	TCTP_HUMAN Translationally-controlled tumor protein OS	22.94494057	23.02570343	22.74299812	21.68440247
P13797-3	PLST_HUMAN Isoform 3 of Plastin-3 OS	20.80325508	21.41012573	20.93984032	21.11914635
P14314-2	GLU2B_HUMAN Isoform 2 of Glucosidase 2 subunit beta OS	20.49462891	20.55646515	20.94670868	20.54952431

P14618	KPYM_HUMAN Pyruvate kinase PKM OS	26.33880234	26.30679893	26.95038033	26.92150307
P14625	ENPL_HUMAN Endoplasmin OS	25.14616013	24.98215675	25.34106064	25.01962471
P14868-2	SYDC_HUMAN Isoform 2 of Aspartate--tRNA ligase, cytoplasmic OS	20.75808716	20.91320229	20.63944626	20.86052704
P15121	ALDR_HUMAN Aldo-keto reductase family 1 member B1 OS	19.60351372	20.02106667	20.2934494	19.91615105
P15170-2	ERF3A_HUMAN Isoform 2 of Eukaryotic peptide chain release factor GTP-binding subunit ERF3A OS	18.81366158	18.34658432	19.01454353	19.65240097
E7EQR4	E7EQR4_HUMAN Ezrin OS	21.33494568	20.75148201	21.29288864	21.32827568
P15531	NDKA_HUMAN Nucleoside diphosphate kinase A OS	20.29949951	21.05039406	21.42157364	20.32256699
B4DLR8	B4DLR8_HUMAN NAD(P)H dehydrogenase [quinone] 1 OS	21.96476173	22.27486229	21.60747528	22.14973068
P15880	RS2_HUMAN 40S ribosomal protein S2 OS	21.47847557	21.86067772	21.50489426	20.85094643
H0YD13	H0YD13_HUMAN CD44 antigen OS	21.84796906	21.62055397	22.34597397	21.94706535
P16152	CBR1_HUMAN Carbonyl reductase [NADPH] 1 OS	20.68893242	20.65210915	20.29670143	21.14008522
P16401	H15_HUMAN Histone H1.5 OS	20.50445747	21.03650856	19.98509789	20.09106827
P16403	H12_HUMAN Histone H1.2 OS	22.56239319	23.6404171	22.6115551	22.15610313
A2A2D0	A2A2D0_HUMAN Stathmin (Fragment) OS	22.06766129	22.17063141	21.99043846	22.18546677
P17066	HSP76_HUMAN Heat shock 70 kDa protein 6 OS	23.97018051	23.79114151	24.3663311	18.36454964
P17301	ITA2_HUMAN Integrin alpha-2 OS	20.62533379	18.01978874	20.27264404	19.34575462
P17844-2	DDX5_HUMAN Isoform 2 of Probable ATP-dependent RNA helicase DDX5 OS	21.91779709	21.96204567	22.16063309	22.15893936
P17931	LEG3_HUMAN Galectin-3 OS	22.04069519	21.6466713	21.1992836	21.85870743
P17987	TCPA_HUMAN T-complex protein 1 subunit alpha OS	21.94663811	20.91830635	22.14678192	22.09316635
P18077	RL35A_HUMAN 60S ribosomal protein L35a OS	21.23876381	21.20012283	20.94927597	20.95183945
P18085	ARF4_HUMAN ADP-ribosylation factor 4 OS	22.76761436	23.49240494	22.76050568	22.95882797
P18124	RL7_HUMAN 60S ribosomal protein L7 OS	22.55255318	22.32608223	22.11359406	22.20711136
P18206-2	VINC_HUMAN Isoform 1 of Vinculin OS	25.51270866	25.16748619	25.25767517	25.19121742
A0A087WXM6	A0A087WXM6_HUMAN 60S ribosomal protein L17 (Fragment) OS	22.04683495	21.91356659	21.91914368	21.42792892
P18669	PGAM1_HUMAN Phosphoglycerate mutase 1 OS	21.50450706	22.3384037	18.76493454	22.02894402
A0A7I2V5M5	A0A7I2V5M5_HUMAN Nucleolin OS	23.5639534	23.83402824	24.17607498	23.00643349
P20340-2	RAB6A_HUMAN Isoform 2 of Ras-related protein Rab-6A OS	20.68260384	20.27082062	19.90782928	18.33300209
P20618	PSB1_HUMAN Proteasome subunit beta type-1 OS	21.38637543	20.9909935	20.79558563	20.46821785
E9PP21	E9PP21_HUMAN Cysteine and glycine-rich protein 1 OS	22.33764267	22.17621231	21.712677	22.27121925
P21333-2	FLNA_HUMAN Isoform 2 of Filamin-A OS	27.50074005	27.26731682	27.49845886	27.23908806
P21796	VDAC1_HUMAN Voltage-dependent anion-selective channel protein 1 OS	20.80317497	21.00257683	19.18766403	21.32289696
P21980	TGM2_HUMAN Protein-glutamine gamma-glutamyltransferase 2 OS	21.63706017	20.52859879	21.82080841	21.45973969
P22234	PUR6_HUMAN Multifunctional protein ADE2 OS	20.32586288	18.53541374	18.37940216	19.8512516
P22307-6	SCP2_HUMAN Isoform 6 of Sterol carrier protein 2 OS	19.93051529	18.27853394	19.50288582	20.16041756
P22314-2	UBA1_HUMAN Isoform 2 of Ubiquitin-like modifier-activating enzyme 1 OS	23.46874046	23.45148849	23.38613892	23.43224335
P22392-2	NDKB_HUMAN Isoform 3 of Nucleoside diphosphate kinase B OS	24.95557785	24.43020248	24.24285316	24.82561111
A0A7I2V4I6	A0A7I2V4I6_HUMAN Heterogeneous nuclear ribonucleoproteins A2/B1 OS	22.79590416	22.79405975	22.6634903	22.38616562
A0A2R8YDM0	A0A2R8YDM0_HUMAN Prostaglandin-endoperoxide synthase (Fragment) OS	19.32447243	19.92104149	20.32586288	20.453022
P23246	SFPQ_HUMAN Splicing factor, proline- and glutamine-rich OS	21.78572464	22.33884048	22.07407951	19.62455559
P23284	PPIB_HUMAN Peptidyl-prolyl cis-trans isomerase B OS	24.42136765	23.90334129	23.9958477	23.69242859
P23381-2	SYWC_HUMAN Isoform 2 of Tryptophan--tRNA ligase, cytoplasmic OS	18.65694618	18.98865128	18.03157043	18.45745659

P23396	RS3_HUMAN 40S ribosomal protein S3 OS	23.78096771	23.62287903	23.62053299	23.94708443
P23526	SAHH_HUMAN Adenosylhomocysteinase OS	21.50300217	21.42700768	21.16337013	21.25948524
P23528	COF1_HUMAN Cofilin-1 OS	24.93597984	24.95938683	24.94060135	25.63765717
P23634-7	AT2B4_HUMAN Isoform ZB of Plasma membrane calcium-transporting ATPase 4 OS	20.08498573	20.69200325	20.50794601	18.06524467
P24534	EF1B_HUMAN Elongation factor 1-beta OS	22.30502129	21.72263336	22.14027405	22.05857468
Q5QNZ2	Q5QNZ2_HUMAN ATP synthase F(0) complex subunit B1, mitochondrial OS	19.32291794	20.23958015	19.95787239	19.57420921
P25398	RS12_HUMAN 40S ribosomal protein S12 OS	22.16864204	21.38205338	21.39037132	20.97330284
P25705	ATPA_HUMAN ATP synthase subunit alpha, mitochondrial OS	24.05150604	24.12273598	24.0110321	23.74488831
F5GX11	F5GX11_HUMAN Proteasome subunit alpha type-1 OS	21.36121178	20.17657661	20.6032238	20.54387474
A0A7I2V2H3	A0A7I2V2H3_HUMAN UPF0415 protein C7orf25 OS	20.29299927	20.44949913	18.5714798	17.94278336
P25788-2	PSA3_HUMAN Isoform 2 of Proteasome subunit alpha type-3 OS	19.95400429	19.35004044	18.62101173	20.80829239
H0YMZ1	H0YMZ1_HUMAN Proteasome subunit alpha type (Fragment) OS	20.44818878	18.83518982	20.33745193	20.11667442
P26038	MOES_HUMAN Moesin OS	24.08448219	24.15236282	24.07667542	23.99576187
P26373	RL13_HUMAN 60S ribosomal protein L13 OS	21.72088051	22.07162666	21.93329811	22.05596352
A6NLN1	A6NLN1_HUMAN Polypyrimidine tract-binding protein 1 OS	21.35498619	22.10261536	21.91195869	22.54333115
P26639	SYTC_HUMAN Threonine--tRNA ligase 1, cytoplasmic OS	18.68282509	18.14849663	20.6827755	20.56978226
P26640	SYVC_HUMAN Valine--tRNA ligase OS	20.64491272	20.36900902	19.86188889	20.05152321
P26641	EF1G_HUMAN Elongation factor 1-gamma OS	24.44909668	23.74570847	23.42226791	23.98589706
P27348	1433T_HUMAN 14-3-3 protein theta OS	21.95311928	21.91830635	22.69824791	21.8007679
F8W7C6	F8W7C6_HUMAN 60S ribosomal protein L10 OS	19.95446968	20.85041237	20.13808632	20.4403019
P27797	CALR_HUMAN Calreticulin OS	24.27582932	24.20321846	24.16361618	24.06488609
P27816-6	MAP4_HUMAN Isoform 6 of Microtubule-associated protein 4 OS	22.30866432	22.13295174	21.96705246	22.24091911
P27824	CALX_HUMAN Calnexin OS	22.58545494	22.43690109	22.57588577	22.74349213
P28066	PSA5_HUMAN Proteasome subunit alpha type-5 OS	19.54440308	21.35697365	18.90184212	22.0509243
P28072	PSB6_HUMAN Proteasome subunit beta type-6 OS	20.35412407	20.73537445	20.70480537	20.0171299
P28074	PSB5_HUMAN Proteasome subunit beta type-5 OS	20.54820824	20.92918587	21.03838539	18.24308014
P29373	RABP2_HUMAN Cellular retinoic acid-binding protein 2 OS	21.69132042	21.58641624	21.46218872	21.75605202
P29401	TKT_HUMAN Transketolase OS	23.89309883	23.9358902	23.79431725	24.02934837
E9PK01	E9PK01_HUMAN Elongation factor 1-delta (Fragment) OS	23.84028625	24.22140312	23.92243195	23.40859795
P29966	MARCS_HUMAN Myristoylated alanine-rich C-kinase substrate OS	21.43135071	21.26441956	21.41369438	20.4724884
P30040	ERP29_HUMAN Endoplasmic reticulum resident protein 29 OS	20.24875641	19.04772758	19.87669754	20.63280678
P30041	PRDX6_HUMAN Peroxiredoxin-6 OS	22.81677246	22.49831009	21.80408287	23.03259659
P30044-2	PRDX5_HUMAN Isoform Cytoplasmic+peroxisomal of Peroxiredoxin-5, mitochondrial OS	20.55496788	19.9026432	20.01576805	20.35175514
P30048-2	PRDX3_HUMAN Isoform 2 of Thioredoxin-dependent peroxide reductase, mitochondrial OS	20.88323021	20.84053421	20.80207062	21.22311401
P30050	RL12_HUMAN 60S ribosomal protein L12 OS	22.99602127	22.84628677	22.77017784	23.10616684
P30086	PEBP1_HUMAN Phosphatidylethanolamine-binding protein 1 OS	21.17937469	20.88226128	21.31118965	20.51691628
P30101	PDIA3_HUMAN Protein disulfide-isomerase A3 OS	24.33892059	24.46351051	24.36833	24.09595299
P30153	2AAA_HUMAN Serine/threonine-protein phosphatase 2A 65 kDa regulatory subunit A alpha isoform OS	20.17438507	17.96764565	20.35347939	20.97889709
P31153-2	METK2_HUMAN Isoform 2 of S-adenosylmethionine synthase isoform type-2 OS	21.7015934	21.30752563	18.02231789	19.35296822
P31939	PUR9_HUMAN Bifunctional purine biosynthesis protein ATIC OS	19.96395111	20.33712578	19.75433922	19.82289505
P31943	HNRH1_HUMAN Heterogeneous nuclear ribonucleoprotein H OS	22.09732056	21.65294075	21.94141769	21.81796265

P31946-2	1433B_HUMAN Isoform Short of 14-3-3 protein beta/alpha OS	21.12395287	22.44609451	22.75191116	21.69510841
P31948	STIP1_HUMAN Stress-induced-phosphoprotein 1 OS	21.68101692	21.71586227	21.76862335	21.52042198
P32119	PRDX2_HUMAN Peroxiredoxin-2 OS	21.18083191	21.54491234	21.79018593	21.64059448
D6RAN4	D6RAN4_HUMAN 60S ribosomal protein L9 (Fragment) OS	21.75902176	21.75474739	21.77499008	21.77527046
P33176	KINH_HUMAN Kinesin-1 heavy chain OS	21.85064125	21.33472633	21.40135002	18.63724709
H0YMM5	H0YMM5_HUMAN Deoxyuridine 5-triphosphate nucleotidohydrolase OS	17.98854065	19.09668159	18.96603775	18.76483917
P34932	HSP74_HUMAN Heat shock 70 kDa protein 4 OS	20.94005585	21.18058968	20.53164864	20.7768383
C9J0J7	C9J0J7_HUMAN Profilin OS	20.86014748	20.92998123	21.36666298	18.95683861
G3XAM7	G3XAM7_HUMAN Catenin (Cadherin-associated protein), alpha 1, 102kDa, isoform CRA_a OS	18.23778915	19.61126328	18.54493904	20.20490456
P35232	PHB_HUMAN Prohibitin OS	21.47288513	21.34759712	21.18289375	21.02654839
P35241	RADI_HUMAN Radixin OS	18.7151165	18.15534973	19.38460732	18.39462662
K7EP65	K7EP65_HUMAN 60S ribosomal protein L22 (Fragment) OS	21.8465538	22.31024742	21.9591465	22.57124138
P35579	MYH9_HUMAN Myosin-9 OS	27.21946526	27.34975815	27.44679451	27.2035923
P35580	MYH10_HUMAN Myosin-10 OS	19.46911812	18.07261276	19.93718338	19.44395065
P35637-2	FUS_HUMAN Isoform Short of RNA-binding protein FUS OS	20.26109314	20.34527016	20.40010071	19.83422089
C9JX88	C9JX88_HUMAN 26S proteasome regulatory subunit 7 OS	20.30295944	18.80281448	19.17874146	20.59313583
P36578	RL4_HUMAN 60S ribosomal protein L4 OS	23.30841446	23.01481628	22.90056229	22.87282562
P37802	TAGL2_HUMAN Transgelin-2 OS	22.95617104	23.49093819	23.52838516	22.38687515
P37837	TALDO_HUMAN Transaldolase OS	21.21501541	21.01120186	20.64121246	19.90301132
A0A7I2V2G2	A0A7I2V2G2_HUMAN Stress-70 protein, mitochondrial OS	22.65066528	23.09741592	22.98363686	23.06202126
P39019	RS19_HUMAN 40S ribosomal protein S19 OS	22.94916916	23.27696419	23.08090973	23.17503929
P39023	RL3_HUMAN 60S ribosomal protein L3 OS	22.28551292	21.49066925	21.54707909	21.69935036
P39656-3	OST48_HUMAN Isoform 3 of Dolichyl-diphosphooligosaccharide--protein glycosyltransferase 48 kDa subunit OS	21.70602798	20.82772446	21.10014725	21.47649956
P40227	TCPZ_HUMAN T-complex protein 1 subunit zeta OS	22.43456078	22.74435425	22.52492142	22.80258369
A0A7I2V2L9	A0A7I2V2L9_HUMAN 60S ribosomal protein L13a OS	22.31454086	22.17834091	22.05029297	22.66062164
P40925	MDHC_HUMAN Malate dehydrogenase, cytoplasmic OS	18.32060432	19.06594086	20.32597351	20.0188961
P40926	MDHM_HUMAN Malate dehydrogenase, mitochondrial OS	22.7376442	22.84955406	22.19084167	23.05339622
P40939	ECHA_HUMAN Trifunctional enzyme subunit alpha, mitochondrial OS	20.05629349	18.65982819	18.91164589	20.71280289
P41091	IF2G_HUMAN Eukaryotic translation initiation factor 2 subunit 3 OS	19.02732849	20.92303085	20.30374146	20.31052399
A0A6Q8PGW4	A0A6Q8PGW4_HUMAN Diadenosine tetraphosphate synthetase OS	22.65839958	20.50096321	22.15035057	22.33134079
A0A0A0MSX9	A0A0A0MSX9_HUMAN Isoleucyl-tRNA synthetase OS	20.78803635	20.23233604	18.30582237	19.70235252
P42677	RS27_HUMAN 40S ribosomal protein S27 OS	21.05291557	21.36292458	21.74365616	21.24103546
P42704	LPPRC_HUMAN Leucine-rich PPR motif-containing protein, mitochondrial OS	20.07887459	20.15930939	19.95375824	19.05296326
P42766	RL35_HUMAN 60S ribosomal protein L35 OS	20.98530579	21.26436234	20.98300934	20.2877121
D6REM6	D6REM6_HUMAN Matrin-3 OS	18.12245369	20.94327927	20.88807106	18.25110435
C9J3L8	C9J3L8_HUMAN Signal sequence receptor subunit alpha OS	20.83352661	20.42552376	19.78462219	20.82826614
P43487-2	RANG_HUMAN Isoform 2 of Ran-specific GTPase-activating protein OS	19.92619133	21.06137848	18.36230278	20.40851974
A0A0A0MR02	A0A0A0MR02_HUMAN Outer mitochondrial membrane protein porin 2 (Fragment) OS	18.93975449	18.82051849	18.63635254	20.91597557
P46060	RAGP1_HUMAN Ran GTPase-activating protein 1 OS	20.7369442	20.84919167	20.60918999	20.90771294
E9PLL6	E9PLL6_HUMAN 60S ribosomal protein L27a OS	20.7542572	19.02553749	18.59032059	20.97994423

A0A2R8Y6J3	A0A2R8Y6J3_HUMAN 60S ribosomal protein L5 (Fragment) OS	21.16484261	20.87919807	21.56648636	20.66553116
P46779	RL28_HUMAN 60S ribosomal protein L28 OS	20.38247681	21.68071747	22.26384735	20.03965759
P46781	RS9_HUMAN 40S ribosomal protein S9 OS	22.76727104	23.10210228	22.92795753	22.23549461
P46783	RS10_HUMAN 40S ribosomal protein S10 OS	22.1238575	21.65560722	21.62880898	22.79249191
P46821	MAP1B_HUMAN Microtubule-associated protein 1B OS	23.13908577	22.94111252	23.00273132	23.0926342
P46940	IQGA1_HUMAN Ras GTPase-activating-like protein IQGAP1 OS	24.00821304	23.67281914	23.76910782	23.76708794
P47756-2	CAPZB_HUMAN Isoform 2 of F-actin-capping protein subunit beta OS	22.01294136	21.34342957	21.38758659	21.88550377
P47914	RL29_HUMAN 60S ribosomal protein L29 OS	19.93747139	21.24417496	18.78913689	19.66221237
P48047	ATPO_HUMAN ATP synthase subunit O, mitochondrial OS	20.76700783	20.39362144	20.49101067	20.20179939
P48444	COPD_HUMAN Coatomer subunit delta OS	19.20639038	18.78091049	19.65928841	20.10495186
P48643	TCPE_HUMAN T-complex protein 1 subunit epsilon OS	19.14135933	19.8029232	21.50741386	21.48978806
P49207	RL34_HUMAN 60S ribosomal protein L34 OS	21.11050606	21.28133011	20.90763855	21.49770164
P49257	LMAN1_HUMAN Protein ERGIC-53 OS	20.85946465	20.31052399	18.4568367	20.73015785
P49327	FAS_HUMAN Fatty acid synthase OS	22.85325241	22.78761864	22.85325241	22.35124207
P49368-2	TCPG_HUMAN Isoform 2 of T-complex protein 1 subunit gamma OS	20.64790154	22.1076355	22.11603928	22.52676201
P49411	EFTU_HUMAN Elongation factor Tu, mitochondrial OS	20.77209282	21.30996895	21.29148293	21.49389648
A0A6Q8PGR9	A0A6Q8PGR9_HUMAN Alanine--tRNA ligase OS	18.80595398	20.223526	20.52410889	20.24435043
P49721	PSB2_HUMAN Proteasome subunit beta type-2 OS	20.19002724	18.74065781	19.61156845	18.52177048
P49748-2	ACADV_HUMAN Isoform 2 of Very long-chain specific acyl-CoA dehydrogenase, mitochondrial OS	20.55730629	20.48492813	18.15488434	20.70100212
P49755	TMEDA_HUMAN Transmembrane emp24 domain-containing protein 10 OS	21.40457535	20.70201683	20.59322739	21.44536209
P50395	GDIB_HUMAN Rab GDP dissociation inhibitor beta OS	23.22912598	22.87820625	22.23777199	23.04550171
P50454	SERPH_HUMAN Serpin H1 OS	25.6435585	25.03980064	24.48965263	25.09281158
P50502	F10A1_HUMAN Hsc70-interacting protein OS	22.07234764	21.534832	20.55421829	21.27537346
P50990	TCPQ_HUMAN T-complex protein 1 subunit theta OS	22.16060257	23.07182312	22.83300591	22.91832542
P50991	TCPD_HUMAN T-complex protein 1 subunit delta OS	21.31318474	21.25112915	22.47221565	21.98971176
P51148	RAB5C_HUMAN Ras-related protein Rab-5C OS	21.26080704	21.59514046	20.97379303	21.83047295
P51149	RAB7A_HUMAN Ras-related protein Rab-7a OS	22.71793556	22.20158958	22.18401527	22.25715637
P51571	SSRD_HUMAN Translocon-associated protein subunit delta OS	20.67676353	19.64981461	19.71739578	20.84383583
P51572	BAP31_HUMAN B-cell receptor-associated protein 31 OS	17.92259598	18.25635529	19.50223923	19.21449471
P52209-2	6PGD_HUMAN Isoform 2 of 6-phosphogluconate dehydrogenase, decarboxylating OS	23.3372879	22.33946419	21.9394455	22.58217239
P52272-2	HNRPM_HUMAN Isoform 2 of Heterogeneous nuclear ribonucleoprotein M OS	21.64072609	21.08628082	22.13599014	21.81710434
J3KTF8	J3KTF8_HUMAN Rho GDP-dissociation inhibitor 1 (Fragment) OS	23.52133179	23.53872108	22.55695534	23.88874054
P52907	CAZA1_HUMAN F-actin-capping protein subunit alpha-1 OS	22.35748482	21.97973442	22.09413338	22.56036568
P53396-2	ACLY_HUMAN Isoform 2 of ATP-citrate synthase OS	21.96105766	21.92288589	22.14724731	22.02553368
P53618	COPB_HUMAN Coatomer subunit beta OS	19.32070923	20.1977253	19.00530243	20.54434586
P53621	COPA_HUMAN Coatomer subunit alpha OS	22.68382454	22.54750252	22.55025291	22.44899559
P54136	SYRC_HUMAN Arginine--tRNA ligase, cytoplasmic OS	20.83776665	20.80009651	20.1692543	20.34559631
P55060-4	XPO2_HUMAN Isoform 4 of Exportin-2 OS	19.82200813	18.66786385	17.65454102	19.97154999
P55072	TERA_HUMAN Transitional endoplasmic reticulum ATPase OS	24.05705452	23.39139366	23.98771858	22.93711281
P55084-2	ECHB_HUMAN Isoform 2 of Trifunctional enzyme subunit beta, mitochondrial OS	20.35067558	18.85640335	19.36937141	19.67572975
H0YHC3	H0YHC3_HUMAN Nucleosome assembly protein 1-like 1 (Fragment) OS	20.18833733	20.7776413	20.59623337	17.94430542

P55884	EIF3B_HUMAN Eukaryotic translation initiation factor 3 subunit B OS	18.57753944	19.83369637	19.02816963	20.20848274
P59998	ARPC4_HUMAN Actin-related protein 2/3 complex subunit 4 OS	22.11470604	22.09377861	22.12316322	22.69166183
P60174	TPIS_HUMAN Triosephosphate isomerase OS	23.27639771	23.84584618	24.09055138	24.59718895
B3KW56	B3KW56_HUMAN Eukaryotic translation initiation factor 3 subunit E OS	19.91165161	19.76900673	18.54272652	20.17791557
F8W1R7	F8W1R7_HUMAN Myosin light polypeptide 6 OS	23.86702919	24.01563263	23.8969841	24.06899071
P60709	ACTB_HUMAN Actin, cytoplasmic 1 OS	29.5298996	29.50846863	29.72000885	29.53129578
P60842	IF4A1_HUMAN Eukaryotic initiation factor 4A-I OS	25.29862595	24.65485382	24.5323143	24.97631264
P60866	RS20_HUMAN 40S ribosomal protein S20 OS	22.93490028	23.04278374	22.17056847	22.09206963
B1ALA9	B1ALA9_HUMAN Ribose-phosphate pyrophosphokinase 1 OS	19.31720924	18.96899223	19.94649506	19.62693977
P60900	PSA6_HUMAN Proteasome subunit alpha type-6 OS	20.35820961	20.8303566	20.40883064	21.42152214
P60953	CDC42_HUMAN Cell division control protein 42 homolog OS	20.50930023	20.43806839	20.9557457	20.54717255
P60981	DEST_HUMAN Destrin OS	21.46418381	21.45563316	21.47516251	21.40431595
P61019	RAB2A_HUMAN Ras-related protein Rab-2A OS	21.1293087	20.28093338	20.36324501	19.8890667
P61088	UBE2N_HUMAN Ubiquitin-conjugating enzyme E2 N OS	20.9978981	21.51595306	21.42306328	21.61162376
P61106	RAB14_HUMAN Ras-related protein Rab-14 OS	20.51431656	20.53525925	20.12325668	17.97779083
B4DXW1	B4DXW1_HUMAN Actin-like protein 3 OS	22.71753693	21.74419022	21.8473568	22.20660591
P61160	ARP2_HUMAN Actin-related protein 2 OS	22.2937851	21.52812195	22.10354424	21.49755478
R4GMT0	R4GMT0_HUMAN Alpha-centractin OS	19.0608387	19.81391144	21.02890968	20.02242279
P84077	ARF1_HUMAN ADP-ribosylation factor 1 OS	22.76844215	22.53793907	22.59048843	23.07713127
P61224-2	RAP1B_HUMAN Isoform 2 of Ras-related protein Rap-1b OS	21.05834389	21.05940056	21.01678848	20.85574532
P61247	RS3A_HUMAN 40S ribosomal protein S3a OS	21.88405037	22.07309914	22.11946297	21.52606964
J3QRI7	J3QRI7_HUMAN 60S ribosomal protein L26 (Fragment) OS	21.34256172	21.26984978	21.22552681	21.58659935
P61313	RL15_HUMAN 60S ribosomal protein L15 OS	19.74180603	21.89163589	21.21720695	19.95475388
P61353	RL27_HUMAN 60S ribosomal protein L27 OS	22.93097305	22.72698212	22.68527985	22.77822304
P61586	RHOA_HUMAN Transforming protein RhoA OS	20.54736137	20.57144928	20.46283722	18.35413361
P61604	CH10_HUMAN 10 kDa heat shock protein, mitochondrial OS	22.73770714	22.60387993	22.33467293	22.72719002
P61619	S61A1_HUMAN Protein transport protein Sec61 subunit alpha isoform 1 OS	18.47943306	20.18628311	20.03442764	19.72177315
P61923	COPZ1_HUMAN Coatomer subunit zeta-1 OS	18.60433006	19.91628265	19.40555191	17.92468262
P61970	NTF2_HUMAN Nuclear transport factor 2 OS	20.49891853	20.18531609	20.22811317	20.33330917
P61978-3	HNRPK_HUMAN Isoform 3 of Heterogeneous nuclear ribonucleoprotein K OS	23.09923172	23.44037819	23.84373856	23.63234138
P61981	1433G_HUMAN 14-3-3 protein gamma OS	18.42302132	22.27104759	17.98696136	20.9958992
P62081	RS7_HUMAN 40S ribosomal protein S7 OS	22.66921234	22.55978203	22.36847687	22.01127052
E9PMD7	E9PMD7_HUMAN Serine/threonine-protein phosphatase OS	20.06539536	19.72168922	18.28643608	20.40395164
P62191-2	PRS4_HUMAN Isoform 2 of 26S proteasome regulatory subunit 4 OS	19.5610466	20.35487747	18.47707939	17.67256355
Q5JR95	Q5JR95_HUMAN 40S ribosomal protein S8 OS	21.89999199	22.16026497	22.126791	22.73442268
P62244	RS15A_HUMAN 40S ribosomal protein S15a OS	22.8121357	22.11825943	22.24895859	22.83686256
P62249	RS16_HUMAN 40S ribosomal protein S16 OS	23.02240562	23.15893936	23.09021187	23.08371925
P62258	1433E_HUMAN 14-3-3 protein epsilon OS	24.48179245	24.88599777	25.01069069	24.21385956
A0A2R8Y811	A0A2R8Y811_HUMAN 40S ribosomal protein S14 (Fragment) OS	22.64425278	22.63916016	22.63143158	23.099617
P62266	RS23_HUMAN 40S ribosomal protein S23 OS	19.49882126	20.69515038	20.42141914	20.35928154
P62269	RS18_HUMAN 40S ribosomal protein S18 OS	22.16429138	22.85625839	22.96545029	22.22022247
P62277	RS13_HUMAN 40S ribosomal protein S13 OS	22.54196167	23.03071213	22.88016891	23.04660225

P62280	RS11_HUMAN 40S ribosomal protein S11 OS	21.46956062	22.00963211	22.20203781	21.24150085
P62424	RL7A_HUMAN 60S ribosomal protein L7a OS	22.38474464	22.31705475	22.33772469	22.15927887
P62495-2	ERF1_HUMAN Isoform 2 of Eukaryotic peptide chain release factor subunit 1 OS	19.9813385	19.69171333	18.8434906	19.57411385
P62701	RS4X_HUMAN 40S ribosomal protein S4, X isoform OS	22.05480385	22.29698181	22.86287308	21.86619759
P62750	RL23A_HUMAN 60S ribosomal protein L23a OS	22.6637516	22.13868141	22.56320763	22.01767349
P62805	H4_HUMAN Histone H4 OS	20.7542572	19.5152607	18.8754425	19.59492302
P62826	RAN_HUMAN GTP-binding nuclear protein Ran OS	23.31575584	23.00792313	23.3066082	24.03263092
P62829	RL23_HUMAN 60S ribosomal protein L23 OS	21.55032349	22.20275497	19.74606705	21.30991364
S4R456	S4R456_HUMAN 40S ribosomal protein S15 (Fragment) OS	18.76415825	18.87331963	18.88997269	18.95011711
P62847-2	RS24_HUMAN Isoform 2 of 40S ribosomal protein S24 OS	18.87836456	20.34256172	20.33690834	21.84049606
P62851	RS25_HUMAN 40S ribosomal protein S25 OS	22.20263481	22.06822014	21.82018471	22.31688881
P62857	RS28_HUMAN 40S ribosomal protein S28 OS	19.75593758	20.7923336	20.42613792	20.1043129
E5RI99	E5RI99_HUMAN 60S ribosomal protein L30 (Fragment) OS	19.77177048	20.74336815	20.14532089	20.04473495
P62899	RL31_HUMAN 60S ribosomal protein L31 OS	21.02472305	21.78508568	21.93844032	21.34321213
P62906	RL10A_HUMAN 60S ribosomal protein L10a OS	22.63526726	22.59279442	21.74996948	22.84684181
D3YTB1	D3YTB1_HUMAN 60S ribosomal protein L32 (Fragment) OS	19.16825104	19.68024254	20.77531052	19.93445015
P62913	RL11_HUMAN 60S ribosomal protein L11 OS	22.14099121	22.10126877	22.33279037	21.17907143
P62917	RL8_HUMAN 60S ribosomal protein L8 OS	20.62220955	20.93660927	21.90142822	21.3046875
P62937	PPIA_HUMAN Peptidyl-prolyl cis-trans isomerase A OS	25.39584541	25.18899345	25.30002213	25.47966576
P63000	RAC1_HUMAN Ras-related C3 botulinum toxin substrate 1 OS	22.02259064	22.02323532	21.77213287	21.61445618
P63104	1433Z_HUMAN 14-3-3 protein zeta/delta OS	23.11859131	24.02478981	24.46967125	23.54427528
P63173	RL38_HUMAN 60S ribosomal protein L38 OS	19.12953377	19.08990479	18.94283485	19.35309029
I3L397	I3L397_HUMAN Eukaryotic translation initiation factor 5A (Fragment) OS	23.20315933	22.88628578	22.66001129	22.99548531
P63244	RACK1_HUMAN Receptor of activated protein C kinase 1 OS	22.68769455	22.40223503	22.33057594	22.37904167
P67809	YBOX1_HUMAN Y-box-binding protein 1 OS	22.74765587	22.75920486	22.52561569	22.25600433
H0YNG3	H0YNG3_HUMAN Signal peptidase complex catalytic subunit SEC11 OS	18.22343063	19.51091194	19.41544914	19.53732872
P67936	TPM4_HUMAN Tropomyosin alpha-4 chain OS	24.36084938	24.38007355	23.59434319	24.00547409
P68032	ACTC_HUMAN Actin, alpha cardiac muscle 1 OS	24.74088097	25.19869232	24.25659561	25.02643776
P68036-2	UB2L3_HUMAN Isoform 2 of Ubiquitin-conjugating enzyme E2 L3 OS	20.16619301	20.69557571	20.87395096	20.99196243
A0A7I2V659	A0A7I2V659_HUMAN Elongation factor 1-alpha 1 OS	28.44517708	28.03574753	27.33125305	28.28034019
P68363	TBA1B_HUMAN Tubulin alpha-1B chain OS	27.3512764	26.94826508	27.13359451	27.01393127
P68371	TBB4B_HUMAN Tubulin beta-4B chain OS	27.17560005	26.76268578	26.85697556	26.43130302
P78371	TCPB_HUMAN T-complex protein 1 subunit beta OS	21.93524361	22.83682251	22.53661156	22.74796295
P78417	GSTO1_HUMAN Glutathione S-transferase omega-1 OS	22.47114944	21.69782448	21.38331985	22.29299927
P78527	PRKDC_HUMAN DNA-dependent protein kinase catalytic subunit OS	21.67137337	21.07391739	19.96395111	19.34712219
C9JXB8	C9JXB8_HUMAN 60S ribosomal protein L24 OS	21.07110405	20.63979912	20.12830162	19.10333824
J3QR09	J3QR09_HUMAN Ribosomal protein L19 OS	18.86495018	17.8894558	18.10998154	19.38549232
P84103-2	SRSF3_HUMAN Isoform 2 of Serine/arginine-rich splicing factor 3 OS	19.94692421	18.28826523	20.18180275	20.56010818
P98179	RBM3_HUMAN RNA-binding protein 3 OS	20.84375763	20.35810089	20.57800865	21.36719704
C9JFR7	C9JFR7_HUMAN Cytochrome c (Fragment) OS	20.96613693	21.44475555	21.244524	21.09841347
F8VVM2	F8VVM2_HUMAN Phosphate carrier protein, mitochondrial OS	17.60062599	18.42212296	21.98811722	22.12107658
A0A024R4E5	A0A024R4E5_HUMAN High density lipoprotein binding protein (Vigilin), isoform CRA_a OS	22.63045311	21.8818512	22.13062859	21.87927246

Q00610-2	CLH1_HUMAN Isoform 2 of Clathrin heavy chain 1 OS	24.28333855	24.4599514	24.52348709	24.4379673
A0A1W2PPS1	A0A1W2PPS1_HUMAN Heterogeneous nuclear ribonucleoprotein U OS	22.81362534	22.8461132	22.21252441	22.80616951
Q01082	SPTB2_HUMAN Spectrin beta chain, non-erythrocytic 1 OS	20.09377861	20.3208046	20.39110565	19.40790939
Q01105-3	SET_HUMAN Isoform 3 of Protein SET OS	22.15761375	21.89371109	21.63688278	21.83174896
Q01469	FABP5_HUMAN Fatty acid-binding protein 5 OS	19.76960945	19.52793121	19.37285995	19.24328041
Q01518-2	CAP1_HUMAN Isoform 2 of Adenylyl cyclase-associated protein 1 OS	23.38811111	22.81166649	22.88028145	22.88689995
Q01813	PFKAP_HUMAN ATP-dependent 6-phosphofructokinase, platelet type OS	21.26161003	20.82593918	20.44929695	20.34667778
Q01995	TAGL_HUMAN Transgelin OS	25.09583282	24.96128654	25.1590786	24.31264496
M0R3D6	M0R3D6_HUMAN 60S ribosomal protein L18a (Fragment) OS	19.75468254	20.95659828	21.43043137	19.5927887
Q02878	RL6_HUMAN 60S ribosomal protein L6 OS	22.6342926	22.74763489	22.59573364	22.70256615
Q03135	CAV1_HUMAN Caveolin-1 OS	22.41717529	22.91661263	22.47375298	21.99565887
Q04637-6	IF4G1_HUMAN Isoform E of Eukaryotic translation initiation factor 4 gamma 1 OS	18.87566185	21.64891052	21.73309898	21.32668686
Q04917	1433F_HUMAN 14-3-3 protein eta OS	22.33043861	21.76672554	21.66422844	21.3857975
Q05682-5	CALD1_HUMAN Isoform 5 of Caldesmon OS	23.44695282	23.52324867	23.57957458	23.55145073
A0A6I8PTT9	A0A6I8PTT9_HUMAN Glutamine--fructose-6-phosphate transaminase (isomerizing) OS	19.03189087	18.82517242	19.52383232	20.12578201
Q06323	PSME1_HUMAN Proteasome activator complex subunit 1 OS	20.07313156	18.79440498	18.25384521	19.6867466
Q06830	PRDX1_HUMAN Peroxiredoxin-1 OS	24.96035957	24.15398598	24.34448624	24.11791039
Q07020	RL18_HUMAN 60S ribosomal protein L18 OS	23.02531433	23.17790031	22.8281498	21.97819901
Q07065	CKAP4_HUMAN Cytoskeleton-associated protein 4 OS	25.25666618	25.28957748	25.32717896	25.23553276
Q08211	DHX9_HUMAN ATP-dependent RNA helicase A OS	20.98454094	20.9061718	21.01065636	21.02614212
Q09666	AHNK_HUMAN Neuroblast differentiation-associated protein AHNAK OS	26.62100792	26.41356087	26.47032356	25.94518661
Q12792	TWF1_HUMAN Twinfilin-1 OS	19.92853546	19.87456703	19.09229469	19.71100426
Q13162	PRDX4_HUMAN Peroxiredoxin-4 OS	18.68662453	20.78700066	18.63160133	21.92972755
Q13200	PSMD2_HUMAN 26S proteasome non-ATPase regulatory subunit 2 OS	20.86831093	20.59623337	20.59614182	21.10174942
A0A7I2YQU2	A0A7I2YQU2_HUMAN Eukaryotic translation initiation factor 3 subunit I OS	18.56655884	19.83174896	18.65626717	19.56917
Q13404	UB2V1_HUMAN Ubiquitin-conjugating enzyme E2 variant 1 OS	24.62405205	24.62823105	24.45481682	24.98215675
Q13509	TBB3_HUMAN Tubulin beta-3 chain OS	20.71665955	20.27344131	20.58306885	19.21914864
Q13813-3	SPTN1_HUMAN Isoform 3 of Spectrin alpha chain, non-erythrocytic 1 OS	20.70902061	21.31744194	20.69905472	20.48424149
Q13885	TBB2A_HUMAN Tubulin beta-2A chain OS	21.21365166	20.09377861	20.43857574	19.739748
Q14019	COTL1_HUMAN Coactosin-like protein OS	21.77386284	21.90142822	22.01573563	21.13652229
H0YA96	H0YA96_HUMAN Heterogeneous nuclear ribonucleoprotein D0 (Fragment) OS	22.32750893	21.78656197	21.28799438	22.0921669
Q14152	EIF3A_HUMAN Eukaryotic translation initiation factor 3 subunit A OS	20.89245033	21.60462761	20.39508629	20.68970108
Q14203-5	DCTN1_HUMAN Isoform 5 of Dynactin subunit 1 OS	17.61199188	19.21425819	17.94719696	18.45355988
Q14204	DYHC1_HUMAN Cytoplasmic dynein 1 heavy chain 1 OS	23.90113258	23.65403366	23.85908508	23.16855049
Q14315	FLNC_HUMAN Filamin-C OS	27.09194374	26.97421265	26.98185349	26.87244034
Q14697	GANAB_HUMAN Neutral alpha-glucosidase AB OS	22.99762344	23.51941299	23.18717575	23.43529892
Q14764	MVP_HUMAN Major vault protein OS	20.39058113	22.77344131	19.33424759	21.94510269
Q14847	LASP1_HUMAN LIM and SH3 domain protein 1 OS	21.31290817	21.60688782	22.53036308	21.82325935
Q14974	IMB1_HUMAN Importin subunit beta-1 OS	22.30866432	21.90517998	22.1890316	21.7320652
Q15019	SEPT2_HUMAN Septin-2 OS	22.23861885	21.11362457	21.44985199	21.60765457
Q15056-2	IF4H_HUMAN Isoform Short of Eukaryotic translation initiation factor 4H OS	20.77305794	20.79827881	18.79834366	21.32558823

Q15084-3	PDIA6_HUMAN Isoform 3 of Protein disulfide-isomerase A6 OS	22.83953667	22.79237175	22.26224136	23.43338966
Q15149-4	PLEC_HUMAN Isoform 4 of Plectin OS	24.71711922	24.969347	24.830019	24.10181427
Q15293	RCN1_HUMAN Reticulocalbin-1 OS	21.11977959	21.70150948	21.04353523	20.97784996
Q15365	PCBP1_HUMAN Poly(rC)-binding protein 1 OS	21.63732529	22.02799988	22.22914124	22.05135727
Q15366-6	PCBP2_HUMAN Isoform 6 of Poly(rC)-binding protein 2 OS	20.50057411	18.698452	20.46483231	20.68294716
B8ZZU8	B8ZZU8_HUMAN Elongin-B OS	19.77781677	19.90050697	19.78297615	20.01876068
F5H365	F5H365_HUMAN Protein transport protein SEC23 OS	17.96944618	18.96937752	18.12153816	21.32542419
Q15691	MARE1_HUMAN Microtubule-associated protein RP/EB family member 1 OS	17.83308029	20.34884071	19.53636169	20.24504662
Q15758	AAAT_HUMAN Neutral amino acid transporter B(0) OS	20.70379257	20.43705368	20.63856316	20.75971222
Q15907	RB11B_HUMAN Ras-related protein Rab-11B OS	22.26252937	22.26258659	22.11524582	22.28587914
Q15942	ZYX_HUMAN Zyxin OS	22.23613739	22.16287804	22.59201813	22.23567009
E7ES33	E7ES33_HUMAN Septin OS	21.20794678	21.85269928	20.24562645	21.16195679
Q16222-3	UAP1_HUMAN Isoform 3 of UDP-N-acetylhexosamine pyrophosphorylase OS	19.39533806	19.98273277	20.26670837	20.1983242
Q16527	CSRP2_HUMAN Cysteine and glycine-rich protein 2 OS	19.78471756	20.29165268	19.84460068	18.88469315
Q16555-2	DPYL2_HUMAN Isoform 2 of Dihydropyrimidinase-related protein 2 OS	22.42393494	22.52125931	22.51662636	22.7605648
Q16658	FSCN1_HUMAN Fascin OS	23.51905441	23.55461693	23.22679138	23.33197021
A0A7I2YQ74	A0A7I2YQ74_HUMAN UTP--glucose-1-phosphate uridylyltransferase OS	20.23350716	20.25118637	20.38004684	20.29949951
E9PIR7	E9PIR7_HUMAN Thioredoxin-disulfide reductase OS	20.91590309	20.79867363	18.58206558	19.95005989
Q6NZI2	CAVN1_HUMAN Caveolae-associated protein 1 OS	22.70372963	23.40080261	23.39309692	23.35272408
Q6UVK1	CSPG4_HUMAN Chondroitin sulfate proteoglycan 4 OS	19.39962006	19.93574715	20.68671227	19.50047684
Q70UQ0-4	IKIP_HUMAN Isoform 4 of Inhibitor of nuclear factor kappa-B kinase-interacting protein OS	19.40643692	18.23005867	19.04209328	20.60503387
Q7KZF4	SND1_HUMAN Staphylococcal nuclease domain-containing protein 1 OS	22.73789215	22.74517441	23.06307602	22.70459366
Q86VP6	CAND1_HUMAN Cullin-associated NEDD8-dissociated protein 1 OS	20.53782082	20.93026924	20.72050476	20.99444962
Q8NBS9-2	TXND5_HUMAN Isoform 2 of Thioredoxin domain-containing protein 5 OS	21.11273384	20.36879539	20.0941658	20.95496559
Q8TED1	GPX8_HUMAN Probable glutathione peroxidase 8 OS	20.08485603	19.09341431	19.99507141	19.04289818
Q8WUM4	PDC6I_HUMAN Programmed cell death 6-interacting protein OS	21.28455353	19.92161369	18.27128601	20.72533989
Q92499-3	DDX1_HUMAN Isoform 3 of ATP-dependent RNA helicase DDX1 OS	18.12132645	20.40613365	18.52245331	18.84397888
Q92598-2	HS105_HUMAN Isoform Beta of Heat shock protein 105 kDa OS	18.6023674	20.34797668	18.33521271	20.21643829
Q92616	GCN1_HUMAN eIF-2-alpha kinase activator GCN1 OS	18.45020676	19.38721085	20.10098076	18.54070282
A0A087WTP3	A0A087WTP3_HUMAN Far upstream element-binding protein 2 OS	21.17169952	20.74197006	20.79891205	20.47704315
Q92973-2	TNPO1_HUMAN Isoform 2 of Transportin-1 OS	18.61182785	20.31959343	18.71065712	18.6649456
Q969G5	CAVN3_HUMAN Caveolae-associated protein 3 OS	21.30969238	21.17846298	20.51595306	21.67878342
Q969H8	MYDGF_HUMAN Myeloid-derived growth factor OS	21.56365013	21.38337326	21.09847641	21.35143089
Q96AE4	FUBP1_HUMAN Far upstream element-binding protein 1 OS	20.86883736	20.4691124	20.22646904	19.21940613
Q96AG4	LRC59_HUMAN Leucine-rich repeat-containing protein 59 OS	21.9192524	22.20353127	22.36327171	22.0500946
Q96AY3	FKB10_HUMAN Peptidyl-prolyl cis-trans isomerase FKBP10 OS	20.18410492	19.36252594	20.24933624	19.78151894
Q96HC4	PDLI5_HUMAN PDZ and LIM domain protein 5 OS	18.70390511	19.27682877	19.87273407	19.69335556
Q96QK1	VPS35_HUMAN Vacuolar protein sorting-associated protein 35 OS	18.32221222	19.24896812	19.19289398	20.00990486
Q96TA1-2	NIBA2_HUMAN Isoform 2 of Protein Niban 2 OS	19.14989853	20.91086197	20.85376549	20.61387253
A0A087X271	A0A087X271_HUMAN Calponin (Fragment) OS	23.69699669	23.3259449	21.96183395	22.62075615

A0A7I2V641	A0A7I2V641_HUMAN 26S proteasome non-ATPase regulatory subunit 1 OS	18.28941727	19.67624664	19.57581902	18.32927704
Q99497	PARK7_HUMAN Parkinson disease protein 7 OS	22.21092033	22.30401993	22.20490456	21.77193069
Q99536	VAT1_HUMAN Synaptic vesicle membrane protein VAT-1 homolog OS	22.63396072	22.03795052	19.75020599	21.72317505
F5GY37	F5GY37_HUMAN Prohibitin OS	21.92788506	21.71962738	20.81550217	21.71895981
Q99715-4	COCA1_HUMAN Isoform 4 of Collagen alpha-1(XII) chain OS	19.68501854	19.96253967	19.78284836	18.75119781
Q99832	TCPH_HUMAN T-complex protein 1 subunit eta OS	21.34884071	20.57800865	21.46856689	21.84352875
Q9BRA2	TXD17_HUMAN Thioredoxin domain-containing protein 17 OS	19.84862518	19.68291283	20.00675964	20.44717979
Q9BSJ8	ESYT1_HUMAN Extended synaptotagmin-1 OS	20.17803764	20.97673225	20.32223701	20.76773453
Q9BUF5	TBB6_HUMAN Tubulin beta-6 chain OS	23.14765167	22.41423607	22.6908741	22.16459846
Q9BVK6	TMED9_HUMAN Transmembrane emp24 domain-containing protein 9 OS	19.98036194	20.52008629	19.68292999	20.33712578
Q9H0U4	RAB1B_HUMAN Ras-related protein Rab-1B OS	22.75906181	22.75963211	22.9252243	22.09326363
Q5T123	Q5T123_HUMAN SH3 domain-binding glutamic acid-rich-like protein 3 OS	21.15189934	18.7892971	18.71455956	20.36292458
Q9H3N1	TMX1_HUMAN Thioredoxin-related transmembrane protein 1 OS	18.19048309	20.78668213	19.18562889	17.42985535
Q9H4M9	EHD1_HUMAN EH domain-containing protein 1 OS	18.41928482	19.01069069	20.92672729	21.23502731
Q9HB71	CYBP_HUMAN Calcyclin-binding protein OS	18.70917511	20.5643959	18.91725349	18.86560249
A0A087X163	A0A087X163_HUMAN Ras-related protein Rab-18 OS	18.61141777	19.37511063	18.93945313	18.47066879
Q9NQC3-2	RTN4_HUMAN Isoform B of Reticulon-4 OS	23.34272385	22.8412838	22.71078682	23.19751549
Q9NR12	PDLI7_HUMAN PDZ and LIM domain protein 7 OS	18.79019356	19.67226219	19.06404877	19.15857887
Q9NRV9	HEBP1_HUMAN Heme-binding protein 1 OS	18.67448997	18.21212578	19.93890762	18.86046219
D6RGI3	D6RGI3_HUMAN Septin OS	22.12164688	21.77996635	21.67998695	21.34651566
Q9NZM1-6	MYOF_HUMAN Isoform 6 of Myoferlin OS	23.84957314	23.01350403	23.11109543	22.56048203
Q9NZN4	EHD2_HUMAN EH domain-containing protein 2 OS	22.09329414	21.28421402	21.56644058	21.16373825
Q9P0L0	VAPA_HUMAN Vesicle-associated membrane protein-associated protein A OS	19.88254547	19.76885033	19.23502541	18.76872063
Q9P2E9	RRBP1_HUMAN Ribosome-binding protein 1 OS	23.50178909	23.40911674	23.15705872	23.19231606
F8VQE1	F8VQE1_HUMAN LIM domain and actin-binding protein 1 OS	21.16974449	20.71749496	18.20223618	20.70480537
Q9UHD8-7	SEPT9_HUMAN Isoform 7 of Septin-9 OS	22.38955688	22.09026146	22.11565781	22.17273712
Q9ULV4	COR1C_HUMAN Coronin-1C OS	20.39267731	20.36591721	21.1221199	20.94320679
Q9UQ80-2	PA2G4_HUMAN Isoform 2 of Proliferation-associated protein 2G4 OS	21.8764267	21.51931763	21.58664513	21.97620773
Q9Y230	RUVB2_HUMAN RuvB-like 2 OS	18.30500984	18.33820915	20.23128128	19.30720139
Q9Y265	RUVB1_HUMAN RuvB-like 1 OS	18.55114746	20.03335381	20.45100975	20.28557014
Q9Y266	NUDC_HUMAN Nuclear migration protein nudC OS	19.0090847	19.68888283	17.75411606	18.9045372
Q9Y3U8	RL36_HUMAN 60S ribosomal protein L36 OS	20.48197746	21.4355793	20.8459034	20.64570427
Q9Y490	TLN1_HUMAN Talin-1 OS	24.84388351	24.7702179	24.88920403	24.74180603
A0A087X054	A0A087X054_HUMAN Hypoxia up-regulated protein 1 OS	20.05642509	20.02485847	21.03106499	19.64225197
Q9Y617-2	SERC_HUMAN Isoform 2 of Phosphoserine aminotransferase OS	21.74176407	21.5323143	21.55982971	21.35681343
Q9Y678	COPG1_HUMAN Coatomer subunit gamma-1 OS	21.22640991	21.85551643	21.95521355	21.34705734
Q9Y696	CLIC4_HUMAN Chloride intracellular channel protein 4 OS	22.36956787	22.27673721	21.01277161	21.85365295

Accession	**Protein**	**LFQ intensity eGFP 48hrs**	**LFQ intensity Envelope 48hrs**	**LFQ intensity Membrane 48hrs**	**LFQ intensity Nucleocapsid 48hrs**
H3BTL1	H3BTL1_HUMAN Microtubule-associated protein 1 light chain 3 beta, isoform CRA_f OS	20.61602783	19.31570053	20.51749229	20.4514122

Q99613-2	EIF3C_HUMAN Isoform 2 of Eukaryotic translation initiation factor 3 subunit C OS	20.29052734	20.32695961	20.18664551	20.28263092
F8VZJ2	F8VZJ2_HUMAN Nascent polypeptide-associated complex subunit alpha OS	21.19904518	18.63215828	21.84230042	22.28022575
O00148	DX39A_HUMAN ATP-dependent RNA helicase DDX39A OS	20.31118965	20.01835251	20.09571075	18.59388924
O00159-2	MYO1C_HUMAN Isoform 2 of Unconventional myosin-Ic OS	22.21106911	21.78320694	21.85733986	22.21380043
O00231	PSD11_HUMAN 26S proteasome non-ATPase regulatory subunit 11 OS	21.21406746	20.9754734	21.56899261	21.15480614
O00232-2	PSD12_HUMAN Isoform 2 of 26S proteasome non-ATPase regulatory subunit 12 OS	20.46513176	19.75865555	19.89496803	18.77387047
O00299	CLIC1_HUMAN Chloride intracellular channel protein 1 OS	24.23066711	24.3347683	24.61071014	23.91988945
O00303	EIF3F_HUMAN Eukaryotic translation initiation factor 3 subunit F OS	19.38295746	18.56738091	20.39571381	18.66461372
O00410	IPO5_HUMAN Importin-5 OS	21.32849503	21.32350159	21.36890221	21.21204948
A0A2R8Y5G6	A0A2R8Y5G6_HUMAN RNA helicase OS	21.15684319	21.00915337	20.47040558	20.73859406
O14818	PSA7_HUMAN Proteasome subunit alpha type-7 OS	22.06785774	22.11581802	22.22925949	22.20669556
P19105	ML12A_HUMAN Myosin regulatory light chain 12A OS	23.62399483	23.00559425	23.69508553	23.48000526
O15143	ARC1B_HUMAN Actin-related protein 2/3 complex subunit 1B OS	21.59700775	20.73809814	21.18755341	21.15455818
O15144	ARPC2_HUMAN Actin-related protein 2/3 complex subunit 2 OS	20.68628502	18.87779427	21.54858398	21.10232735
A0A286YF22	A0A286YF22_HUMAN D-3-phosphoglycerate dehydrogenase OS	22.08229065	21.99603844	21.67499733	21.21092033
O43242	PSMD3_HUMAN 26S proteasome non-ATPase regulatory subunit 3 OS	20.24411774	20.6088295	20.23899651	20.32794762
O43707	ACTN4_HUMAN Alpha-actinin-4 OS	23.97561264	23.64603424	23.7552166	24.17119598
O43795-2	MYO1B_HUMAN Isoform 2 of Unconventional myosin-Ib OS	20.40114212	19.9607029	19.70079803	20.30529976
O43852	CALU_HUMAN Calumenin OS	23.17360687	23.74375916	23.61862946	22.98340988
O60506-4	HNRPQ_HUMAN Isoform 4 of Heterogeneous nuclear ribonucleoprotein Q OS	23.01831818	21.88136482	21.81979561	22.45603371
O60664-4	PLIN3_HUMAN Isoform 4 of Perilipin-3 OS	22.88912964	22.62209702	22.99765778	22.50491905
O60701	UGDH_HUMAN UDP-glucose 6-dehydrogenase OS	23.14577103	23.81723976	23.6198616	23.17949677
O60763	USO1_HUMAN General vesicular transport factor p115 OS	20.40062141	19.94377899	19.95503616	20.12338448
O75083	WDR1_HUMAN WD repeat-containing protein 1 OS	23.52169228	23.40483665	23.53575897	23.6003685
E5RIW3	E5RIW3_HUMAN Tubulin-specific chaperone A OS	20.54745483	20.4355278	20.63129807	18.83438873
O75369-2	FLNB_HUMAN Isoform 2 of Filamin-B OS	23.62878609	23.7702179	23.60614204	23.62667084
B4DJV2	B4DJV2_HUMAN Citrate synthase OS	21.43903351	20.50106049	21.43786621	21.09029388
O75396	SC22B_HUMAN Vesicle-trafficking protein SEC22b OS	22.06887627	21.81323242	21.65285301	22.25245667
O76003	GLRX3_HUMAN Glutaredoxin-3 OS	18.77362633	19.87885284	18.01993942	18.97174072
O94979-3	SC31A_HUMAN Isoform 3 of Protein transport protein Sec31A OS	21.21501541	20.64640808	21.30123138	21.05867386
O95373	IPO7_HUMAN Importin-7 OS	21.0726738	20.87882233	20.47050476	20.38479614
O95782-2	AP2A1_HUMAN Isoform B of AP-2 complex subunit alpha-1 OS	19.65579987	19.41734505	19.11441422	18.37331772
O95816	BAG2_HUMAN BAG family molecular chaperone regulator 2 OS	20.03778267	19.60074043	19.6768322	19.50629997
P00338	LDHA_HUMAN L-lactate dehydrogenase A chain OS	25.59931946	24.21178246	25.64121819	25.35194969
P00367	DHE3_HUMAN Glutamate dehydrogenase 1, mitochondrial OS	20.1382122	21.23257065	20.90771294	21.21199036
P00387-2	NB5R3_HUMAN Isoform 2 of NADH-cytochrome b5 reductase 3 OS	22.25161934	20.54113388	22.09635544	22.2870369
P00403	COX2_HUMAN Cytochrome c oxidase subunit 2 OS	20.18519402	20.31030273	20.06276321	17.92194557
P00505-2	AATM_HUMAN Isoform 2 of Aspartate aminotransferase, mitochondrial OS	20.38711357	19.84133339	19.64602089	20.5334549

P00558	PGK1_HUMAN Phosphoglycerate kinase 1 OS	23.70038795	24.01077652	23.98085022	23.66231728
P00568	KAD1_HUMAN Adenylate kinase isoenzyme 1 OS	20.12691689	19.76556778	19.90935326	20.07156181
P02452	CO1A1_HUMAN Collagen alpha-1(I) chain OS	25.26054955	25.17157745	25.11787033	25.20407677
P02545	LMNA_HUMAN Prelamin-A/C OS	25.40291786	25.47512627	25.71319008	25.26456261
P02751-5	FINC_HUMAN Isoform 5 of Fibronectin OS	21.25902557	21.49921227	20.68551445	21.11426163
P02786	TFR1_HUMAN Transferrin receptor protein 1 OS	21.27685165	20.27161789	20.21714783	21.07365608
P04075	ALDOA_HUMAN Fructose-bisphosphate aldolase A OS	25.17352295	25.48793602	24.71093369	25.2035923
P04080	CYTB_HUMAN Cystatin-B OS	21.09596825	20.51152039	20.36099625	21.31986809
P04083	ANXA1_HUMAN Annexin A1 OS	25.85984421	25.46245003	25.31451225	25.27191734
P04181	OAT_HUMAN Ornithine aminotransferase, mitochondrial OS	19.77516747	20.05576515	20.26899338	18.02760124
P04350	TBB4A_HUMAN Tubulin beta-4A chain OS	21.51821327	20.98974609	21.78831482	20.72966003
P04406	G3P_HUMAN Glyceraldehyde-3-phosphate dehydrogenase OS	26.29617691	25.36649704	25.45741844	25.5820179
K7EM73	K7EM73_HUMAN Calcium-activated neutral proteinase small subunit (Fragment) OS	21.22205162	21.29473877	21.43822098	21.59363747
A0A6Q8PFK8	A0A6Q8PFK8_HUMAN Heat shock protein beta-1 OS	24.37245369	24.6660614	24.20254517	24.95628738
P04843	RPN1_HUMAN Dolichyl-diphosphooligosaccharide--protein glycosyltransferase subunit 1 OS	23.33046532	23.2104454	22.76013947	23.20088577
P04844-2	RPN2_HUMAN Isoform 2 of Dolichyl-diphosphooligosaccharide--protein glycosyltransferase subunit 2 OS	22.18365097	21.64403152	21.6032238	21.49658012
P05023-3	AT1A1_HUMAN Isoform 3 of Sodium/potassium-transporting ATPase subunit alpha-1 OS	21.11057091	21.35525513	20.99113083	21.16263199
P05141	ADT2_HUMAN ADP/ATP translocase 2 OS	21.48365021	22.39949989	22.11069679	22.44609451
P05387	RLA2_HUMAN 60S acidic ribosomal protein P2 OS	20.08770561	20.49589729	19.80579185	20.27514648
P05388	RLA0_HUMAN 60S acidic ribosomal protein P0 OS	22.57147217	22.75007057	22.37530708	22.33992767
P05455	LA_HUMAN Lupus La protein OS	20.00429153	21.74291611	20.257761	20.50193405
H7C4K3	H7C4K3_HUMAN Integrin beta-1 OS	22.8581562	23.02396202	23.01133919	22.98018837
P06576	ATPB_HUMAN ATP synthase subunit beta, mitochondrial OS	24.12344742	23.96410942	23.83740044	24.01996422
R4GN98	R4GN98_HUMAN Protein S100 (Fragment) OS	20.72208977	21.599823	20.35906792	20.35767174
P06733	ENOA_HUMAN Alpha-enolase OS	26.74111176	26.54545403	26.79426765	26.75684547
P06744	G6PI_HUMAN Glucose-6-phosphate isomerase OS	22.42864418	22.34499931	22.41763878	22.10261536
P06748-3	NPM_HUMAN Isoform 3 of Nucleophosmin OS	22.79336548	22.7108078	22.87464523	23.0128746
P06753-2	TPM3_HUMAN Isoform 2 of Tropomyosin alpha-3 chain OS	24.54250526	25.21337891	24.96886253	24.77700806
P07195	LDHB_HUMAN L-lactate dehydrogenase B chain OS	23.85880089	23.40002251	23.93409157	23.63289642
P07237	PDIA1_HUMAN Protein disulfide-isomerase OS	24.70054626	24.93111801	24.70677757	24.89254379
P07355	ANXA2_HUMAN Annexin A2 OS	26.59733009	26.1086483	26.18290901	26.60865402
Q5JP53	Q5JP53_HUMAN Tubulin beta chain OS	25.12904167	25.62220955	25.58840752	25.11521339
P07737	PROF1_HUMAN Profilin-1 OS	25.58626175	25.19636726	25.59391594	25.46323013
P07741-2	APT_HUMAN Isoform 2 of Adenine phosphoribosyltransferase OS	19.62508392	19.3804493	19.40645027	18.29244232
P07814	SYEP_HUMAN Bifunctional glutamate/proline--tRNA ligase OS	21.41245461	21.20251656	21.11711884	20.71498299
A0A7I2V668	A0A7I2V668_HUMAN Cathepsin B OS	21.01352119	21.11222649	18.72297287	21.22864342
P07900	HS90A_HUMAN Heat shock protein HSP 90-alpha OS	25.17866135	25.23066711	25.19490433	25.04485321
P07954-2	FUMH_HUMAN Isoform Cytoplasmic of Fumarate hydratase, mitochondrial OS	20.41069603	20.77940559	20.80970573	18.50860214

A0A087WTA8	A0A087WTA8_HUMAN Collagen alpha-2(I) chain OS	24.04009247	24.18971062	23.89050484	23.835186
P08133-2	ANXA6_HUMAN Isoform 2 of Annexin A6 OS	23.14861298	22.47397614	22.0764637	23.00011826
P08195-2	4F2_HUMAN Isoform 2 of 4F2 cell-surface antigen heavy chain OS	21.80278206	21.16545677	18.55701637	21.57846832
P08238	HS90B_HUMAN Heat shock protein HSP 90-beta OS	26.72103691	27.03601074	26.61259651	26.97278976
P08670	VIME_HUMAN Vimentin OS	27.92643166	27.78144264	27.94642639	27.59967422
P08708	RS17_HUMAN 40S ribosomal protein S17 OS	19.34197617	20.06999016	20.12401581	20.2693367
P08758	ANXA5_HUMAN Annexin A5 OS	25.90728951	24.90370941	26.21661949	25.90274429
C9J9K3	C9J9K3_HUMAN 40S ribosomal protein SA (Fragment) OS	22.93883514	22.66955757	22.58297539	23.36932945
P09211	GSTP1_HUMAN Glutathione S-transferase P OS	23.5114727	24.15506744	24.5366478	24.07879448
P09382	LEG1_HUMAN Galectin-1 OS	24.75139046	25.20910645	25.52966499	25.35910797
P09493-3	TPM1_HUMAN Isoform 3 of Tropomyosin alpha-1 chain OS	23.28686714	22.82801437	23.23216057	23.02414894
P09651-3	ROA1_HUMAN Isoform 2 of Heterogeneous nuclear ribonucleoprotein A1 OS	22.3688221	23.61031723	22.52075768	22.28940201
P09936	UCHL1_HUMAN Ubiquitin carboxyl-terminal hydrolase isozyme L1 OS	22.0267849	21.69947815	21.65302849	22.27463531
J3QS39	J3QS39_HUMAN Polyubiquitin-B (Fragment) OS	25.43083954	25.14230728	25.24793243	25.28866386
P0DMV8-2	HS71A_HUMAN Isoform 2 of Heat shock 70 kDa protein 1A OS	23.30480003	22.37289238	22.56043625	23.17430878
P0DP25	CALM3_HUMAN Calmodulin-3 OS	22.3113842	21.35563087	22.31705475	21.82609558
P10599	THIO_HUMAN Thioredoxin OS	23.29516029	22.97388077	22.84155273	22.73783112
A0A7I2V599	A0A7I2V599_HUMAN 60 kDa heat shock protein, mitochondrial OS	23.77655602	24.07373619	24.05191994	24.16629982
P11021	BIP_HUMAN Endoplasmic reticulum chaperone BiP OS	26.22101593	26.02892685	25.72832298	26.22131157
P11142	HSP7C_HUMAN Heat shock cognate 71 kDa protein OS	26.54633713	26.52459335	26.42298889	26.63339424
P11279	LAMP1_HUMAN Lysosome-associated membrane glycoprotein 1 OS	21.02884293	21.24504662	18.07195663	18.31446075
P11413	G6PD_HUMAN Glucose-6-phosphate 1-dehydrogenase OS	23.51159286	23.81303787	23.84249306	23.78954887
V9GYY3	V9GYY3_HUMAN C-1-tetrahydrofolate synthase, cytoplasmic OS	20.76902771	20.7466526	20.46463394	20.99133873
P11940-2	PABP1_HUMAN Isoform 2 of Polyadenylate-binding protein 1 OS	22.49689674	22.47951126	21.75678444	22.63325119
P12004	PCNA_HUMAN Proliferating cell nuclear antigen OS	19.69995117	19.57966614	19.51034355	19.98189545
A0A087X0S5	A0A087X0S5_HUMAN Collagen alpha-1(VI) chain OS	20.94756508	20.67796707	20.38131523	20.73900604
P12110-3	CO6A2_HUMAN Isoform 2C2A of Collagen alpha-2(VI) chain OS	20.41379738	19.88619614	19.87937737	19.74571609
P12111-2	CO6A3_HUMAN Isoform 2 of Collagen alpha-3(VI) chain OS	21.92321205	22.11158943	22.16177177	21.7786026
P12236	ADT3_HUMAN ADP/ATP translocase 3 OS	20.45402527	20.4596405	21.09699821	21.72953606
E7ETK5	E7ETK5_HUMAN Inosine-5-monophosphate dehydrogenase 2 OS	19.78273582	20.56504631	20.41751099	20.21204948
P12814	ACTN1_HUMAN Alpha-actinin-1 OS	23.76698685	23.12697983	23.49191666	23.29516029
P12956	XRCC6_HUMAN X-ray repair cross-complementing protein 6 OS	22.56695175	22.32465553	21.75319672	22.34519005
P13010	XRCC5_HUMAN X-ray repair cross-complementing protein 5 OS	21.67856979	21.08582687	20.87199783	21.24736595
P13489	RINI_HUMAN Ribonuclease inhibitor OS	21.70446777	18.20135307	21.84804535	21.52387047
P13639	EF2_HUMAN Elongation factor 2 OS	25.30218697	25.73259735	26.16109848	25.58972359
P13667	PDIA4_HUMAN Protein disulfide-isomerase A4 OS	22.57482529	22.61261368	22.5365181	22.94567299
P13693	TCTP_HUMAN Translationally-controlled tumor protein OS	22.15591812	21.87428856	21.91148376	22.06292725
P13797-3	PLST_HUMAN Isoform 3 of Plastin-3 OS	21.77096367	21.26080704	20.74098396	21.45347404

P14314-2	GLU2B_HUMAN Isoform 2 of Glucosidase 2 subunit beta OS	21.38047028	21.60086823	22.08255005	21.5177803
P14618	KPYM_HUMAN Pyruvate kinase PKM OS	27.30426025	27.35951042	26.99269676	27.45615005
P14625	ENPL_HUMAN Endoplasmin OS	25.62522316	25.66901207	25.58588982	25.55218506
P14868-2	SYDC_HUMAN Isoform 2 of Aspartate--tRNA ligase, cytoplasmic OS	20.97568321	21.10290337	20.97098732	21.48084259
P15121	ALDR_HUMAN Aldo-keto reductase family 1 member B1 OS	20.20012283	19.66695213	20.00072098	20.58710289
P15170-2	ERF3A_HUMAN Isoform 2 of Eukaryotic peptide chain release factor GTP-binding subunit ERF3A OS	19.17871857	18.8816967	18.65241432	18.97840881
E7EQR4	E7EQR4_HUMAN Ezrin OS	21.62408447	21.44637299	21.66353416	21.60648155
P15531	NDKA_HUMAN Nucleoside diphosphate kinase A OS	20.1347065	20.28353691	19.48254776	20.32454491
B4DLR8	B4DLR8_HUMAN NAD(P)H dehydrogenase [quinone] 1 OS	22.44753265	21.86578369	22.30376816	22.73442268
P15880	RS2_HUMAN 40S ribosomal protein S2 OS	21.24411774	18.87893677	21.9693718	21.77503014
H0YD13	H0YD13_HUMAN CD44 antigen OS	22.43895721	23.2060833	23.46063995	22.74071503
P16152	CBR1_HUMAN Carbonyl reductase [NADPH] 1 OS	20.7833271	20.15400314	20.06276321	21.21957207
P16401	H15_HUMAN Histone H1.5 OS	18.7462368	19.19828224	20.49921227	18.50682259
P16403	H12_HUMAN Histone H1.2 OS	22.38640213	18.74824715	22.90209007	22.68478775
A2A2D0	A2A2D0_HUMAN Stathmin (Fragment) OS	22.34226227	22.94529915	22.71406174	22.72735596
P17066	HSP76_HUMAN Heat shock 70 kDa protein 6 OS	24.61397362	18.26551056	24.45437813	23.79897118
P17301	ITA2_HUMAN Integrin alpha-2 OS	20.31406975	20.44505882	21.03624153	19.52389908
P17844-2	DDX5_HUMAN Isoform 2 of Probable ATP-dependent RNA helicase DDX5 OS	21.87075806	21.69782448	21.48718834	22.00747681
P17931	LEG3_HUMAN Galectin-3 OS	21.06651306	20.39863968	20.80388451	21.38120842
P17987	TCPA_HUMAN T-complex protein 1 subunit alpha OS	22.82805443	22.23224831	22.20341301	21.87271309
P18077	RL35A_HUMAN 60S ribosomal protein L35a OS	21.2151947	20.62952042	20.89533806	18.39235115
P18085	ARF4_HUMAN ADP-ribosylation factor 4 OS	23.32635689	23.1848774	23.47691917	23.37491035
P18124	RL7_HUMAN 60S ribosomal protein L7 OS	22.77858353	22.86116982	22.92049026	21.71276093
P18206-2	VINC_HUMAN Isoform 1 of Vinculin OS	25.69399643	25.5762043	25.60995102	25.6798687
A0A087WXM6	A0A087WXM6_HUMAN 60S ribosomal protein L17 (Fragment) OS	21.83194351	22.09371376	22.00915337	22.17660713
P18669	PGAM1_HUMAN Phosphoglycerate mutase 1 OS	22.57996559	22.89827538	22.50629997	22.94472694
A0A7I2V5M5	A0A7I2V5M5_HUMAN Nucleolin OS	24.28376198	24.15305901	23.8727684	24.26492119
P20340-2	RAB6A_HUMAN Isoform 2 of Ras-related protein Rab-6A OS	20.35035133	20.64728546	19.22706413	20.53772736
P20618	PSB1_HUMAN Proteasome subunit beta type-1 OS	21.58879662	21.0796566	21.55314064	21.32756424
E9PP21	E9PP21_HUMAN Cysteine and glycine-rich protein 1 OS	22.84471703	22.3922596	22.31274033	23.36546326
P21333-2	FLNA_HUMAN Isoform 2 of Filamin-A OS	27.62086868	27.82468796	27.72916603	27.72227478
P21796	VDAC1_HUMAN Voltage-dependent anion-selective channel protein 1 OS	20.6687355	18.72044563	21.33848572	21.56583595
P21980	TGM2_HUMAN Protein-glutamine gamma-glutamyltransferase 2 OS	21.30513382	21.54787827	20.48079491	21.22193336
P22234	PUR6_HUMAN Multifunctional protein ADE2 OS	19.85329437	20.30039215	20.32926178	19.82730484
P22307-6	SCP2_HUMAN Isoform 6 of Sterol carrier protein 2 OS	20.27605629	20.05999374	19.90847397	19.79895973
P22314-2	UBA1_HUMAN Isoform 2 of Ubiquitin-like modifier-activating enzyme 1 OS	23.89458084	23.74201202	23.80262375	23.73923302
P22392-2	NDKB_HUMAN Isoform 3 of Nucleoside diphosphate kinase B OS	24.87084198	24.58703423	25.027071	24.5736351
A0A7I2V4I6	A0A7I2V4I6_HUMAN Heterogeneous nuclear ribonucleoproteins A2/B1 OS	22.01185036	21.45728683	22.39076424	21.95822716

A0A2R8YDM0	A0A2R8YDM0_HUMAN Prostaglandin-endoperoxide synthase (Fragment) OS	20.32586288	20.18046761	18.31494141	20.08160782
P23246	SFPQ_HUMAN Splicing factor, proline- and glutamine-rich OS	21.93700409	22.39204979	22.44929695	22.170784
P23284	PPIB_HUMAN Peptidyl-prolyl cis-trans isomerase B OS	24.49307823	24.43083954	24.33203888	24.61801338
P23381-2	SYWC_HUMAN Isoform 2 of Tryptophan--tRNA ligase, cytoplasmic OS	19.58361816	19.61547089	19.94206238	19.09093857
P23396	RS3_HUMAN 40S ribosomal protein S3 OS	24.05589676	23.84661102	24.10717392	23.0134201
P23526	SAHH_HUMAN Adenosylhomocysteinase OS	21.42639351	21.24341965	21.40374374	21.49896812
P23528	COF1_HUMAN Cofilin-1 OS	25.63425446	25.41902351	25.51023483	25.02356529
P23634-7	AT2B4_HUMAN Isoform ZB of Plasma membrane calcium-transporting ATPase 4 OS	19.09305573	18.99697495	19.97070694	19.05999374
P24534	EF1B_HUMAN Elongation factor 1-beta OS	22.53945541	22.28398895	23.46699905	18.71809959
Q5QNZ2	Q5QNZ2_HUMAN ATP synthase F(0) complex subunit B1, mitochondrial OS	19.74175644	19.88176727	19.82468224	20.20717239
P25398	RS12_HUMAN 40S ribosomal protein S12 OS	21.24010468	21.19111252	20.75702858	21.18960571
P25705	ATPA_HUMAN ATP synthase subunit alpha, mitochondrial OS	24.06899071	24.1180687	24.17554283	23.322649
F5GX11	F5GX11_HUMAN Proteasome subunit alpha type-1 OS	20.89326668	21.15776825	21.75991631	20.15721321
A0A7I2V2H3	A0A7I2V2H3_HUMAN UPF0415 protein C7orf25 OS	18.28251839	20.25395775	20.9078598	21.27560234
P25788-2	PSA3_HUMAN Isoform 2 of Proteasome subunit alpha type-3 OS	21.40504456	21.23473549	20.93437958	18.14051628
H0YMZ1	H0YMZ1_HUMAN Proteasome subunit alpha type (Fragment) OS	20.68918991	20.87342644	20.73355484	20.08511543
P26038	MOES_HUMAN Moesin OS	24.19355011	24.49405479	24.2624855	24.43338966
P26373	RL13_HUMAN 60S ribosomal protein L13 OS	22.53971481	22.312603	22.59839249	22.6654644
A6NLN1	A6NLN1_HUMAN Polypyrimidine tract-binding protein 1 OS	21.72538185	22.15412521	21.51383591	22.02242279
P26639	SYTC_HUMAN Threonine--tRNA ligase 1, cytoplasmic OS	20.62551308	20.51951027	20.79177666	21.08634567
P26640	SYVC_HUMAN Valine--tRNA ligase OS	20.20836258	20.69752693	20.3126297	20.14307976
P26641	EF1G_HUMAN Elongation factor 1-gamma OS	23.89993668	23.68474579	24.16851997	23.83026123
P27348	1433T_HUMAN 14-3-3 protein theta OS	22.66890907	22.60295296	22.68429565	22.8053627
F8W7C6	F8W7C6_HUMAN 60S ribosomal protein L10 OS	20.09777069	20.208601	20.27491951	20.58737755
P27797	CALR_HUMAN Calreticulin OS	24.5749054	23.92524338	23.95287132	24.04518509
P27816-6	MAP4_HUMAN Isoform 6 of Microtubule-associated protein 4 OS	22.35584641	22.31890297	21.99334526	22.26524925
P27824	CALX_HUMAN Calnexin OS	23.38640213	22.6495018	22.55510712	22.92092514
P28066	PSA5_HUMAN Proteasome subunit alpha type-5 OS	22.57500839	22.02958298	21.85919952	22.3742733
P28072	PSB6_HUMAN Proteasome subunit beta type-6 OS	21.40836525	21.35380173	21.3002243	21.63878441
P28074	PSB5_HUMAN Proteasome subunit beta type-5 OS	20.89548683	20.46093941	20.28973961	20.46303749
P29373	RABP2_HUMAN Cellular retinoic acid-binding protein 2 OS	19.99479485	21.08102226	18.70096016	18.61837006
P29401	TKT_HUMAN Transketolase OS	24.20776749	24.15282631	24.09884644	24.58141327
E9PK01	E9PK01_HUMAN Elongation factor 1-delta (Fragment) OS	23.50324631	23.40379715	23.96895027	23.96956635
P29966	MARCS_HUMAN Myristoylated alanine-rich C-kinase substrate OS	21.71082878	21.66674423	22.72317505	21.75747681
P30040	ERP29_HUMAN Endoplasmic reticulum resident protein 29 OS	20.35423279	20.56987381	20.70716667	20.00030899
P30041	PRDX6_HUMAN Peroxiredoxin-6 OS	22.99870872	22.94952583	22.97891426	23.0866375
P30044-2	PRDX5_HUMAN Isoform Cytoplasmic+peroxisomal of Peroxiredoxin-5, mitochondrial OS	20.39424896	20.23911285	20.7653904	20.62871933
P30048-2	PRDX3_HUMAN Isoform 2 of Thioredoxin-dependent peroxide reductase, mitochondrial OS	21.37225533	21.13570976	21.50533104	20.64755058

P30050	RL12_HUMAN 60S ribosomal protein L12 OS	23.00829887	22.51156998	23.46687508	22.59689331
P30086	PEBP1_HUMAN Phosphatidylethanolamine-binding protein 1 OS	21.32652092	21.54429817	21.36442184	21.65983772
P30101	PDIA3_HUMAN Protein disulfide-isomerase A3 OS	24.80548096	24.68051338	24.6496563	24.82914734
P30153	2AAA_HUMAN Serine/threonine-protein phosphatase 2A 65 kDa regulatory subunit A alpha isoform OS	21.11946297	21.01950645	20.6721077	20.49355507
P31153-2	METK2_HUMAN Isoform 2 of S-adenosylmethionine synthase isoform type-2 OS	20.46223831	18.66385651	20.77442741	20.27013588
P31939	PUR9_HUMAN Bifunctional purine biosynthesis protein ATIC OS	20.63023186	20.10674095	18.97669983	20.52878952
P31943	HNRH1_HUMAN Heterogeneous nuclear ribonucleoprotein H OS	22.08086014	21.91002083	21.93419838	21.38184357
P31946-2	1433B_HUMAN Isoform Short of 14-3-3 protein beta/alpha OS	22.59208679	22.45312119	22.50772858	22.56241608
P31948	STIP1_HUMAN Stress-induced-phosphoprotein 1 OS	21.73326492	21.64601135	21.98728561	21.84712791
P32119	PRDX2_HUMAN Peroxiredoxin-2 OS	21.55093384	21.07515717	21.79970169	21.80872345
D6RAN4	D6RAN4_HUMAN 60S ribosomal protein L9 (Fragment) OS	21.66657066	21.72671127	22.05543327	21.66882324
P33176	KINH_HUMAN Kinesin-1 heavy chain OS	21.65136528	21.56090164	21.58627892	21.76987457
H0YMM5	H0YMM5_HUMAN Deoxyuridine 5-triphosphate nucleotidohydrolase OS	19.21546173	19.30972672	18.38822746	19.26233101
P34932	HSP74_HUMAN Heat shock 70 kDa protein 4 OS	20.9091053	20.69845963	21.35186195	21.7148571
C9J0J7	C9J0J7_HUMAN Profilin OS	21.2540741	20.90793228	21.47990608	20.59194946
G3XAM7	G3XAM7_HUMAN Catenin (Cadherin-associated protein), alpha 1, 102kDa, isoform CRA_a OS	19.64450836	19.77747917	18.35654449	19.63878632
P35232	PHB_HUMAN Prohibitin OS	20.84597969	21.70281982	22.01991463	21.68589973
P35241	RADI_HUMAN Radixin OS	19.45977974	18.48234367	19.02935028	19.17589569
K7EP65	K7EP65_HUMAN 60S ribosomal protein L22 (Fragment) OS	21.96232796	22.31664085	21.82442665	21.80778122
P35579	MYH9_HUMAN Myosin-9 OS	27.69298744	27.68772507	27.64972496	27.52260399
P35580	MYH10_HUMAN Myosin-10 OS	19.84689903	20.07169342	20.23467636	19.03425407
P35637-2	FUS_HUMAN Isoform Short of RNA-binding protein FUS OS	20.17621231	19.37597466	20.66005516	18.87025833
C9JX88	C9JX88_HUMAN 26S proteasome regulatory subunit 7 OS	20.50494385	20.25925636	20.85916138	20.70708275
P36578	RL4_HUMAN 60S ribosomal protein L4 OS	23.41066933	22.97846031	23.07975388	23.05467224
P37802	TAGL2_HUMAN Transgelin-2 OS	23.55894279	23.16295433	23.46737289	23.71931458
P37837	TALDO_HUMAN Transaldolase OS	21.08679962	19.02413177	20.32860565	20.90719795
A0A7I2V2G2	A0A7I2V2G2_HUMAN Stress-70 protein, mitochondrial OS	23.15665817	22.81215668	22.90218353	23.21714783
P39019	RS19_HUMAN 40S ribosomal protein S19 OS	23.29810143	22.96102142	23.22679138	23.2208271
P39023	RL3_HUMAN 60S ribosomal protein L3 OS	21.65757179	21.20717239	21.90216446	21.84892464
P39656-3	OST48_HUMAN Isoform 3 of Dolichyl-diphosphooligosaccharide--protein glycosyltransferase 48 kDa subunit OS	21.79780388	21.1774292	21.31942749	22.05870628
P40227	TCPZ_HUMAN T-complex protein 1 subunit zeta OS	23.08307076	22.75735474	23.01816559	23.13899231
A0A7I2V2L9	A0A7I2V2L9_HUMAN 60S ribosomal protein L13a OS	22.39610672	22.25571632	22.15625763	21.81225395
P40925	MDHC_HUMAN Malate dehydrogenase, cytoplasmic OS	20.48000526	19.65826797	20.6313858	17.91763306
P40926	MDHM_HUMAN Malate dehydrogenase, mitochondrial OS	22.90459251	21.84318352	22.86039352	22.60844612
P40939	ECHA_HUMAN Trifunctional enzyme subunit alpha, mitochondrial OS	20.74032402	18.74769402	17.91740227	20.55496788
P41091	IF2G_HUMAN Eukaryotic translation initiation factor 2 subunit 3 OS	20.78268814	20.32816696	19.31460571	18.8465004
A0A6Q8PGW4	A0A6Q8PGW4_HUMAN Diadenosine tetraphosphate synthetase OS	22.81164742	22.85264397	22.54077911	22.37007523
A0A0A0MSX9	A0A0A0MSX9_HUMAN Isoleucyl-tRNA synthetase OS	20.7786026	20.84766388	20.14631462	20.0578804

P42677	RS27_HUMAN 40S ribosomal protein S27 OS	21.11457825	20.45813751	20.52238655	20.73297501
P42704	LPPRC_HUMAN Leucine-rich PPR motif-containing protein, mitochondrial OS	19.63912964	19.58732414	19.86545753	20.08692932
P42766	RL35_HUMAN 60S ribosomal protein L35 OS	21.38621902	21.34992027	21.19502449	19.02222824
D6REM6	D6REM6_HUMAN Matrin-3 OS	20.65132141	20.34353638	20.30016899	20.57837677
C9J3L8	C9J3L8_HUMAN Signal sequence receptor subunit alpha OS	20.50037956	18.08462524	19.95730591	18.94451141
P43487-2	RANG_HUMAN Isoform 2 of Ran-specific GTPase-activating protein OS	20.61486053	21.50828362	19.3814888	19.36341476
A0A0A0MR02	A0A0A0MR02_HUMAN Outer mitochondrial membrane protein porin 2 (Fragment) OS	21.10053062	18.61115074	21.37655449	20.70682907
P46060	RAGP1_HUMAN Ran GTPase-activating protein 1 OS	21.03113365	21.17292023	21.28551292	21.48074532
E9PLL6	E9PLL6_HUMAN 60S ribosomal protein L27a OS	20.7218399	20.5857296	18.10736084	20.9452095
A0A2R8Y6J3	A0A2R8Y6J3_HUMAN 60S ribosomal protein L5 (Fragment) OS	21.12704277	20.5799427	21.10437584	21.60580254
P46779	RL28_HUMAN 60S ribosomal protein L28 OS	19.70502472	20.13583374	19.93286705	20.12376213
P46781	RS9_HUMAN 40S ribosomal protein S9 OS	22.77623558	22.41799927	22.1380558	22.41975021
P46783	RS10_HUMAN 40S ribosomal protein S10 OS	22.18255997	22.0206604	22.16977501	22.31843376
P46821	MAP1B_HUMAN Microtubule-associated protein 1B OS	22.97861862	23.17653084	23.35649109	22.91104507
P46940	IQGA1_HUMAN Ras GTPase-activating-like protein IQGAP1 OS	24.22956657	24.04301643	24.16415215	24.13124084
P47756-2	CAPZB_HUMAN Isoform 2 of F-actin-capping protein subunit beta OS	21.83491516	18.75108147	21.58765221	21.50455475
P47914	RL29_HUMAN 60S ribosomal protein L29 OS	18.63410187	19.77980232	20.04072762	19.09104729
P48047	ATPO_HUMAN ATP synthase subunit O, mitochondrial OS	21.42290878	20.24458313	20.49823761	21.00819588
P48444	COPD_HUMAN Coatomer subunit delta OS	19.85680771	19.67188263	20.21608353	20.0283699
P48643	TCPE_HUMAN T-complex protein 1 subunit epsilon OS	22.21299934	21.5017395	21.18095398	22.19628525
P49207	RL34_HUMAN 60S ribosomal protein L34 OS	21.33707047	21.1965847	20.83622551	21.05979538
P49257	LMAN1_HUMAN Protein ERGIC-53 OS	20.11120605	20.76571274	20.66908264	20.18131638
P49327	FAS_HUMAN Fatty acid synthase OS	23.05225182	22.79459572	22.67712784	22.94050407
P49368-2	TCPG_HUMAN Isoform 2 of T-complex protein 1 subunit gamma OS	23.14796066	22.38255501	22.19117165	22.48458481
P49411	EFTU_HUMAN Elongation factor Tu, mitochondrial OS	21.58476639	21.36959457	21.82578468	21.39503479
A0A6Q8PGR9	A0A6Q8PGR9_HUMAN Alanine--tRNA ligase OS	22.0797863	22.1624794	21.7981987	22.03415871
P49721	PSB2_HUMAN Proteasome subunit beta type-2 OS	20.43440819	18.70707512	20.25418854	20.5731144
P49748-2	ACADV_HUMAN Isoform 2 of Very long-chain specific acyl-CoA dehydrogenase, mitochondrial OS	21.2420826	20.63174248	17.81671143	20.72284126
P49755	TMEDA_HUMAN Transmembrane emp24 domain-containing protein 10 OS	21.50949287	21.12905693	20.75066376	20.81464195
P50395	GDIB_HUMAN Rab GDP dissociation inhibitor beta OS	23.33483696	23.04206467	23.48775291	23.14231682
P50454	SERPH_HUMAN Serpin H1 OS	25.20258331	25.42825508	25.41969872	25.27831268
P50502	F10A1_HUMAN Hsc70-interacting protein OS	21.56267357	20.98516655	21.51200294	20.1685524
P50990	TCPQ_HUMAN T-complex protein 1 subunit theta OS	23.54557228	23.41209221	23.56115913	23.53990555
P50991	TCPD_HUMAN T-complex protein 1 subunit delta OS	23.07407951	22.80142021	22.39876938	22.98285294
P51148	RAB5C_HUMAN Ras-related protein Rab-5C OS	21.3372879	21.36693001	21.72121429	21.43119812
P51149	RAB7A_HUMAN Ras-related protein Rab-7a OS	22.55817032	22.36644936	22.36946297	22.44447899
P51571	SSRD_HUMAN Translocon-associated protein subunit delta OS	18.66031456	20.03684425	20.51422119	19.06433678
P51572	BAP31_HUMAN B-cell receptor-associated protein 31 OS	19.22668076	19.28956032	19.14118385	19.75802231

P52209-2	6PGD_HUMAN Isoform 2 of 6-phosphogluconate dehydrogenase, decarboxylating OS	22.70541763	22.59386444	22.85699844	22.75509453
P52272-2	HNRPM_HUMAN Isoform 2 of Heterogeneous nuclear ribonucleoprotein M OS	21.94966888	22.02789879	21.52257729	21.77916527
J3KTF8	J3KTF8_HUMAN Rho GDP-dissociation inhibitor 1 (Fragment) OS	23.87201691	24.0578804	24.23118019	23.78835487
P52907	CAZA1_HUMAN F-actin-capping protein subunit alpha-1 OS	22.37268066	21.3631382	22.77495003	22.74015999
P53396-2	ACLY_HUMAN Isoform 2 of ATP-citrate synthase OS	22.4673233	22.21912956	22.16695786	22.45645905
P53618	COPB_HUMAN Coatomer subunit beta OS	21.08290863	18.38897133	17.43130112	20.36303139
P53621	COPA_HUMAN Coatomer subunit alpha OS	22.91932678	22.40603065	22.80846786	22.60731697
P54136	SYRC_HUMAN Arginine--tRNA ligase, cytoplasmic OS	20.94877815	20.63156509	20.39100075	20.99748611
P55060-4	XPO2_HUMAN Isoform 4 of Exportin-2 OS	20.3780365	20.3042984	20.11895561	20.2455101
P55072	TERA_HUMAN Transitional endoplasmic reticulum ATPase OS	24.27362633	24.4832077	24.09361649	24.43224335
P55084-2	ECHB_HUMAN Isoform 2 of Trifunctional enzyme subunit beta, mitochondrial OS	19.71219826	19.80769539	20.84176445	18.28129005
H0YHC3	H0YHC3_HUMAN Nucleosome assembly protein 1-like 1 (Fragment) OS	20.54425049	20.63147545	20.22387886	21.2160244
P55884	EIF3B_HUMAN Eukaryotic translation initiation factor 3 subunit B OS	20.8956337	19.67891312	18.57518959	19.43682861
P59998	ARPC4_HUMAN Actin-related protein 2/3 complex subunit 4 OS	22.28813553	22.78680038	22.48726273	22.39286232
P60174	TPIS_HUMAN Triosephosphate isomerase OS	24.44556427	24.71088028	24.43942642	24.62934303
B3KW56	B3KW56_HUMAN Eukaryotic translation initiation factor 3 subunit E OS	19.85682297	20.29221344	19.07779694	18.93789291
F8W1R7	F8W1R7_HUMAN Myosin light polypeptide 6 OS	24.57894135	24.75409508	24.40210533	24.60438919
P60709	ACTB_HUMAN Actin, cytoplasmic 1 OS	29.33001328	29.86727905	28.66478729	29.2647686
P60842	IF4A1_HUMAN Eukaryotic initiation factor 4A-I OS	24.70872498	24.78875351	25.12892342	24.72108841
P60866	RS20_HUMAN 40S ribosomal protein S20 OS	22.42526627	22.77039909	22.66459656	22.66938591
B1ALA9	B1ALA9_HUMAN Ribose-phosphate pyrophosphokinase 1 OS	18.88178253	19.33992577	19.43888092	18.15581894
P60900	PSA6_HUMAN Proteasome subunit alpha type-6 OS	21.58536148	21.45156288	21.56369781	21.6724968
P60953	CDC42_HUMAN Cell division control protein 42 homolog OS	20.10200691	20.73908806	20.56941032	20.01848793
P60981	DEST_HUMAN Destrin OS	21.72313309	21.87286186	21.45256996	21.26384735
P61019	RAB2A_HUMAN Ras-related protein Rab-2A OS	20.43135071	20.34992027	20.78612328	21.72454834
P61088	UBE2N_HUMAN Ubiquitin-conjugating enzyme E2 N OS	21.16637611	21.61108208	21.29916382	21.65403366
P61106	RAB14_HUMAN Ras-related protein Rab-14 OS	21.25638008	20.82010651	20.78420639	20.41565514
B4DXW1	B4DXW1_HUMAN Actin-like protein 3 OS	22.37387466	21.79665565	22.07910347	22.25179291
P61160	ARP2_HUMAN Actin-related protein 2 OS	21.78783798	22.01410103	18.80467796	21.74394417
R4GMT0	R4GMT0_HUMAN Alpha-centractin OS	20.42224121	20.82314301	19.00419807	20.38426971
P84077	ARF1_HUMAN ADP-ribosylation factor 1 OS	22.8700428	22.76237106	22.99137306	22.64961243
P61224-2	RAP1B_HUMAN Isoform 2 of Ras-related protein Rap-1b OS	21.52367783	21.00374222	20.86944008	20.72275734
P61247	RS3A_HUMAN 40S ribosomal protein S3a OS	21.48301125	21.54382706	21.85064125	21.55669785
J3QRI7	J3QRI7_HUMAN 60S ribosomal protein L26 (Fragment) OS	21.39634132	21.09384346	20.63927078	21.47867203
P61313	RL15_HUMAN 60S ribosomal protein L15 OS	20.59541321	19.92959023	20.48709106	20.49394608
P61353	RL27_HUMAN 60S ribosomal protein L27 OS	22.97445869	22.77056122	22.63060951	22.8403244
P61586	RHOA_HUMAN Transforming protein RhoA OS	19.98759651	20.52305603	20.76449966	20.54283524
P61604	CH10_HUMAN 10 kDa heat shock protein, mitochondrial OS	22.4226265	22.30744171	22.5920639	22.50717163

P61619	S61A1_HUMAN Protein transport protein Sec61 subunit alpha isoform 1 OS	19.67051888	19.80440521	19.67796707	19.7062397
P61923	COPZ1_HUMAN Coatomer subunit zeta-1 OS	20.11540413	20.36559677	20.05814552	19.71450615
P61970	NTF2_HUMAN Nuclear transport factor 2 OS	21.28427124	20.87530327	20.36581039	20.86135864
P61978-3	HNRPK_HUMAN Isoform 3 of Heterogeneous nuclear ribonucleoprotein K OS	23.69338608	24.02622604	23.7654705	23.6595974
P61981	1433G_HUMAN 14-3-3 protein gamma OS	22.70366478	21.37623596	22.02516174	18.85562325
P62081	RS7_HUMAN 40S ribosomal protein S7 OS	22.80146027	21.96789551	21.70977783	22.33535385
E9PMD7	E9PMD7_HUMAN Serine/threonine-protein phosphatase OS	20.32025337	18.63227081	20.4649334	20.40405655
P62191-2	PRS4_HUMAN Isoform 2 of 26S proteasome regulatory subunit 4 OS	19.86011696	20.93409157	20.52707291	20.58113861
Q5JR95	Q5JR95_HUMAN 40S ribosomal protein S8 OS	22.29476738	22.55027771	22.76634026	23.05617714
P62244	RS15A_HUMAN 40S ribosomal protein S15a OS	22.37276077	22.1238575	22.46480751	22.78208733
P62249	RS16_HUMAN 40S ribosomal protein S16 OS	23.22833443	23.08633041	23.2766819	22.66839027
P62258	1433E_HUMAN 14-3-3 protein epsilon OS	24.36452866	24.86258888	25.07246971	24.43898201
A0A2R8Y811	A0A2R8Y811_HUMAN 40S ribosomal protein S14 (Fragment) OS	22.77832222	22.81025505	22.53226662	22.7710247
P62266	RS23_HUMAN 40S ribosomal protein S23 OS	19.91680717	19.80626297	19.22837257	18.28453445
P62269	RS18_HUMAN 40S ribosomal protein S18 OS	22.22270012	22.41444206	22.35568428	22.2277317
P62277	RS13_HUMAN 40S ribosomal protein S13 OS	22.7966156	23.0280323	22.61820412	22.66405487
P62280	RS11_HUMAN 40S ribosomal protein S11 OS	20.74246407	21.16796875	20.88106537	21.46313667
P62424	RL7A_HUMAN 60S ribosomal protein L7a OS	22.42378044	18.94994545	22.51169014	22.22290611
P62495-2	ERF1_HUMAN Isoform 2 of Eukaryotic peptide chain release factor subunit 1 OS	19.04307556	19.20320129	20.02512932	20.0318737
P62701	RS4X_HUMAN 40S ribosomal protein S4, X isoform OS	22.58244705	22.62417412	22.77918434	21.74505234
P62750	RL23A_HUMAN 60S ribosomal protein L23a OS	22.83425903	22.25822067	22.62305832	22.96326447
P62805	H4_HUMAN Histone H4 OS	18.8910141	18.83523941	18.29583359	18.90744781
P62826	RAN_HUMAN GTP-binding nuclear protein Ran OS	24.46176338	24.08675194	24.00204468	24.21393394
P62829	RL23_HUMAN 60S ribosomal protein L23 OS	21.83140182	21.14948082	21.43623924	21.33276176
S4R456	S4R456_HUMAN 40S ribosomal protein S15 (Fragment) OS	18.87330055	18.98317909	18.99887657	19.39975548
P62847-2	RS24_HUMAN Isoform 2 of 40S ribosomal protein S24 OS	20.687397	20.51902962	20.27775955	20.34212685
P62851	RS25_HUMAN 40S ribosomal protein S25 OS	22.21341515	22.18392372	22.04143143	22.04383469
P62857	RS28_HUMAN 40S ribosomal protein S28 OS	19.09625053	19.2377243	20.52764511	18.82063293
E5RI99	E5RI99_HUMAN 60S ribosomal protein L30 (Fragment) OS	19.09628296	19.47548103	19.1880722	18.9431839
P62899	RL31_HUMAN 60S ribosomal protein L31 OS	21.51287079	21.52960014	21.51566505	21.56034279
P62906	RL10A_HUMAN 60S ribosomal protein L10a OS	23.07394981	22.79193497	23.26742363	23.41557693
D3YTB1	D3YTB1_HUMAN 60S ribosomal protein L32 (Fragment) OS	19.64353943	19.51476097	19.31690025	20.50988007
P62913	RL11_HUMAN 60S ribosomal protein L11 OS	21.7864418	22.02482414	21.53957367	22.34472847
P62917	RL8_HUMAN 60S ribosomal protein L8 OS	21.62894249	21.89788818	21.69459724	21.11114311
P62937	PPIA_HUMAN Peptidyl-prolyl cis-trans isomerase A OS	24.97683716	25.02812576	25.21404457	25.09904671
P63000	RAC1_HUMAN Ras-related C3 botulinum toxin substrate 1 OS	21.93102837	21.89285851	21.86351585	22.38924217
P63104	1433Z_HUMAN 14-3-3 protein zeta/delta OS	24.56778717	24.90577698	24.856287	24.80626678
P63173	RL38_HUMAN 60S ribosomal protein L38 OS	18.49188423	18.88479614	19.83377266	17.66793251

I3L397	I3L397_HUMAN Eukaryotic translation initiation factor 5A (Fragment) OS	22.95351028	22.89330292	22.57346153	22.53803444
P63244	RACK1_HUMAN Receptor of activated protein C kinase 1 OS	21.35024452	21.170784	22.76941109	22.2841301
P67809	YBOX1_HUMAN Y-box-binding protein 1 OS	22.65237236	22.907547	22.40080261	22.9051609
H0YNG3	H0YNG3_HUMAN Signal peptidase complex catalytic subunit SEC11 OS	19.40270424	19.7603302	19.68708801	19.88902283
P67936	TPM4_HUMAN Tropomyosin alpha-4 chain OS	24.1532917	24.04901505	24.21252441	24.52007294
P68032	ACTC_HUMAN Actin, alpha cardiac muscle 1 OS	25.18899345	24.83465576	24.26076317	25.29858971
P68036-2	UB2L3_HUMAN Isoform 2 of Ubiquitin-conjugating enzyme E2 L3 OS	20.33745193	20.60421944	20.35863876	20.6382103
A0A7I2V659	A0A7I2V659_HUMAN Elongation factor 1-alpha 1 OS	28.03396416	27.76287651	28.18669128	28.00961304
P68363	TBA1B_HUMAN Tubulin alpha-1B chain OS	27.35766602	27.515028	27.62247467	27.29640388
P68371	TBB4B_HUMAN Tubulin beta-4B chain OS	27.19788742	26.8773632	27.41264153	27.12129402
P78371	TCPB_HUMAN T-complex protein 1 subunit beta OS	22.8313427	23.25364113	23.14559937	23.05617714
P78417	GSTO1_HUMAN Glutathione S-transferase omega-1 OS	22.32882309	22.48089218	22.40794945	22.57431602
P78527	PRKDC_HUMAN DNA-dependent protein kinase catalytic subunit OS	21.72587967	21.63214111	21.56630135	21.7286644
C9JXB8	C9JXB8_HUMAN 60S ribosomal protein L24 OS	21.09680557	21.11190796	20.88524437	21.43806839
J3QR09	J3QR09_HUMAN Ribosomal protein L19 OS	19.01748276	19.72578812	19.72573853	20.3035183
P84103-2	SRSF3_HUMAN Isoform 2 of Serine/arginine-rich splicing factor 3 OS	18.7894001	20.36474228	20.44384575	20.59705162
P98179	RBM3_HUMAN RNA-binding protein 3 OS	20.38131523	20.97477341	19.7901535	20.52735901
C9JFR7	C9JFR7_HUMAN Cytochrome c (Fragment) OS	21.03999329	21.10935974	20.71129036	21.25257301
F8VVM2	F8VVM2_HUMAN Phosphate carrier protein, mitochondrial OS	21.65123367	22.38389969	22.223526	21.95840454
A0A024R4E5	A0A024R4E5_HUMAN High density lipoprotein binding protein (Vigilin), isoform CRA_a OS	22.42157364	22.21563911	21.96490288	22.32011604
Q00610-2	CLH1_HUMAN Isoform 2 of Clathrin heavy chain 1 OS	24.97928238	24.67298126	24.81972694	24.59576607
A0A1W2PPS1	A0A1W2PPS1_HUMAN Heterogeneous nuclear ribonucleoprotein U OS	22.69313049	22.85212898	23.09529305	22.65429688
Q01082	SPTB2_HUMAN Spectrin beta chain, non-erythrocytic 1 OS	21.80770302	21.04853249	21.25919914	20.98607063
Q01105-3	SET_HUMAN Isoform 3 of Protein SET OS	18.95907784	19.06279373	21.68461609	22.34600258
Q01469	FABP5_HUMAN Fatty acid-binding protein 5 OS	19.00317574	18.85256577	18.67992592	18.67603683
Q01518-2	CAP1_HUMAN Isoform 2 of Adenylyl cyclase-associated protein 1 OS	22.56090164	23.20096016	23.59479904	22.99465752
Q01813	PFKAP_HUMAN ATP-dependent 6-phosphofructokinase, platelet type OS	22.05208588	21.34212685	21.14033508	21.37607574
Q01995	TAGL_HUMAN Transgelin OS	24.7683506	24.65518188	24.50609398	24.88539314
M0R3D6	M0R3D6_HUMAN 60S ribosomal protein L18a (Fragment) OS	19.92990875	19.86867142	20.1021347	20.40062141
Q02878	RL6_HUMAN 60S ribosomal protein L6 OS	22.42675209	22.08929062	22.28757095	22.91342163
Q03135	CAV1_HUMAN Caveolin-1 OS	22.72075462	22.38677025	22.3856926	22.21545982
Q04637-6	IF4G1_HUMAN Isoform E of Eukaryotic translation initiation factor 4 gamma 1 OS	21.82915688	21.39131546	21.84586525	21.52061272
Q04917	1433F_HUMAN 14-3-3 protein eta OS	22.6102047	22.48047447	22.50006294	22.64180756
Q05682-5	CALD1_HUMAN Isoform 5 of Caldesmon OS	22.96497345	23.71408272	23.85367203	23.31340599
A0A6I8PTT9	A0A6I8PTT9_HUMAN Glutamine--fructose-6-phosphate transaminase (isomerizing) OS	20.48404312	20.22470284	20.57653236	20.77828217
Q06323	PSME1_HUMAN Proteasome activator complex subunit 1 OS	18.18373871	19.07732773	19.4559536	20.34460831
Q06830	PRDX1_HUMAN Peroxiredoxin-1 OS	25.09470558	24.84536743	24.84856987	25.20018959
Q07020	RL18_HUMAN 60S ribosomal protein L18 OS	22.49071693	22.67646217	22.55506134	22.72008705

Q07065	CKAP4_HUMAN Cytoskeleton-associated protein 4 OS	25.88105774	25.56537819	25.3656292	25.76638031
Q08211	DHX9_HUMAN ATP-dependent RNA helicase A OS	20.88554192	20.41586113	20.59841537	20.43298149
Q09666	AHNK_HUMAN Neuroblast differentiation-associated protein AHNAK OS	26.80919075	26.82784081	26.60752487	26.89585114
Q12792	TWF1_HUMAN Twinfilin-1 OS	19.77402496	19.71676636	19.71513367	18.12091637
Q13162	PRDX4_HUMAN Peroxiredoxin-4 OS	21.9103508	21.42147064	21.97952652	21.31523132
Q13200	PSMD2_HUMAN 26S proteasome non-ATPase regulatory subunit 2 OS	20.71833229	20.72974396	20.90778542	20.67719269
A0A7I2YQU2	A0A7I2YQU2_HUMAN Eukaryotic translation initiation factor 3 subunit I OS	20.01031494	18.65255928	19.58714485	19.62633324
Q13404	UB2V1_HUMAN Ubiquitin-conjugating enzyme E2 variant 1 OS	25.04034424	25.15054321	24.50536728	24.32244301
Q13509	TBB3_HUMAN Tubulin beta-3 chain OS	20.62729454	21.03704643	20.46293831	20.93919373
Q13813-3	SPTN1_HUMAN Isoform 3 of Spectrin alpha chain, non-erythrocytic 1 OS	22.29094887	22.0790062	22.85004997	21.93340683
Q13885	TBB2A_HUMAN Tubulin beta-2A chain OS	20.257761	20.23139954	20.50067139	18.76807785
Q14019	COTL1_HUMAN Coactosin-like protein OS	21.47476768	21.88110352	21.42188263	21.59609604
H0YA96	H0YA96_HUMAN Heterogeneous nuclear ribonucleoprotein D0 (Fragment) OS	21.51460648	21.17053795	21.23800659	21.82178116
Q14152	EIF3A_HUMAN Eukaryotic translation initiation factor 3 subunit A OS	21.46453285	21.34044266	21.08679962	21.03402519
Q14203-5	DCTN1_HUMAN Isoform 5 of Dynactin subunit 1 OS	19.51335335	19.29692459	19.15960503	19.35968971
Q14204	DYHC1_HUMAN Cytoplasmic dynein 1 heavy chain 1 OS	24.34435081	24.31035805	24.19730568	24.18714523
Q14315	FLNC_HUMAN Filamin-C OS	27.12149239	27.11723709	27.25349617	27.0048542
Q14697	GANAB_HUMAN Neutral alpha-glucosidase AB OS	23.36292458	22.8890934	22.88393974	23.58060837
Q14764	MVP_HUMAN Major vault protein OS	22.82702637	22.94881439	22.78640175	23.10726929
Q14847	LASP1_HUMAN LIM and SH3 domain protein 1 OS	21.25678253	22.18474007	21.33788681	21.2075882
Q14974	IMB1_HUMAN Importin subunit beta-1 OS	22.3130188	22.37877655	22.22552681	22.31893158
Q15019	SEPT2_HUMAN Septin-2 OS	21.82667732	21.78524399	20.0318737	21.30557823
Q15056-2	IF4H_HUMAN Isoform Short of Eukaryotic translation initiation factor 4H OS	21.22146225	21.41622162	21.5228653	22.01229477
Q15084-3	PDIA6_HUMAN Isoform 3 of Protein disulfide-isomerase A6 OS	23.18219757	23.13641357	23.43948936	23.43109512
Q15149-4	PLEC_HUMAN Isoform 4 of Plectin OS	25.25093269	24.91988945	25.1126709	25.1349659
Q15293	RCN1_HUMAN Reticulocalbin-1 OS	20.77378273	21.71234131	17.98793602	21.14108467
Q15365	PCBP1_HUMAN Poly(rC)-binding protein 1 OS	21.73677826	21.9072361	21.34472847	21.80565643
Q15366-6	PCBP2_HUMAN Isoform 6 of Poly(rC)-binding protein 2 OS	20.30106354	20.06736565	20.74131203	20.65499687
B8ZZU8	B8ZZU8_HUMAN Elongin-B OS	18.43782806	18.92963982	19.85376549	20.35638237
F5H365	F5H365_HUMAN Protein transport protein SEC23 OS	21.41926003	21.0653286	20.91568375	21.73454666
Q15691	MARE1_HUMAN Microtubule-associated protein RP/EB family member 1 OS	18.58977509	19.15172577	19.41030312	18.99092293
Q15758	AAAT_HUMAN Neutral amino acid transporter B(0) OS	20.91210556	21.30374146	21.05629349	21.60082245
Q15907	RB11B_HUMAN Ras-related protein Rab-11B OS	22.33606339	22.42513847	22.12543488	22.69670105
Q15942	ZYX_HUMAN Zyxin OS	22.87152863	22.36383247	22.08916283	22.49947929
E7ES33	E7ES33_HUMAN Septin OS	21.02823448	21.39937019	21.57740784	20.84544373
Q16222-3	UAP1_HUMAN Isoform 3 of UDP-N-acetylhexosamine pyrophosphorylase OS	20.71774673	20.5890255	21.29092026	20.81362534
Q16527	CSRP2_HUMAN Cysteine and glycine-rich protein 2 OS	20.24898911	19.03178215	20.2585659	20.15177536
Q16555-2	DPYL2_HUMAN Isoform 2 of Dihydropyrimidinase-related protein 2 OS	22.89191437	22.48387146	22.51535225	22.79141808

Q16658	FSCN1_HUMAN Fascin OS	23.12012863	23.95774841	23.68880463	23.29151154
A0A7I2YQ74	A0A7I2YQ74_HUMAN UTP--glucose-1-phosphate uridylyltransferase OS	20.73040771	20.23572922	20.22599792	20.52821732
E9PIR7	E9PIR7_HUMAN Thioredoxin-disulfide reductase OS	20.13520813	22.20421982	20.66031647	20.95347404
Q6NZI2	CAVN1_HUMAN Caveolae-associated protein 1 OS	23.55027771	23.35231972	23.77846336	23.37583733
Q6UVK1	CSPG4_HUMAN Chondroitin sulfate proteoglycan 4 OS	22.93912315	22.35345078	22.73419571	22.38031006
Q70UQ0-4	IKIP_HUMAN Isoform 4 of Inhibitor of nuclear factor kappa-B kinase-interacting protein OS	20.96169281	20.2250576	19.98814011	20.65970612
Q7KZF4	SND1_HUMAN Staphylococcal nuclease domain-containing protein 1 OS	23.31686211	23.32649422	23.29291534	23.51544952
Q86VP6	CAND1_HUMAN Cullin-associated NEDD8-dissociated protein 1 OS	20.88084221	20.96027946	20.43338966	20.77313995
Q8NBS9-2	TXND5_HUMAN Isoform 2 of Thioredoxin domain-containing protein 5 OS	20.94105911	20.64702225	21.04286766	20.72916222
Q8TED1	GPX8_HUMAN Probable glutathione peroxidase 8 OS	18.95015335	20.26796532	20.07535362	20.22776222
Q8WUM4	PDC6I_HUMAN Programmed cell death 6-interacting protein OS	21.52750206	21.55651093	21.44924736	20.98523521
Q92499-3	DDX1_HUMAN Isoform 3 of ATP-dependent RNA helicase DDX1 OS	21.01780891	20.79344368	20.19544411	20.9557457
Q92598-2	HS105_HUMAN Isoform Beta of Heat shock protein 105 kDa OS	20.23642921	20.25234222	20.68208885	19.83480835
Q92616	GCN1_HUMAN eIF-2-alpha kinase activator GCN1 OS	19.96268082	19.60320663	19.48883629	18.87059975
A0A087WTP3	A0A087WTP3_HUMAN Far upstream element-binding protein 2 OS	21.19490433	21.02018547	21.56917953	21.09732056
Q92973-2	TNPO1_HUMAN Isoform 2 of Transportin-1 OS	20.04566956	20.53402519	18.87665558	20.35315514
Q969G5	CAVN3_HUMAN Caveolae-associated protein 3 OS	21.82442665	20.65438461	21.56267357	21.22334862
Q969H8	MYDGF_HUMAN Myeloid-derived growth factor OS	21.44091034	21.9212532	21.48394585	21.342453
Q96AE4	FUBP1_HUMAN Far upstream element-binding protein 1 OS	20.93272209	20.83684158	20.31506538	21.13345337
Q96AG4	LRC59_HUMAN Leucine-rich repeat-containing protein 59 OS	22.75144196	21.95095062	22.62464333	22.54898453
Q96AY3	FKB10_HUMAN Peptidyl-prolyl cis-trans isomerase FKBP10 OS	20.19568443	20.47447014	20.399683	20.26132393
Q96HC4	PDLI5_HUMAN PDZ and LIM domain protein 5 OS	19.94792175	19.39408112	19.55939865	19.54916763
Q96QK1	VPS35_HUMAN Vacuolar protein sorting-associated protein 35 OS	20.62987518	20.65831184	20.38900566	21.01726532
Q96TA1-2	NIBA2_HUMAN Isoform 2 of Protein Niban 2 OS	21.71686745	20.96402168	20.68157387	21.38052177
A0A087X271	A0A087X271_HUMAN Calponin (Fragment) OS	23.08953476	22.62776184	22.79120064	22.18797493
A0A7I2V641	A0A7I2V641_HUMAN 26S proteasome non-ATPase regulatory subunit 1 OS	20.179739	19.58616829	19.29665565	20.6661377
Q99497	PARK7_HUMAN Parkinson disease protein 7 OS	22.87517166	22.71793556	22.83803558	22.54533577
Q99536	VAT1_HUMAN Synaptic vesicle membrane protein VAT-1 homolog OS	21.73098755	21.59368324	22.00295448	21.65678596
F5GY37	F5GY37_HUMAN Prohibitin OS	21.46203804	18.62091637	21.73525047	21.64891052
Q99715-4	COCA1_HUMAN Isoform 4 of Collagen alpha-1(XII) chain OS	23.96322823	24.28029633	23.71826935	23.67012024
Q99832	TCPH_HUMAN T-complex protein 1 subunit eta OS	22.27301407	22.31215858	21.68286133	22.31942749
Q9BRA2	TXD17_HUMAN Thioredoxin domain-containing protein 17 OS	20.04393578	20.12754631	19.92491722	20.79519081
Q9BSJ8	ESYT1_HUMAN Extended synaptotagmin-1 OS	21.77591324	21.3288784	21.09029388	21.22605705
Q9BUF5	TBB6_HUMAN Tubulin beta-6 chain OS	22.85214806	22.76218987	22.93560219	22.94660187
Q9BVK6	TMED9_HUMAN Transmembrane emp24 domain-containing protein 9 OS	20.93358612	20.93574715	21.05231857	21.12647438
Q9H0U4	RAB1B_HUMAN Ras-related protein Rab-1B OS	22.43270111	22.57503319	22.97305679	22.72486115
Q5T123	Q5T123_HUMAN SH3 domain-binding glutamic acid-rich-like protein 3 OS	20.5874691	20.44748306	20.63484573	20.56458092
Q9H3N1	TMX1_HUMAN Thioredoxin-related transmembrane protein 1 OS	20.38553429	20.24435043	19.96592522	18.50144386

Q9H4M9	EHD1_HUMAN EH domain-containing protein 1 OS	21.21626091	21.05609512	21.66209984	21.61800194
Q9HB71	CYBP_HUMAN Calcyclin-binding protein OS	21.07012177	21.29193306	21.10667801	21.24196625
A0A087X163	A0A087X163_HUMAN Ras-related protein Rab-18 OS	19.9343071	19.69951057	18.67591667	19.63078308
Q9NQC3-2	RTN4_HUMAN Isoform B of Reticulon-4 OS	22.88684464	22.36828995	23.12352562	22.69799423
Q9NR12	PDLI7_HUMAN PDZ and LIM domain protein 7 OS	19.44159889	19.90405464	20.33527184	20.15003967
Q9NRV9	HEBP1_HUMAN Heme-binding protein 1 OS	20.5460434	20.23923111	19.58080673	18.86299706
D6RGI3	D6RGI3_HUMAN Septin OS	22.09519577	21.59099007	22.53848457	21.22364426
Q9NZM1-6	MYOF_HUMAN Isoform 6 of Myoferlin OS	23.33456421	23.35930824	23.51941299	23.40561485
Q9NZN4	EHD2_HUMAN EH domain-containing protein 2 OS	21.6853447	21.87582779	22.1516819	21.82842255
Q9P0L0	VAPA_HUMAN Vesicle-associated membrane protein-associated protein A OS	20.19111252	20.65377235	21.08173752	19.89276123
Q9P2E9	RRBP1_HUMAN Ribosome-binding protein 1 OS	23.14600372	23.28489113	23.42598343	23.22552681
F8VQE1	F8VQE1_HUMAN LIM domain and actin-binding protein 1 OS	20.20669556	20.37708282	20.42419052	20.58884239
Q9UHD8-7	SEPT9_HUMAN Isoform 7 of Septin-9 OS	22.22393799	22.41959572	22.67260361	22.53791618
Q9ULV4	COR1C_HUMAN Coronin-1C OS	20.28059387	21.59382057	20.74935532	20.60855865
Q9UQ80-2	PA2G4_HUMAN Isoform 2 of Proliferation-associated protein 2G4 OS	21.73144341	21.54198456	22.05075836	21.95191002
Q9Y230	RUVB2_HUMAN RuvB-like 2 OS	20.31572914	20.23186874	20.65342331	20.00360489
Q9Y265	RUVB1_HUMAN RuvB-like 1 OS	20.3109684	20.10174942	19.86678696	19.98036194
Q9Y266	NUDC_HUMAN Nuclear migration protein nudC OS	19.5786705	20.15721321	19.76089859	19.83787346
Q9Y3U8	RL36_HUMAN 60S ribosomal protein L36 OS	20.25614929	20.49882126	20.18652534	18.73384285
Q9Y490	TLN1_HUMAN Talin-1 OS	24.98315811	25.01260948	25.03216743	24.93251419
A0A087X054	A0A087X054_HUMAN Hypoxia up-regulated protein 1 OS	21.84796906	21.17876625	20.70235443	21.04979515
Q9Y617-2	SERC_HUMAN Isoform 2 of Phosphoserine aminotransferase OS	21.61265755	21.64315224	21.30635834	21.52750206
Q9Y678	COPG1_HUMAN Coatomer subunit gamma-1 OS	22.16438293	21.94998932	21.65744019	22.20573997
Q9Y696	CLIC4_HUMAN Chloride intracellular channel protein 4 OS	22.25942802	22.63710403	22.63955688	22.24251938

Appendix Table 2
The key materials and reagents used in the current study.

Primary antibodies (Immunofluorescence)					
Protein	**Figure**	**Final working concentration (µg/ml)**	**Company**	**Cat. No.**	**Batch No.**
ACE2	1B, 1D, 1F	5	Proteintech	66699-1-Ig	-
APC His-Tag conjugated antibody	1G, 1H	10 µl/10^6 cells	R&D	IC050A	ABUH0521061
Collagen I	3I, 5H	5	RockLand	600-401-103	46588
MMP1	3K	5	Genetex	GTX24043	18912
TMPRSS2	1C, 1D, 1F	8.86	Abcam	ab109131	GR3343890-9
Vimentin	1B	1	Abcam	ab92547	GR219216-24
Vimentin	1C	1	R&D	MAB2015	UUQ021041

Secondary antibodies (Immunofluorescence)				
Target	**Final working concentration (µg/ml)**	**Company**	**Cat. No.**	**Batch No.**
Alexa 488 donkey anti-rabbit IgG	6.67	Life Technologies	A21206	2072687
Alexa 488 donkey anti-rat IgG	6.67	Life Technologies	A21208	1932496
Alexa 568 donkey anti-mouse IgG	4	Life Technologies	A10037	1303018
Alexa 568 donkey anti-rabbit IgG	4	Life Technologies	A10042	1964370

Antibody (FACS)					
Protein	**Figure**	**Final working concentration (µg/ml)**	**Company**	**Cat. No.**	**Batch No.**
APC His-Tag conjugated antibody	1I, IJ	10 µl/10^6 cells	R&D	IC050A	ABUH0521061

Primary antibodies (Western Blotting)

Protein	Figure	Final working concentration (µg/ml)	Company	Cat. No.	Batch No.
ACE2	1E	1	Proteintech	66699-1-Ig	-
Collagen I	3A, 3D, 5F	2	RockLand	600-401-103	46588
Lamin B1	1D, 5F	1	Abcam	ab16048	GR3417466-1
MMP1	3A, 3D	2	Genetex	GTX24043	18912
GAPDH	3A, 3D	0.2	Santa Cruz	SC-32233	H2114
TMPRSS 2	1D	1.77	Abcam	ab109131	GR3343890-9

Secondary antibodies (Western Blotting)				
Target	**Final working concentration (µg/ml)**	**Company**	**Cat. No.**	**Batch No.**
HRP mouse	0.184	Cell Signalling	7076	33
HRP rabbit	0.06	Cell Signalling	7074	28

Primers			
Gene (human)	**Forward primer ('5-'3)**	**Reverse primer ('5-'3)**	**PCR Product size**
COL1A1	GTGCTAAAGGTGCCAATGGT	ACCAGGTTCACCGCTGTTAC	128
GapDH	ATCACTGCCACCCAGAAGAC	CAGTGAGCTTCCCGTTCAG	148
MMP1	TGCTCATGCTTTTCAACCAG	AGTTCATGAGCTGCAACACG	117
36b4	GCAATGTTGCCAGTGTCTGT	GCCTTGACCTTTTCAGCAAG	142

Recombinant Protein		
Protein	**Company**	**Cat. No.**
SARS-CoV-2 Spike His tag Protein	R&D	10549-CV-100

Plasmids		
Vector	**Company**	**Cat. No.**
pLVX-EF1alpha-eGFP-2xStrep-IRES-Puro	Addgene	141395
pLVX-EF1alpha-SARS-CoV-2-E-2xStrep-IRES-Puro	Addgene	141385
pLVX-EF1alpha-SARS-CoV-2-M-2xStrep-IRES-Puro	Addgene	141386
pLVX-EF1alpha-SARS-CoV-2-N-2xStrep-IRES-Puro	Addgene	141391
pWPI-IRES-Puro-Ak	Addgene	154984
pWPI-IRES-Puro-Ak-ACE2	Addgene	154985

Mitochondrial inhibitor	Company	Cat. No.
Etomoxir	Sigma	236020